J. Mech. Phys. Solids 192 (2024) 105833

Contents lists available at ScienceDirect

Journal of the Mechanics and Physics of Solids

journal homepage: www.elsevier.com/locate/jmps

The importance of a full chemo-poro-mechanical coupling for the modeling of subcutaneous injections

Ludovic Gil [a], Michel Jabbour [b,c], Nicolas Triantafyllidis [b,c,d,*]

[a] BD Medical - Pharmaceutical Systems, 11 rue Aristide Bergès, Le Pont-de-Claix Cedex, Isère 38801, France
[b] Laboratoire de Mécanique des Solides (CNRS UMR 7649), Ecole Polytechnique, Institut Polytechnique de Paris, France
[c] Département de Mécanique, École Polytechnique, Route de Saclay, Palaiseau 91128, France
[d] Aerospace Engineering Department & Mechanical Engineering Department (emeritus) The University of Michigan, Ann Arbor, MI 48109-2140, USA

ARTICLE INFO

Keywords:
Subcutaneous injections
Finite strain
Chemo-mechanical couplings

ABSTRACT

Modeling of subcutaneous injections in soft adipose tissue – a common way to administer pharmaceutical medication – is a challenging multiphysics problem which has recently attracted the attention of the engineering community, as it could help optimize medical devices and treatments. The underlying continuum mechanics of this process is complex and involves finite strain poro-mechanics – where a viscous fluid, containing different charged species, is injected into a porous viscoelastic matrix and absorbed by blood and lymph vessels – as well as electrochemistry, that generates osmotic pressure due to electrical charges attached to the tissue. In this paper, we present a chemo-mechanical model of subcutaneous injections that accounts for the diffusion of electrically charged chemical species – contained in the interstitial fluid – into the tissue, blood and lymph vessels. This work provides the methodology to derive a general theory accounting for the electro-chemo-poro-mechanical couplings in a thermodynamically consistent framework, avoiding phenomenological biases or inconsistencies likely to arise in the derivation of nonlinear theories with many couplings. To motivate its use for the modeling of subcutaneous injections, it is complemented by a simplified, linearized boundary value problem that illustrates the importance of considering these couplings for the prediction of subcutaneous injections key performance indicators.

1. Introduction

The subcutaneous[1] injection is a widely used method of drug administration since it does not need patient hospitalization and can easily be performed at home. While the convenience of the procedure is appreciated by the medical community, the range of treatments that can be injected in the subcutaneous tissue could be limited due to patient acceptability, along with concerns associated to the effect of such injections on the receiving tissue. Understanding the physics involved and developing a chemo-mechanical model of the subcutaneous injection can give tools to better analyze and then control the parameters of this procedure in order to optimize its effectiveness and patient acceptability.

The biomechanics community has already investigated the subject from the experimental side with observations, tests, measurements, e.g. see Thomsen et al. (2012, 2014, 2015), and more specifically focusing on the feasibility of large volume subcutaneous

* Corresponding author at: Département de Mécanique, École Polytechnique, Route de Saclay, Palaiseau 91128, France.
E-mail address: nicolas.triantafyllidis@polytechnique.edu (N. Triantafyllidis).

[1] The term *subcutaneous tissue* is used to describe to the fat layer that is located between the skin and the muscle.

https://doi.org/10.1016/j.jmps.2024.105833
Received 31 December 2023; Received in revised form 2 August 2024; Accepted 17 August 2024
Available online 27 August 2024

injections of viscous drugs, e.g. see Schwarzenbach et al. (2015), Woodley et al. (2021, 2022), Rini et al. (2022) and references quoted therein. In spite of the complexity of the problem, the modeling side has also received attention from the mechanics community. Initially solid and fluid mechanics models were used, e.g. see Comley and Fleck (2011), gradually evolving to more sophisticated recent ones involving finite strain poro-elasticity including viscous effects and diffusion of chemical species, e.g. see Zheng et al. (2021), Leng et al. (2021a,b), de Lucio et al. (2023) and references therein.

An essential aspect for the correct modeling of injections must rely on taking into account the various and complex underlying physical phenomena. There is a vast continuum mechanics literature on problems related to the physical mechanisms involved in subcutaneous injections, motivated by different engineering and physics applications involving one or more of these mechanisms. One could thus cite the modeling of clay (Gajo and Loret, 2003, 2007), cartilage (Lai et al., 1991; Sun et al., 1999; Loret and Simões, 2004; Huyghe and Janssen, 1999), tissue growth (Loret and Simões, 2005), ionic polymers (Xiao and Bhattacharya, 2001), hydrogels (Chester and Anand, 2010, 2011; Brassart and Suo, 2013), chemical diffusion in solids (Fried and Gurtin, 1999; Anand, 2012), electronic couplings in semi-conductors (Guin et al., 2018), fluid flow in porous media (Coussy, 2004), the biphasic approach of poro-mechanics (Biot, 1941, 1972), microstructure and homogenization problems in the same topic (Coussy et al., 1998; Dormieux et al., 1991), just to name a few. Given the extreme microstructural complexity of biological tissue and the macroscopic nature of the phenomena of interest, we focus henceforth on the continuum modeling of the problem at hand.

Starting with the purely mechanical aspect of the problem, Gil et al. (2022) have recently proposed an objective, finite strain poro-elasticity model. Since the complete modeling of subcutaneous injections must involve the diffusion and absorption of chemical species as well as electroneutrality considerations – essential for the prediction of pressure and the associated osmotic contribution – and based on the recent work by Gil (2020), we present here a thermodynamically consistent, objective and fully coupled finite strain theory for electro-chemo-poro-elasticity to serve as a complete model for the boundary value problem of subcutaneous injections.

Although continuum models for this problem have already appeared in the literature, with different models covering different aspects, the previous work of Gil (2020) and Gil et al. (2022) highlighted the risk of introducing inconsistencies with objectivity in finite strain, especially in the case where multiple couplings are phenomenologically postulated when writing balance laws. The present thermodynamically consistent formulation that includes the multiphysics aspects of the problem at hand is novel and hence, in our opinion, merits a separate presentation. To emphasize the necessity of a full electro-chemo-poro-mechanical coupling for modeling subcutaneous injections, the general theory is complemented by the inclusion of a simplified, linearized model injection problem that shows the importance of the osmotic efficiency coefficient and the fixed charges in the tissue for predicting the pressure, volume changes, interstitial fluid and chemical species velocities as well as absorption rates, which are key performance indicators of subcutaneous injections.

After the introduction in Section 1, the presentation continues with some notation and other preliminaries in Section 2, followed by the general principles using the direct (current configuration Eulerian) approach of continuum mechanics in Section 3. Using the Coleman–Noll framework of thermodynamics, we establish in Section 4 constitutive restrictions for the volume and surface field quantities involved, followed in Section 5 by the corresponding constitutive choices. A summary of the system of governing equations and interface conditions is given in Section 6. We illustrate the interplay between mechanics, chemistry and electroneutrality in Section 7 via a simplified, time-independent linearized injection model and conclude in Section 8. The derivation details for the general theory are given in Appendix A and the details of the linearized boundary problem in Appendix B.

2. Preliminaries

To set the stage for the continuum modeling of subcutaneous injections, we start with a brief description of the relevant physics, biology and chemistry of the problem in Section 2.1, followed by the notations, assumptions and definitions of the basic field quantities for the proposed continuum model in Section 2.2.

2.1. Problem description

A general pattern can be used to describe the human skin-subcutaneous complex (Herlin et al., 2014, 2015). This medium is distinguished in three main parallel layers (see Fig. 1): the skin which represents the impermeable membrane separating the inner body from the atmosphere, one stiff deep layer (muscle) and, in between, the so-called subcutaneous region into which the subcutaneous injections are performed.

Structural description The subcutaneous region is not homogeneous and to a first level, is structured by skin ligaments and membranes that partition the *adipose tissue*, as sketched in Fig. 1. Extensive work has been done to observe and mechanically characterize the adipose tissue (Comley and Fleck, 2010, 2011, 2012; Alkhouli et al., 2013; Wu et al., 2007). It consists of a network of collagen fibers that support lipid cells called *adipocytes*. Adipocytes contain a single lipid droplet held in a phospholipid bilayer. They are inserted in a collagen meshed membrane whose role is to reinforce the adipocytes membranes.

The interlobular septa and the absorption system The reinforcement membrane surrounding each adipocyte is commonly described as a closed-cell foam, hence it is barely permeable. The adipocytes are gathered in clusters called *lobules* that are separated by a matrix made of oriented collagen fibers, called the *interlobular septa* (Comley and Fleck, 2010). Due to the fibril structure of the interlobular septa, it is described as a fully saturated open-cell foam, in which the *interstitial fluid*[2] can flow. Therefore, the injected

[2] It refers to the fluid filling the interlobular septa in the natural configuration, it is mixed with the injected fluid during injection.

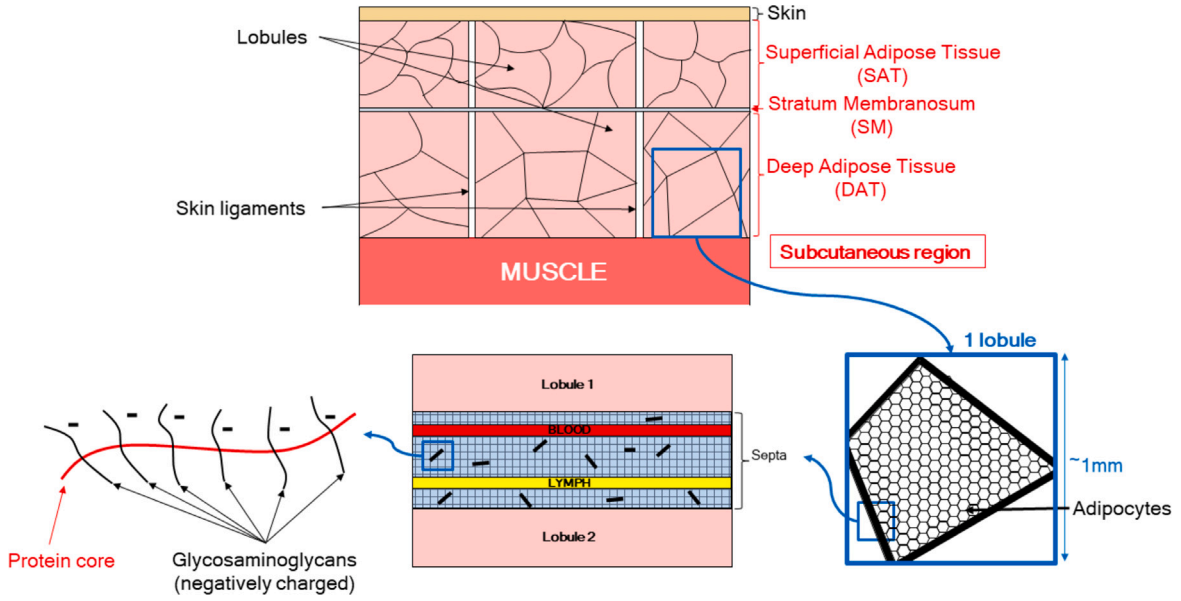

Fig. 1. Schematic of the subcutaneous region showing different scales involved in the injection process.

fluid mainly flows through the interlobular septa as it can be observed in experimental visualizations of injected depots in porcine adipose tissue (Thomsen et al., 2012, 2015).

The injected fluid contains chemical molecules that may react with each other and be absorbed by the body through the septa into blood and lymph vessels (see Fig. 1). For an extensive description of the septa, one can refer to Swartz and Fleury (2007), Aukland and Nicolaysen (1981), McGurk (2010), Richter et al. (2012), Richter and Jacobsen (2014), Levitt (2003) and Wiig and Swartz (2012). It is vascularized by both blood and lymphatic vessels that absorb and release the molecules of the *interstitial fluid*.

The blood system is a closed loop whose convection is forced by the heart beats whereas the lymphatic system is an open system. The lymph flows at low speed from the lymphatic capillaries towards the lymphatic nodes. Consequently, the absorption by blood capillaries is a lot faster than the absorption by the lymphatic system. However, the permeability of the blood capillaries membrane decreases with the size of the molecules. It has been shown that after injection in subcutaneous tissue, large molecules are slowly absorbed by the lymphatic system while smaller molecules are absorbed by the blood system (McLennan et al., 2005).

Fixed charge density At physiological pH, the hydrated subcutaneous tissue is electrically charged due to the presence of proteins, called *proteoglycans*. Proteoglycans are made of a protein core holding *glycosaminoglycans* that carry electric charges (see Fig. 1). Proteoglycans are in the interstitial fluid but are trapped in the collagen fibers network due to their size. Therefore, they cannot move through the interlobullar septa or be absorbed by the blood or the lymph. This is usually modeled by a fixed charge density carried by the tissue. The value of the electric charge may vary depending on individuals and body location. Extensive work has been done on the modeling of connective tissue and cartilage which is made of hydrated collagen carrying negatively charged proteoglycans (see for instance (Sun et al., 1999; Loret and Simões, 2004; Lai et al., 1981, 1991)).

2.2. Assumptions, notations and definitions

Dyadic notation convention is followed here; since several variations exist in the literature, a brief overview of the version used in this paper is presented below.[3]

- *Scalars* are denoted by *script* Latin or Greek letters (e.g. a, b, c, m, α, β, γ, ψ, M, Ψ, etc.).
- *Vectors* are denoted by **bold small case** Latin or Greek letters, e.g. $\mathbf{a}$, $\mathbf{b}$, $\mathbf{c}$, $\boldsymbol{\alpha}$, $\boldsymbol{\beta}$, $\boldsymbol{\gamma}$, etc. Their components are denoted using the script version of the same symbols a_i, α_i, etc.
- *Second-order tensors* are denoted by **BOLD UPPER CASE** Latin or Greek letters, e.g. $\mathbf{A}$, $\boldsymbol{\Sigma}$. Their components are denoted using the script versions of the corresponding symbol A_{ij}, Σ_{ij}.
- *Sets* of variables are denoted by script uppercase calligraphic $\mathcal{FONT}$, e.g. $\mathcal{L}$, $\mathcal{S}$, $\mathcal{V}$.

[3] It is tacitly assumed that all boundary value problems here are set in the three-dimensional Euclidean space $\mathbb{R}^3$. A Cartesian basis is used for all field quantities, although the proposed dyadic notation allows for a straightforward extension to curvilinear coordinates.

There are two notable exceptions to the aforementioned convention; to stay consistent with usual notations in solid mechanics, we denote the spatial position of a point in the current configuration by the vector $\mathbf{x}$ and reference coordinate vector of the corresponding material point by $\mathbf{X}$. Moreover, the Cauchy stress (second order tensor) is denoted by the bold small case letter $\boldsymbol{\sigma}$.

Spatial differentiation is indicated by two nabla operators: the small nabla operator $\boldsymbol{\nabla}$ for the current configuration and the corresponding large nabla operator $\boldsymbol{\nabla}$ for the reference configuration

$$\boldsymbol{\nabla} := \frac{\partial}{\partial \mathbf{x}}, \quad \boldsymbol{\nabla} := \frac{\partial}{\partial \mathbf{X}}.$$

Dyadic notation uses a dot ($\cdot$) for the *single contraction operation*, a double dot ($:$) for the *double contraction operation*, a triple dot ($\vdots$) for the *triple contraction operation* and so on.

We consider a porous skeleton saturated with an interstitial fluid. A point of the skeleton (tissue) with reference coordinate $\mathbf{X}$ moves to its current position $\mathbf{x}$ and the resulting skeleton displacement $\mathbf{u}$ is given by $\mathbf{x} = \boldsymbol{\chi}(\mathbf{X}, t) = \mathbf{X} + \mathbf{u}(\mathbf{X}, t)$. As fluid flows through the solid, we adopt an Eulerian description of mass transfer in the continuum and make the following hypotheses:

(H-1) The thermodynamic system is composed of the solid skeleton (tissue), an impermeable surface membrane (skin), the interstitial fluid and the absorption systems. Any interaction between them is considered as internal to the system and does not contribute to the balance laws. There is no internal source of momentum or energy.[4]

(H-2) There is no mass exchange between the solid skeleton and the fluids (interstitial or absorption system).

(H-3) The skeleton moves with velocity $\mathbf{v}_s(\mathbf{x}, t) = \dot{\boldsymbol{\chi}} = \dot{\mathbf{u}}$, where the upper dot represents the material time derivative as usually defined in continuum mechanics. i.e. derivation where the material point with reference configuration coordinate $\mathbf{X}$ is held fixed.

(H-4) To each material point of the continuum we assign an *apparent density*[5] *of skeleton*[6] $m_s(\mathbf{x}, t)$, an *apparent density of interstitial fluid*[7] $m_f(\mathbf{x}, t)$, and an *apparent density of fluid in the absorption system* $m_f^a(\mathbf{x}, t)$. For the sake of simplicity, we will only consider one system of absorption: the blood vessels network. Note that there is no obstacle to the extension of this model to account for several absorption systems. In the rest of this work, the term *fluid* will systematically refer to the *interstitial fluid*. Also, any quantity with the superscript a will refer to the absorption (blood) system.

(H-5) Both the fluid and the blood contain n electrically charged chemical species of apparent densities $m_i(\mathbf{x}, t)$ and $m_i^a(\mathbf{x}, t)$ respectively,[8] $1 \leq i \leq n$, in solution in a neutral solvent ($i = 0$).

(H-6) The fluid mass flows with velocity $\mathbf{v}_f(\mathbf{x}, t)$, the blood mass flows with velocity $\mathbf{v}_f^a(\mathbf{x}, t)$.[9]

(H-7) The flux of chemical species i is the sum of its average flux $m_i \mathbf{v}_f$ – due to the average fluid motion by velocity $\mathbf{v}_f$ – plus a *relative to the average fluid mass flux* $\mathbf{j}_i(\mathbf{x}, t)$. Analogous definitions hold for the blood with a *relative to the average blood mass flux* $\mathbf{j}_i^a(\mathbf{x}, t)$.

(H-8) The fluid and blood chemical mass densities can change due to mass transfer of species between them. Chemical species i can be absorbed/released at a mass rate r_i, per unit current volume of the continuum, by/to the blood vessels.

(H-9) We do not distinguish between a solid and a fluid temperature (thermal equilibrium at miscroscale). However, we derive the set of equation in the general context of a non-isothermal framework to account for the fact that a drug can be injected at a lower temperature than the body's physiological temperature. This can impact the physics of the injection as the thawing of the drug can change its viscosity and the cooling of the tissue by the drug can also change its mechanical properties.

(H-10) Chemicals in the fluids can be charged, but the continuum must have *no net electrical charge*. We further assume that *both the fluid and the blood* are individually electrically neutral.

An immediate consequence of (H-5) is the following relation between the total and chemical species mass densities for the fluid and the blood

$$m_f(\mathbf{x}, t) = \sum_{i=0}^{n} m_i(\mathbf{x}, t), \quad m_f^a(\mathbf{x}, t) = \sum_{i=0}^{n} m_i^a(\mathbf{x}, t), \tag{2.1}$$

and from (H-6), the absolute velocities of species i in the fluid $\mathbf{v}_i$ and in the blood $\mathbf{v}_i^a$ satisfy

$$m_f \mathbf{v}_f = \sum_{i=0}^{n} m_i \mathbf{v}_i, \quad m_f^a \mathbf{v}_f^a = \sum_{i=0}^{n} m_i^a \mathbf{v}_i^a. \tag{2.2}$$

[4] The presence of the interstitial fluid and absorption systems is similar to the framework used in multiple-porosity networks (Coussy, 2004). The difference with existing poromechanics theories (single or multiple porosity networks) lies in the consistent thermodynamic treatment – that preserves objectivity and requires a minimum set of hypotheses – developed by the authors (Gil et al., 2022).

[5] Mass per unit current volume of the continuum as opposed to true density which is mass per unit volume of pure material.

[6] In *skeleton* we gather all the solid components of the tissue: collagen fibers, closed-cell foams, adipocytes, membranes...

[7] By *interstitial*, we describe the fluid that flows within the interstitial network.

[8] There is no loss of generality in assuming that the interstitial fluid and the blood are composed of the same chemical species; absence of a particular species in either fluid system is accounted for by setting the corresponding mass density to zero.

[9] Note that, in accordance with the standard works on chemical species diffusion (Gurtin, 1971; Gurtin and Vargas, 1971; Fried and Gurtin, 1999; Jabbour and Bhattacharya, 2003), the fluid (resp. blood) absolute velocity is equivalent to the mass averaged velocity of the species in the fluid (resp. blood).

According to the assumption (H-7), $\mathbf{j}_i$ and $\mathbf{j}_i^a$ the relative fluxes of species i in the fluid and the blood, are expressed in terms of the corresponding absolute velocities $\mathbf{v}_i$ and $\mathbf{v}_i^a$ and the fluid velocities $\mathbf{v}_f$ and $\mathbf{v}_f^a$

$$\mathbf{j}_i = m_i(\mathbf{v}_i - \mathbf{v}_f), \quad \mathbf{j}_i^a = m_i^a(\mathbf{v}_i^a - \mathbf{v}_f^a); \quad i = 0 \cdots n. \tag{2.3}$$

In deriving the governing equations, we write the balance laws in Section 3 in the *current configuration* on an arbitrary *material* control volume υ which *follows the motion of the solid skeleton material points*. We allow the volume υ to be crossed by a *material* discontinuity surface $\hat{\mathrm{s}}$, which can be of use to model some membranes or ligaments that may be present in the tissue and contribute as elastic discontinuities. We further assume there is no sliding or debonding of the continuum at the discontinuity surface, i.e. that $\hat{\mathrm{s}}$ deforms with the continuum following the mapping $\chi(\mathbf{X}, t)$ and the skeleton displacement and velocities are thus continuous across s

$$[\![\mathbf{x}]\!] = \mathbf{0}, \quad [\![\mathbf{v}_s]\!] = \mathbf{0}, \ \mathbf{x} \in \hat{\mathrm{s}}. \tag{2.4}$$

An important role is played in the theory by the concept of *relative* fluid $\mathbf{v}_r$ and blood $\mathbf{v}_r^a$ velocities

$$\mathbf{v}_r := \mathbf{v}_f - \mathbf{v}_s, \quad \mathbf{v}_r^a := \mathbf{v}_f^a - \mathbf{v}_s. \tag{2.5}$$

Following the introduction of the *primitive variables* m_s, m_f and m_f^a describing the state of the system, we define the *total mass density* of the continuum m_t, its *average velocity* $\mathbf{v}$ and the *mass ratios* c_s, c_f, c_f^a

$$m_t := m_s + m_f + m_f^a, \quad c_s := \frac{m_s}{m_t}, \quad c_f := \frac{m_f}{m_t}, \quad c_f^a := \frac{m_f^a}{m_t}, \quad \mathbf{v} := c_s\mathbf{v}_s + c_f\mathbf{v}_f + c_f^a\mathbf{v}_f^a. \tag{2.6}$$

Note also the identities that follow directly from the definitions (2.6)

$$m_t\mathbf{v} = m_s\mathbf{v}_s + m_f\mathbf{v}_f + m_f^a\mathbf{v}_f^a, \quad \mathbf{v} = \mathbf{v}_s + c_f\mathbf{v}_r + c_f^a\mathbf{v}_r^a, \quad c_s + c_f + c_f^a = 1. \tag{2.7}$$

It is also useful to introduce the definition of the *material time derivative*, denoted by a superposed dot for scalars $a(\mathbf{x}, t)$ and vectors $\mathbf{a}(\mathbf{x}, t)$ defined in an Eulerian description $(\mathbf{x}(\mathbf{X}, t), t)$ (derivation at $\mathbf{X}$ fixed)

$$\dot{a}(\mathbf{x}, t) := \frac{\partial a}{\partial t} + (\boldsymbol{\nabla} a)\cdot\mathbf{v}_s, \quad \dot{\mathbf{a}}(\mathbf{x}, t) := \frac{\partial \mathbf{a}}{\partial t} + (\boldsymbol{\nabla}\mathbf{a})^{\mathsf{T}}\cdot\mathbf{v}_s. \tag{2.8}$$

The *Reynolds transport theorem* is recorded here as it is repeatedly used in the following work. Consider a material control volume in the current configuration υ moving with the skeleton at speed $\mathbf{v}_s$. For any for scalar field $a(\mathbf{x}, t)$ or vector field $\mathbf{a}(\mathbf{x}, t)$, the following identities hold

$$\frac{\mathrm{d}}{\mathrm{d}t}\int_\upsilon a \,\mathrm{d}\upsilon = \int_\upsilon \left[\dot{a} + a\left(\boldsymbol{\nabla}\cdot\mathbf{v}_s\right)\right] \mathrm{d}\upsilon, \quad \frac{\mathrm{d}}{\mathrm{d}t}\int_\upsilon \mathbf{a} \,\mathrm{d}\upsilon = \int_\upsilon \left[\dot{\mathbf{a}} + \mathbf{a}\left(\boldsymbol{\nabla}\cdot\mathbf{v}_s\right)\right] \mathrm{d}\upsilon. \tag{2.9}$$

The stage is now set for the derivation of the general governing equations for the continuum modeling of the subcutaneous injection problem.

3. General principles

Using the direct approach of continuum mechanics (current configuration, arbitrary material control volume υ with boundary $\partial\upsilon$), we present here the mass conservation laws in Section 3.1. Regarding the linear momentum, angular momentum and energy balance laws respectively in Section 3.2, Section 3.3 and Section 3.4 and the entropy imbalance law in Section 3.5, we follow the methodology of the author's previous work (Gil et al., 2022) which was motivated by some inconsistencies (e.g. with objectivity) that could arise in continuum poromechanics theories, as well as the difficulty of choosing phenomenological terms for momentum and energy fluxes in mixture theories. The schematics of the boundary value problem are shown in Fig. 2.

3.1. Mass conservation

We write the mass conservation separately for the skeleton, the fluid, the blood, as well as for each one of the chemical species contained in each of the two fluid systems.

Skeleton The integral form of mass conservation for the solid skeleton is

$$\frac{\mathrm{d}}{\mathrm{d}t}\int_\upsilon m_s \,\mathrm{d}\upsilon = 0. \tag{3.1}$$

Applying to (3.1) the Reynolds transport theorem (2.9) yields the local form[10]

$$\dot{m}_s + m_s\left(\boldsymbol{\nabla}\cdot\mathbf{v}_s\right) = 0, \ \mathbf{x} \in \upsilon. \tag{3.2}$$

[10] The corresponding jump condition is automatically satisfied in view of the assumption (2.4).

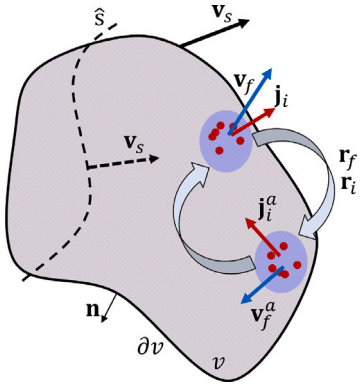

Fig. 2. Schematic of the material control volume v with boundary ∂v and discontinuity surface $\hat{\mathrm{s}}$.

(Interstitial) fluid The control volume moves with the skeleton at velocity $\mathbf{v}_s$ and the fluid flows with an absolute velocity $\mathbf{v}_f$, creating a relative flux with velocity $\mathbf{v}_r$ of fluid through the control volume boundary[11]

$$\frac{\mathrm{d}}{\mathrm{d}t}\int_v m_f\ \mathrm{d}v = -\int_{\partial v} m_f\ (\mathbf{v}_r\cdot\mathbf{n})\ \mathrm{d}a + \int_v r_f\ \mathrm{d}v, \tag{3.3}$$

where r_f is the rate of fluid mass absorption/release by the blood per unit current volume and $\mathbf{n}$ denotes the outward unit normal to ∂v, resulting with the help of (2.9) in the following local form and associated interface condition

$$\dot{m}_f + m_f\,(\boldsymbol{\nabla}\cdot\mathbf{v}_s) + \boldsymbol{\nabla}\cdot\ (m_f\mathbf{v}_r) = r_f,\ \mathbf{x}\in v,\quad \mathbf{n}\cdot[\![m_f\mathbf{v}_r]\!] = 0,\ \mathbf{x}\in\hat{\mathrm{s}}. \tag{3.4}$$

Chemical species in fluid At the border of the control volume ∂v, the mass flux of species i corresponds to the mass brought by the fluid motion, corrected by the species motion relative to the fluid. Hence, for all chemical species solved in the fluid,[12] the integral form of the mass balance reads

$$\frac{\mathrm{d}}{\mathrm{d}t}\int_v m_i\ \mathrm{d}v = -\int_{\partial v}\left[\,\mathbf{j}_i + m_i\mathbf{v}_r\right]\cdot\mathbf{n}\ \mathrm{d}a + \int_v r_i\ \mathrm{d}v,\quad 1\le i\le n. \tag{3.5}$$

The localization process yields the following governing equation and interface condition

$$\dot{m}_i + m_i\,(\boldsymbol{\nabla}\cdot\mathbf{v}_s) + \boldsymbol{\nabla}\cdot\ (\,\mathbf{j}_i + m_i\mathbf{v}_r) = r_i,\ \mathbf{x}\in v,\quad \mathbf{n}\cdot[\![\,\mathbf{j}_i + m_i\mathbf{v}_r]\!] = 0,\ \mathbf{x}\in\hat{\mathrm{s}},\quad 1\le i\le n. \tag{3.6}$$

According to (H-8), the term r_f appearing in (3.3) is the sum of the absorption rates of all the chemical species r_i, including the solvent's r_0

$$r_f = \sum_{i=0}^{n} r_i. \tag{3.7}$$

Also note that since $\mathbf{v}_f$ is the mass average velocity of all species, it follows from (H-7)

$$\sum_{i=0}^{n}\mathbf{j}_i = \mathbf{0}, \tag{3.8}$$

where $\mathbf{j}_0$ is the mass flow of the solvent, relative to the fluid motion.

Absorption system (blood) In analogy to (3.3) for the fluid flowing through the skeleton, one can write the corresponding balance for the blood flowing in the absorption system

$$\frac{\mathrm{d}}{\mathrm{d}t}\int_v m_f^a\ \mathrm{d}v = -\int_{\partial v} m_f^a\ (\mathbf{v}_r^a\cdot\mathbf{n})\ \mathrm{d}a - \int_v r_f\ \mathrm{d}v, \tag{3.9}$$

where we have already accounted for the fact that $r_f^a = -r_f$ since what is absorbed from (or released in) the interstitial fluid is released in (or absorbed from) the blood. The corresponding governing equation and interface condition are

$$\dot{m}_f^a + m_f^a\,(\boldsymbol{\nabla}\cdot\mathbf{v}_s) + \boldsymbol{\nabla}\cdot\ \left(m_f^a\mathbf{v}_r^a\right) = -r_f,\ \mathbf{x}\in v,\quad \mathbf{n}\cdot\left[\!\left[m_f^a\mathbf{v}_r^a\right]\!\right] = 0,\ \mathbf{x}\in\hat{\mathrm{s}}. \tag{3.10}$$

[11] Following the chemical transport theories (Gurtin, 1971; Gurtin and Vargas, 1971; Fried and Gurtin, 1999; Jabbour and Bhattacharya, 2003), this mass balance is exact from the mixture point of view since it is equivalent to the sum of the mass balances of all the species, including the solvent.

[12] We only write the mass balance for chemical species $i = 1,\dots,n$ in solution (not for the solvent $i = 0$) since the solvent mass balance is implicitly satisfied through (3.3).

Chemical species in blood Similarly to (3.5), and recalling that $r_i^a = -r_i$, the mass balance for the chemical species i solved in the blood yields

$$\frac{\mathrm{d}}{\mathrm{d}t}\int_{\upsilon} m_i^a \,\mathrm{d}\upsilon = -\int_{\partial\upsilon}\left[\,\mathbf{j}_i^a + m_i^a\left(\mathbf{v}_r^a\cdot\mathbf{n}\right)\right]\,\mathrm{d}a - \int_{\upsilon} r_i\,\mathrm{d}\upsilon, \quad 1\le i\le n, \tag{3.11}$$

while the localization process yields the following governing equation and interface condition

$$\dot{m}_i^a + m_i^a\left(\boldsymbol{\nabla}\cdot\mathbf{v}_s\right) + \boldsymbol{\nabla}\cdot\left(\,\mathbf{j}_i^a + m_i^a\mathbf{v}_r^a\right) = -r_i,\ \mathbf{x}\in\upsilon, \quad \mathbf{n}\cdot\left[\!\left[\,\mathbf{j}_i^a + m_i^a\mathbf{v}_r^a\right]\!\right] = 0,\ \mathbf{x}\in\hat{\mathrm{s}}, \quad 1\le i\le n. \tag{3.12}$$

Finally, from (H-7), the mass fluxes $\mathbf{j}_i^a$ satisfy a relation similar to (3.8)

$$\sum_{i=0}^{n}\mathbf{j}_i^a = \mathbf{0}. \tag{3.13}$$

3.2. Linear momentum balance

We define $\mathbf{b}$ as the *external body force* density (per unit current volume of the continuum) and the *generalized traction vector* $\mathbf{t}$ (per unit current surface area of the continuum) associated to a *generalized Cauchy stress tensor* $\boldsymbol{\sigma}$ such that $\mathbf{t} = \mathbf{n}\cdot\boldsymbol{\sigma}$. Moreover, we allow the discontinuity surface $\hat{\mathrm{s}}$ to sustain a traction.[13] Following the formalism of evolving surfaces of Gurtin and Jabbour (2002), we define $\boldsymbol{\nu}$ as the outward unit normal vector to the boundary curve, defined as the intersection $\hat{\mathrm{s}}\cap\partial\upsilon$.[14] Define $\mathbf{t}_{\hat{\mathrm{s}}}$ the *surface tension vector* applied to the boundary curve $\hat{\mathrm{s}}\cap\partial\upsilon$, associated to a *surface Cauchy stress tensor* such that $\mathbf{t}_{\hat{\mathrm{s}}} = \boldsymbol{\nu}\cdot\boldsymbol{\sigma}_{\hat{\mathrm{s}}}$. Accordingly from (2.7), the integral form of the linear momentum balance is[15]

$$\frac{\mathrm{d}}{\mathrm{d}t}\int_{\upsilon}\left(m_t\mathbf{v}\right)\,\mathrm{d}\upsilon = \frac{\mathrm{d}}{\mathrm{d}t}\int_{\upsilon}\left(m_s\mathbf{v}_s + m_f\mathbf{v}_f + m_f^a\mathbf{v}_f^a\right)\,\mathrm{d}\upsilon = \int_{\upsilon} m_t\mathbf{b}\,\mathrm{d}\upsilon + \int_{\partial\upsilon}\mathbf{t}\,\mathrm{d}a + \int_{\hat{\mathrm{s}}\cap\partial\upsilon}\mathbf{t}_{\hat{\mathrm{s}}}\,\mathrm{d}l. \tag{3.14}$$

Note that both the interstitial fluid and the blood are part of the thermodynamic system. Therefore in accordance to (H-1), all interactions are internal to the system and should not appear in the linear momentum balance.

Using (3.2), (3.4), (3.10), the pointwise form of the linear momentum governing equation and interface condition are:

$$m_t\dot{\mathbf{v}} - \boldsymbol{\nabla}\cdot\left(m_f\mathbf{v}_r + m_f^a\mathbf{v}_r^a\right)\mathbf{v} - \boldsymbol{\nabla}\cdot\boldsymbol{\sigma} - m_t\mathbf{b} = \mathbf{0},\ \mathbf{x}\in\upsilon, \quad \mathbf{n}\cdot[\![\boldsymbol{\sigma}]\!] + \boldsymbol{\nabla}_{\hat{\mathrm{s}}}\cdot\boldsymbol{\sigma}_{\hat{\mathrm{s}}} = \mathbf{0},\ \mathbf{x}\in\hat{\mathrm{s}}, \tag{3.15}$$

where $\boldsymbol{\nabla}_{\hat{\mathrm{s}}}$ denotes the surface gradient operator.

At this stage, this work follows the framework of Gil et al. (2022) and differs from most approaches where momentum fluxes through the boundary $\partial\upsilon$ would have been phenomenologically postulated, such as a decomposition of momentum brought by the interstitial fluid, chemical species, just to cite a few. With this approach, we avoid any phenomenological bias brought at this stage of the derivation.

3.3. Angular momentum balance

In accordance with (3.14), the balance of angular momentum of a control volume υ takes the form

$$\frac{\mathrm{d}}{\mathrm{d}t}\int_{\upsilon}\mathbf{x}\wedge\left(m_t\mathbf{v}\right)\,\mathrm{d}\upsilon = \int_{\upsilon} m_t\mathbf{x}\wedge\mathbf{b}\,\mathrm{d}\upsilon + \int_{\partial\upsilon}\mathbf{x}\wedge\mathbf{t}\,\mathrm{d}a + \int_{\hat{\mathrm{s}}\cap\partial\upsilon}\mathbf{x}\wedge\mathbf{t}_{\hat{\mathrm{s}}}\,\mathrm{d}l. \tag{3.16}$$

Taking the pointwise form and substituting (3.2), (3.4), (3.10) and (3.15) gives the following condition[16]

$$\boldsymbol{\sigma} + \left(m_f\mathbf{v}_r + m_f^a\mathbf{v}_r^a\right)\mathbf{v}_s = \left[\boldsymbol{\sigma} + \left(m_f\mathbf{v}_r + m_f^a\mathbf{v}_r^a\right)\mathbf{v}_s\right]^{\mathsf{T}},\ \mathbf{x}\in\upsilon, \quad \boldsymbol{\sigma}_{\hat{\mathrm{s}}} = \boldsymbol{\sigma}_{\hat{\mathrm{s}}}^{\mathsf{T}},\ \mathbf{x}\in\hat{\mathrm{s}}. \tag{3.17}$$

3.4. Energy balance

The total energy of the control volume υ can usually be decomposed into the sum of its internal energy and its kinetic energy. In this work, we follow instead the approach developed in Gil et al. (2022) to avoid inconsistencies with thermodynamics and objectivity and introduce a total energy density ϵ, resulting in an energy $\int_{\upsilon}\epsilon\,\mathrm{d}\upsilon$ of the control volume, plus the surface energy density $\epsilon_{\hat{\mathrm{s}}}$ which contributes $\int_{\hat{\mathrm{s}}\cap\upsilon}\epsilon_{\hat{\mathrm{s}}}\,\mathrm{d}a$ to the total energy. Since $\mathbf{b}$ is assumed uniform and identical for all continua (e.g. gravity), we write its power expenditure on the control volume as $\int_{\upsilon} m_t\mathbf{v}\cdot\mathbf{b}\,\mathrm{d}\upsilon$.

The surface contribution to the energy is associated to a directional flux vector $\mathbf{h}$ of the form $-\int_{\partial\upsilon}\mathbf{h}\cdot\mathbf{n}\,\mathrm{d}a$. Similarly to the linear momentum balance, this work differs from most approaches where energy fluxes through the boundary $\partial\upsilon$ would have been phenomenologically postulated such as a decomposition of internal and kinetic energies brought by the interstitial fluid, chemical species, the absorption system, as well as work expenditures of the solid, fluid and even sometimes chemical constituents. With this

[13] Such discontinuity surface can be used to model the contribution of elastic membranes, such as surface-covering skin.

[14] The vector $\boldsymbol{\nu}$ is tangent to the surface $\hat{\mathrm{s}}$ and normal to the curve $\hat{\mathrm{s}}\cap\partial\upsilon$, but is not necessarily normal to $\partial\upsilon$.

[15] Following Noll (1974), we make a *type-I* constitutive assumption, which corresponds to the standard inertial form of the linear momentum for the control volume.

[16] No further restriction is obtained from the interface/jump relations.

approach, we avoid any phenomenological bias brought at this stage of the derivation as well as potential inconsistencies with the objectivity principle. Instead, the use an unknown flux $\mathbf{h}$ is enough to derive the thermodynamic restrictions: the thermodynamics principles and mathematics alone will allow to identify the unique form of $\mathbf{h}$ in an isotropic framework (Gil et al., 2022).

Due the presence of a surface energy $\epsilon_{\hat{\mathrm{s}}}$,[17] we must add the corresponding discontinuity surface power input $\int_{\partial\upsilon\cap\hat{\mathrm{s}}} \boldsymbol{\nu}\cdot\mathbf{t}_{\hat{\mathrm{s}}}\ \mathrm{d}l$. Introducing the external energy source density q, the integral form of the energy balance is then

$$\frac{\mathrm{d}}{\mathrm{d}t}\left[\int_{\upsilon}\epsilon\ \mathrm{d}\upsilon+\int_{\hat{\mathrm{s}}\cap\upsilon}\epsilon_{\hat{\mathrm{s}}}\ \mathrm{d}a\right]=-\int_{\partial\upsilon}\mathbf{h}\cdot\mathbf{n}da+\int_{\upsilon}m_t\mathbf{v}\cdot\mathbf{b}\ \mathrm{d}\upsilon+\int_{\upsilon}q\ \mathrm{d}\upsilon+\int_{\partial\upsilon\cap\hat{\mathrm{s}}}\boldsymbol{\nu}\cdot\mathbf{t}_{\hat{\mathrm{s}}}\ \mathrm{d}l. \tag{3.18}$$

The governing equations and corresponding interface conditions resulting from (3.18) are

$$\dot{\epsilon}+\epsilon\ \boldsymbol{\nabla}\cdot\mathbf{v}_s-m_t\mathbf{v}\cdot\mathbf{b}-q+\boldsymbol{\nabla}\cdot\mathbf{h}=0,\ \mathbf{x}\in\upsilon,\quad \mathbf{n}\cdot[\![\mathbf{h}]\!]+\dot{\epsilon}_{\hat{\mathrm{s}}}-\boldsymbol{\nabla}_{\hat{\mathrm{s}}}\cdot\left(\boldsymbol{\sigma}_{\hat{\mathrm{s}}}\cdot\mathbf{v}_s\right)=0,\ \mathbf{x}\in\hat{\mathrm{s}}. \tag{3.19}$$

Using (3.15) to eliminate the external body force $\mathbf{b}$ in $(3.19)_1$, one obtains an alternative expression

$$\dot{\epsilon}-m_t\mathbf{v}\cdot\dot{\mathbf{v}}+\epsilon\boldsymbol{\nabla}\cdot\mathbf{v}_s+\boldsymbol{\nabla}\cdot\left(m_f\mathbf{v}_r+m_f^a\mathbf{v}_r^a\right)\mathbf{v}^2+(\boldsymbol{\nabla}\cdot\boldsymbol{\sigma})\cdot\mathbf{v}-q+\boldsymbol{\nabla}\cdot\mathbf{h}=0,\ \mathbf{x}\in\upsilon. \tag{3.20}$$

3.5. Entropy imbalance

Let η be the volume entropy density of the continuum and $\eta_{\hat{\mathrm{s}}}$ the surface entropy density associated to $\hat{\mathrm{s}}$. Denote by θ the absolute temperature of the continuum, assumed uniform through all its constituents (solid, fluid, blood) by (H-9). The second law of thermodynamics (Clausius–Duhem inequality) gives

$$\frac{\mathrm{d}}{\mathrm{d}t}\left[\int_{\upsilon}\eta\ \mathrm{d}\upsilon+\int_{\upsilon\cap\hat{\mathrm{s}}}\eta_{\hat{\mathrm{s}}}da\right]\geq-\int_{\partial\upsilon}\frac{\mathbf{q}}{\theta}\cdot\mathbf{n}\ \mathrm{d}a+\int_{\upsilon}\frac{q}{\theta}\ \mathrm{d}\upsilon. \tag{3.21}$$

In (3.21), we follow again the formalism of Gil et al. (2022) by using a single flux vector $\mathbf{q}$ and the external energy source q, thus explaining the entropy contribution of q/θ with the same source q as in the energy balance (3.18). Following the same approach as for the energy balance, there is no need to split the entropy flux in postulated phenomenological terms.

In local form, the entropy inequality and the associated interface condition are

$$\dot{\eta}+\eta\left(\boldsymbol{\nabla}\cdot\mathbf{v}_s\right)+\frac{\boldsymbol{\nabla}\cdot\mathbf{q}}{\theta}-\frac{\mathbf{q}\cdot(\boldsymbol{\nabla}\theta)}{\theta^2}-\frac{q}{\theta}\geq0,\ \mathbf{x}\in\upsilon,\quad \mathbf{n}\cdot\left[\!\left[\frac{\mathbf{q}}{\theta}\right]\!\right]+\dot{\eta}_{\hat{\mathrm{s}}}\geq0,\ \mathbf{x}\in\hat{\mathrm{s}}. \tag{3.22}$$

Instead of working with the total volume ϵ and surface $\epsilon_{\hat{\mathrm{s}}}$ energy densities, it is more convenient to introduce their *free-energy* counterparts ψ and $\psi_{\hat{\mathrm{s}}}$

$$\psi:=\epsilon-\frac{m_t}{2}\mathbf{v}^2-\theta\eta,\quad \psi_{\hat{\mathrm{s}}}:=\epsilon_{\hat{\mathrm{s}}}-\theta\eta_{\hat{\mathrm{s}}}, \tag{3.23}$$

and upon combining (3.23) with (3.20) and (3.22) to eliminate the external energy source q and assuming a continuous temperature, i.e. $[\![\theta]\!]=0,\ \mathbf{x}\in\hat{\mathrm{s}}$, we obtain the following governing equations and corresponding interface conditions

$$\begin{aligned}&-\dot{\psi}-\eta\dot{\theta}-\psi\boldsymbol{\nabla}\cdot\mathbf{v}_s-\boldsymbol{\nabla}\cdot\left(m_f\mathbf{v}_r+m_f^a\mathbf{v}_r^a\right)\frac{\mathbf{v}^2}{2}-(\boldsymbol{\nabla}\cdot\boldsymbol{\sigma})\cdot\mathbf{v}-\boldsymbol{\nabla}\cdot\ (\mathbf{h}-\mathbf{q})-\frac{\mathbf{q}}{\theta}\cdot\boldsymbol{\nabla}\theta\geq0,\ \mathbf{x}\in\upsilon,\\&-\dot{\psi}_{\hat{\mathrm{s}}}-\eta_{\hat{\mathrm{s}}}\dot{\theta}+\boldsymbol{\nabla}_{\hat{\mathrm{s}}}\cdot\left(\boldsymbol{\sigma}_{\hat{\mathrm{s}}}\cdot\mathbf{v}_s\right)-\mathbf{n}\cdot[\![\mathbf{h}-\mathbf{q}]\!]\geq0,\ \mathbf{x}\in\hat{\mathrm{s}},\end{aligned} \tag{3.24}$$

thus concluding the presentation of the general balance/imbalance principles in integral and local form.

4. Constitutive restrictions

In this section, we apply the principles of the thermodynamics of nonequilibrium processes in order to derive constitutive restrictions from the inequality (3.24), based on the Coleman–Noll procedure which is presented in Section 4.1. The details of the derivation following the approach of Gil et al. (2022) are reported in Appendix A and the associated conclusions are gathered in Section 4.2.

4.1. Framework of the coleman–noll procedure

To complete the set of governing equations derived from the general principles, we need to specify the expressions of ψ, $\psi_{\hat{\mathrm{s}}}$, η, $\eta_{\hat{\mathrm{s}}}$, $\mathbf{q}$, $\mathbf{v}_r$, $\mathbf{v}_r^a$, $\boldsymbol{\sigma}$, $\boldsymbol{\sigma}_{\hat{\mathrm{s}}}$, $\mathbf{j}_i$, r_i, $\mathbf{j}_i^a$ and $\mathbf{h}$. We follow the methodology exposed in Gil et al. (2022) to ensure consistency with the principles

[17] We assume there is no mass density, no fluid and no chemical charge carried by the membrane and that its contribution is only mechanical with no kinetic terms. For an extension to a model with such couplings see Gurtin and Jabbour (2002).

of material frame indifference in the derivation of constitutive restrictions. We *postulate* here the following set of thermodynamic variables[18] with the assumption of homogeneous[19] material

$$\mathcal{L} := \Big\{ \overbrace{\underbrace{m_s, m_f, m_f^a, \{m_i\}_1^n, \{m_i^a\}_1^n, \theta}_{\mathcal{S}}, \overbrace{\nabla m_s, \nabla m_f, \nabla m_f^a, \{\nabla m_i\}_1^n, \{\nabla m_i^a\}_1^n, \nabla\theta}^{\mathcal{G}}, \mathbf{F}, \nabla\mathbf{F}}^{\mathcal{L}_O} \Big\} \cup \{\mathbf{v}_s\}, \tag{4.1}$$

where $\mathbf{F} = (\nabla\boldsymbol{\chi})^{\intercal}$ is the continuum's deformation gradient, $\mathcal{S}$ is the set of scalar thermodynamic variables and $\mathcal{G}$ the set of the first spatial gradients of $\mathcal{S}$. We henceforth make a distinction between the set $\mathcal{L}_O$ and the skeleton velocity field $\mathbf{v}_s$. It can be shown (Gil et al., 2022) that an objective quantity cannot depend on $\mathbf{v}_s$ and hence only the set $\mathcal{L}_O$ can be used to describe objective fields. The thermodynamic state of the continuum is thus defined by the following fields

$$\psi(\mathcal{L}),\ \psi_{\hat{\mathcal{S}}}(\mathcal{L}),\ \eta(\mathcal{L}),\ \eta_{\hat{\mathcal{S}}}(\mathcal{L}),\ \boldsymbol{\sigma}(\mathcal{L}),\ \boldsymbol{\sigma}_{\hat{\mathcal{S}}}(\mathcal{L}),\ \mathbf{q}(\mathcal{L}),\ \mathbf{v}_r(\mathcal{L}),\ \mathbf{v}_r^a(\mathcal{L}),\ \{\mathbf{j}_i(\mathcal{L})\}_1^n,\ \{\mathbf{j}_i^a(\mathcal{L})\}_1^n,\ \{r_i(\mathcal{L})\}_0^n,\ \mathbf{h}(\mathcal{L}). \tag{4.2}$$

Note that the above list includes the relative fluid velocities $\mathbf{v}_r$ and $\mathbf{v}_r^a$ which are treated as a constitutive variables; different alternatives where these fields are primitive quantities can be explored, as described in Gil et al. (2022). In defining the set of thermodynamic variables (4.1), we chose not to introduce any constraint such as incompressibility or electroneutrality. The system's (small, but physically realistic) deviation from such constrained states will be accounted for by using appropriate penalty energies. Nevertheless, in the case of an analytical solving in simplified frameworks an alternative formulation involving Lagrange multipliers can be more tractable (see e.g. Section 7 for the use of a Lagrange multiplier to enforce electroneutrality). Some of the quantities in (4.2) can still be linked to inertial effects, hence their potential dependence on $\mathbf{v}_s$, which is not an admissible dependence for objective fields. In the forthcoming derivations, when a term of (4.2) is required to be objective, it will depend on the objective restriction of $\mathcal{L}$, denoted $\mathcal{L}_O$, as indicated in (4.1).

Applying the chain rule of time derivation to $\dot{\psi}$ and after substitution of mass balances (3.2), (3.4), (3.6), (3.10), (3.12) in the free-energy imbalance (3.24), time derivatives and higher order spatial gradients of $\mathcal{L}$ will appear. In order to apply the Coleman–Noll procedure, one must identify the terms that can have arbitrarily assigned values for a given set $\mathcal{L}$. We denote the set of these arbitrarily assignable quantities $\mathcal{L}^{\star}$[20] Gil et al. (2022)

$$\mathcal{L}^{\star} = \Big\{ \underbrace{\dot{\theta}, \dot{\overbrace{\nabla m_s}}, \dot{\overbrace{\nabla m_f}}, \dot{\overbrace{\nabla m_f^a}}, \dot{\overbrace{\{\nabla m_i\}_1^n}}, \dot{\overbrace{\{\nabla m_i^a\}_1^n}}, \dot{\overbrace{\nabla\theta}}, \dot{\mathbf{F}}, \dot{\mathbf{v}}_s, \dot{\overbrace{\nabla\mathbf{F}}}}_{\text{Time rates}}, \underbrace{\nabla^2 m_s, \nabla^2 m_f, \nabla^2 m_f^a, \{\nabla^2 m_i\}_1^n, \{\nabla^2 m_i^a\}_1^n, \nabla^2\theta, \nabla^2\mathbf{F}}_{\text{Second order gradients}} \Big\}, \tag{4.3}$$

where all the fields of (4.3) are independent[21] and the symbol $\dot{\overbrace{\ \ }}$ is used to illustrate that the "dot" operator applies to the whole field.

The Coleman–Noll procedure consists in finding the restrictions on the fields (4.2) that ensure that the inequality (3.24) is satisfied for any arbitrary values of the fields in (4.3) (Coleman and Noll, 1963). For the sake of clarity, the full derivation following the procedure introduced by Gil et al. (2022) is reported in Appendix A.

4.2. Results of the application of nonequilibrium thermodynamics principles

Following the derivation of Appendix A, the necessary constitutive restrictions in the volume are gathered in (4.4) below

$$\begin{aligned}
&\frac{\partial\psi}{\partial\nabla m_s} = \frac{\partial\psi}{\partial\nabla m_f} = \frac{\partial\psi}{\partial\nabla m_f^a} = \mathbf{0}, \quad \frac{\partial\psi}{\partial\nabla m_i} = \frac{\partial\psi}{\partial\nabla m_i^a} = \mathbf{0},\ 1 \le i \le n,\\
&\eta = -\frac{\partial\psi}{\partial\theta}, \quad \frac{\partial\psi}{\partial\nabla\theta} = \mathbf{0}, \quad \frac{\partial\psi}{\partial\nabla\mathbf{F}} = \mathbf{0}, \quad \frac{\partial\psi}{\partial\mathbf{v}_s} = \mathbf{0},\\
&\boldsymbol{\sigma} = 2\mathbf{B}\cdot\frac{\partial\psi}{\partial\mathbf{B}} + \left(\psi - m_s\mu_s - m_f\mu_f - m_f^a\mu_f^a - \sum_{i=1}^{n}\left\{m_i\mu_i + m_i^a\mu_i^a\right\}\right)\mathbf{I} - \left(m_f\mathbf{v}_r + m_f^a\mathbf{v}_r^a\right)\mathbf{v},
\end{aligned} \tag{4.4}$$

[18] This approach is a generalization of the procedure proposed by Coleman and Noll (1963) and complemented by Müller (1967, 1968), Gurtin (1971), Gurtin and Vargas (1971) and Truesdell and Noll (1992).

[19] This assumption allows to drop the dependence on χ.

[20] Note that the set (4.3) is not a new postulated set of variables but these time derivative terms and spatial gradients appear in (3.24) when applying the chain rule of time derivation.

[21] In the following work $\nabla\mathbf{v}_s$ will be used when convenient instead of $\dot{\mathbf{F}}$ as the independent time rate variable.

together with a unique expression found for the unknown flux $\mathbf{h}$ in the case of an *isotropic* material

$$\begin{aligned}\mathbf{h} = \quad & \mathbf{q} + \underbrace{\frac{\mathbf{v}^2}{2}\left(m_f\mathbf{v}_r + m_f^a\mathbf{v}_r^a\right)}_{①} - \underbrace{\left[\boldsymbol{\sigma} + \left(m_f\mathbf{v}_r + m_f^a\mathbf{v}_r^a\right)\mathbf{v}\right]\cdot\mathbf{v}_s}_{②} \\ & + \underbrace{\left(m_f\mu_f + \sum_{i=1}^{n} m_i\mu_i\right)\mathbf{v}_r}_{③} + \underbrace{\sum_{i=1}^{n}\mu_i\mathbf{j}_i}_{④} + \underbrace{\left(m_f^a\mu_f^a + \sum_{i=1}^{n} m_i^a\mu_i^a\right)\mathbf{v}_r^a}_{⑤} + \underbrace{\sum_{i=1}^{n}\mu_i^a\mathbf{j}_i^a}_{⑥}.\end{aligned} \tag{4.5}$$

For the sake of simplicity in the subsequent derivations, the *relative chemical potentials* were introduced in (4.4) and (4.5) as a renaming such that

$$\mu_s(\mathcal{L}) := \frac{\partial\psi}{\partial m_s},\ \mu_f(\mathcal{L}) := \frac{\partial\psi}{\partial m_f},\ \mu_f^a(\mathcal{L}) := \frac{\partial\psi}{\partial m_f^a},\quad \mu_i(\mathcal{L}) := \frac{\partial\psi}{\partial m_i},\ \mu_i^a(\mathcal{L}) := \frac{\partial\psi}{\partial m_i^a},\ 1\le i\le n, \tag{4.6}$$

and also the *absolute chemical potentials* as[22]

$$\tilde{\mu}_0(\mathcal{L}) := \mu_f,\ \tilde{\mu}_0^a(\mathcal{L}) := \mu_f^a,\quad \tilde{\mu}_i(\mathcal{L}) := \mu_i + \mu_f,\ \tilde{\mu}_i^a(\mathcal{L}) := \mu_i^a + \mu_f^a,\ 1\le i\le n. \tag{4.7}$$

Note that in this work, the *chemical potentials are introduced as a renaming of variables* as also proposed by Gurtin (1971) and Gurtin and Vargas (1971). Since they were not introduced as primitive variables, they do not come from constitutive restrictions as it is usually the case (see e.g. Fried and Gurtin (1999), Gurtin et al. (2010), Chester and Anand (2011), Gajo and Loret (2007), Hong et al. (2008) and Loret and Simões (2004)). This notation allows for easy manipulation of these partial derivatives in the calculations and is consistent with the common definition of chemical potential as the derivative of the free energy with respect to concentrations or densities (depending on whether the energy is expressed per unit volume or per unit mass).

An important result to note in (4.4) and (4.5) is the constitutive restrictions derived for the stress tensor $\boldsymbol{\sigma}$ and the flux $\mathbf{h}$ which where introduced in Sections 3.2 and 3.4 following the general framework of Gil et al. (2022). The only possible energy fluxes and power expenditures terms naturally appear in the expression of $\mathbf{h}$ without any phenomenological assumption at the stage of the energy balance. One can see in ① the form of the kinetic energy flux with only a contribution of the averaged velocity conveyed by the relative fluid velocities.[23] The terms ③ and ⑤ represent the internal energy fluxes brought by the interstitial and absorption fluids while the terms ④ and ⑥ show the contribution of the diffusion of the chemical species with respect to the fluids.

Moreover, the general stress tensor expression contains a momentum flux term and one can also identify the following elastic stress tensor for easier manipulation of the coming calculation and identification of the elastic power expenditure ②

$$\boldsymbol{\sigma}^e := 2\mathbf{B}\cdot\frac{\partial\psi}{\partial\mathbf{B}} + \left(\psi - m_s\mu_s - m_f\mu_f - m_f^a\mu_f^a - \sum_{i=1}^{n}\left\{m_i\mu_i + m_i^a\mu_i^a\right\}\right)\mathbf{I} = \boldsymbol{\sigma} + \left(m_f\mathbf{v}_r + m_f^a\mathbf{v}_r^a\right)\mathbf{v}. \tag{4.8}$$

The remaining terms in the entropy imbalance represent *dissipation* D of the system

$$\begin{aligned}D(\mathcal{L}_O) := \ & -\frac{\mathbf{q}}{\theta}\cdot\boldsymbol{\nabla}\theta - \mathbf{v}_r\cdot\left[c_f\boldsymbol{\nabla}\cdot\boldsymbol{\sigma}^e + m_f\boldsymbol{\nabla}\mu_f + \sum_{i=1}^{n} m_i\boldsymbol{\nabla}\mu_i\right] - \sum_{i=1}^{n}\mathbf{j}_i\cdot\boldsymbol{\nabla}\mu_i \\ & -\mathbf{v}_r^a\cdot\left[c_f^a\boldsymbol{\nabla}\cdot\boldsymbol{\sigma}^e + m_f^a\boldsymbol{\nabla}\mu_f^a + \sum_{i=1}^{n} m_i^a\boldsymbol{\nabla}\mu_i^a\right] - \sum_{i=1}^{n}\mathbf{j}_i^a\cdot\boldsymbol{\nabla}\mu_i^a - \sum_{i=0}^{n} r_i\left(\tilde{\mu}_i - \tilde{\mu}_i{}^a\right) \ge 0.\end{aligned} \tag{4.9}$$

[22] Here, we follow the terminology used by Gurtin and Vargas (1971) and Fried and Gurtin (1999). Indeed, our expression of μ_i corresponds to the definition of the *relative chemical potential* in their work.

[23] Note that at the stage of the energy balance (3.18), one could have postulated many different forms of the kinetic energy flux involving kinetic energies of fluids or chemical species extrapolated from the microscopic phenomenology (see section 4.3.3 of Gil et al. (2022)). This current approach allowed to converge to a single form, compliant with the objectivity principle at the macroscopic scale.

The next steps of the derivation of constitutive restrictions in the volume in Appendix A give the following expressions of $\mathbf{q}$, $\mathbf{v}_r$, $\mathbf{v}_r^a$, $\mathbf{j}_i$, $\mathbf{j}_i^a$ and r_i, at first order close to the equilibrium state

$$\begin{aligned}
\mathbf{q} &= -\mathbf{K}_{\theta,\theta}\cdot\nabla\theta - \mathbf{K}_{\theta,p}\cdot\nabla p - \mathbf{K}_{\theta,p^a}\cdot\nabla p^a - \sum_{j=1}^{n}\left\{\mathbf{K}_{\theta,j}\cdot\nabla\mu_j + \mathbf{K}_{\theta,j^a}\cdot\nabla\mu_j^a\right\},\\
\mathbf{v}_r &= -\mathbf{K}_{f,\theta}\cdot\nabla\theta - \mathbf{K}_{f,p}\cdot\nabla p - \mathbf{K}_{f,p^a}\cdot\nabla p^a - \sum_{j=1}^{n}\left\{\mathbf{K}_{f,j}\cdot\nabla\mu_j + \mathbf{K}_{f,j^a}\cdot\nabla\mu_j^a\right\},\\
\mathbf{v}_r^a &= -\mathbf{K}_{f^a,\theta}\cdot\nabla\theta - \mathbf{K}_{f^a,p}\cdot\nabla p - \mathbf{K}_{f^a,p^a}\cdot\nabla p^a - \sum_{j=1}^{n}\left\{\mathbf{K}_{f^a,j}\cdot\nabla\mu_j + \mathbf{K}_{f^a,j^a}\cdot\nabla\mu_j^a\right\},\\
\mathbf{j}_i &= -\mathbf{K}_{i,\theta}\cdot\nabla\theta - \mathbf{K}_{i,p}\cdot\nabla p - \mathbf{K}_{i,p^a}\cdot\nabla p^a - \sum_{j=1}^{n}\left\{\mathbf{K}_{i,j}\cdot\nabla\mu_j + \mathbf{K}_{i,j^a}\cdot\nabla\mu_j^a\right\},\ 1\le i\le n,\\
\mathbf{j}_i^a &= -\mathbf{K}_{i^a,\theta}\cdot\nabla\theta - \mathbf{K}_{i^a,p}\cdot\nabla p - \mathbf{K}_{i^a,p^a}\cdot\nabla p^a - \sum_{j=1}^{n}\left\{\mathbf{K}_{i^a,j}\cdot\nabla\mu_j + \mathbf{K}_{i^a,j^a}\cdot\nabla\mu_j^a\right\},\ 1\le i\le n,\\
r_i &= -\sum_{j=0}^{n}\mathsf{R}_{i,j}\left[\tilde{\mu}_j - \tilde{\mu}_j{}^a - \left(\tilde{\mu}_j{}^e - \tilde{\mu}_j{}^{a,e}\right)\right],\ 1\le i\le n.
\end{aligned}\tag{4.10}$$

where the *pressure gradient-like terms* ∇p and ∇p^a were introduced – by abuse of notation since no pressure is defined here – to allow comparison with poro-mechanics literature[24]

$$\nabla p := c_f\nabla\cdot\boldsymbol{\sigma}^e + m_f\nabla\mu_f + \sum_{i=1}^{n} m_i\nabla\mu_i,\quad \nabla p^a := c_f^a\nabla\cdot\boldsymbol{\sigma}^e + m_f^a\nabla\mu_f^a + \sum_{i=1}^{n} m_i^a\nabla\mu_i^a.\tag{4.11}$$

The second order tensors $\mathbf{K}_{\dots}$ appearing in (4.10) are objective functions of $\mathcal{L}_O^h := \{\mathcal{S},\mathbf{0},\mathbf{B},\mathbf{0}\}$ as are the scalar coefficients $\mathsf{R}_{i,j}$. The direct application of representation theorems (Truesdell and Noll, 1992) implies that they must have the following form

$$\mathbf{K}_{\dots} = k_{\dots,0}\mathbf{I} + k_{\dots,1}\mathbf{B} + k_{\dots,2}\mathbf{B}^2\tag{4.12}$$

where $k_{\dots,J}$ (with $J=0,1,2$), are scalar functions of $\mathcal{L}_O^h$. Finally, from (4.10), the positivity of the dissipation (4.9) also implies that the matrix

$$\begin{bmatrix}
\mathbf{K}_{\theta,\theta} & \mathbf{K}_{\theta,p} & \mathbf{K}_{\theta,p^a} & \mathbf{K}_{\theta,1} & .. & \mathbf{K}_{\theta,n} & \mathbf{K}_{\theta,1^a} & .. & \mathbf{K}_{\theta,n^a} & \mathbf{0}\\
\mathbf{K}_{f,\theta} & \mathbf{K}_{f,p} & \mathbf{K}_{f,p^a} & \mathbf{K}_{f,1} & .. & \mathbf{K}_{f,n} & \mathbf{K}_{f,1^a} & .. & \mathbf{K}_{f,n^a} & \mathbf{0}\\
\mathbf{K}_{f^a,\theta} & \mathbf{K}_{f^a,p} & \mathbf{K}_{f^a,p^a} & \mathbf{K}_{f^a,1} & .. & \mathbf{K}_{f^a,n} & \mathbf{K}_{f^a,1^a} & .. & \mathbf{K}_{f^a,n^a} & \mathbf{0}\\
\mathbf{K}_{1,\theta} & \mathbf{K}_{1,p} & \mathbf{K}_{1,p^a} & \mathbf{K}_{1,1} & .. & \mathbf{K}_{1,n} & \mathbf{K}_{1,1^a} & .. & \mathbf{K}_{1,n^a} & \mathbf{0}\\
\mathbf{K}_{1^a,\theta} & \mathbf{K}_{1^a,p} & \mathbf{K}_{1^a,p^a} & \mathbf{K}_{1^a,1} & .. & \mathbf{K}_{1^a,n} & \mathbf{K}_{1^a,1^a} & .. & \mathbf{K}_{1^a,n^a} & \mathbf{0}\\
: & : & : & : & : & : & : & : & : & :\\
\mathbf{K}_{n,\theta} & \mathbf{K}_{n,p} & \mathbf{K}_{n,p^a} & \mathbf{K}_{n,1} & .. & \mathbf{K}_{n,n} & \mathbf{K}_{n,1^a} & .. & \mathbf{K}_{n,n^a} & \mathbf{0}\\
\mathbf{K}_{n^a,\theta} & \mathbf{K}_{n^a,p} & \mathbf{K}_{n^a,p^a} & \mathbf{K}_{n^a,1} & .. & \mathbf{K}_{n^a,n} & \mathbf{K}_{n^a,1^a} & .. & \mathbf{K}_{n^a,n^a} & \mathbf{0}\\
\mathbf{0} & \mathbf{0} & \mathbf{0} & \mathbf{0} & \mathbf{0} & \mathbf{0} & \mathbf{0} & \mathbf{0} & \mathbf{0} & \left(\mathsf{R}_{i,j}\right)_{\{1,n\}^2}
\end{bmatrix}\tag{4.13}$$

is positive semi-definite.

Moreover, as shown in Appendix A, the following restriction holds

$$\sum_{i=0}^{n}\mathsf{R}_{i,j}\left(\tilde{\mu}_i{}^e - \tilde{\mu}_i{}^{a,e}\right) = 0,\ 0\le j\le n,\tag{4.14}$$

which means that, in case $\left(\mathsf{R}_{i,j}\right)_{\{1,n\}^2}$ is symmetric, $(4.10)_6$ becomes

$$r_i = -\sum_{j=0}^{n}\mathsf{R}_{i,j}\left(\tilde{\mu}_j - \tilde{\mu}_j{}^a\right),\ 1\le i\le n.\tag{4.15}$$

Finally, the constitutive restrictions on the surface $\mathbf{x}\in\hat{\mathsf{s}}$ derived in Appendix A are

$$\eta_{\hat{\mathsf{s}}} = -\frac{\partial\psi_{\hat{\mathsf{s}}}}{\partial\theta},\quad \boldsymbol{\sigma}_{\hat{\mathsf{s}}} = \left(\frac{\partial\psi_{\hat{\mathsf{s}}}}{\partial\mathbf{F}_{\hat{\mathsf{s}}}}\cdot\mathbf{F}_{\hat{\mathsf{s}}}^{\mathsf{T}}\right)^{\mathsf{T}},\tag{4.16}$$

together with the jump conditions

$$\left[\!\left[\mu_f + \left(c_f\mathbf{v}_r\right)^2/2\right]\!\right] = 0,\quad \left[\!\left[\mu_f^a + \left(c_f^a\mathbf{v}_r^a\right)^2/2\right]\!\right] = 0,\quad \left[\!\left[\mu_i\right]\!\right] = 0,\quad \left[\!\left[\mu_i^a\right]\!\right] = 0,\ 1\le i\le n.\tag{4.17}$$

The continuity conditions (4.17) show an important feature of the boundary conditions for a chemoporomechanical model. Notice that the continuity applies for a dynamic-like chemical potential of the fluid. In case of an incompressible fluid, the chemical

[24] In the dissipation Eq. (4.9) the term $c_f\nabla\cdot\boldsymbol{\sigma}^e + m_f\nabla\mu_f + \sum_{i=1}^{n} m_i\nabla\mu_i$ appears as the conjugate of $\mathbf{v}_r$ and the term $c_f^a\nabla\cdot\boldsymbol{\sigma}^e + m_f^a\nabla\mu_f^a + \sum_{i=1}^{n} m_i^a\nabla\mu_i^a$ appears as the conjugate of $\mathbf{v}_r^a$.

potential is usually equivalent to pressure divided by the mass density of the fluid. Hence (4.17) looks like the continuity of a Bernoulli quantity.

Regarding the chemical species, one can note that the continuity condition applies to the relative chemical potentials and not to the species concentrations. This is a very important feature since, in the case of the presence of fixed charges in the continuum, the species concentrations cannot be continuous at the boundary, but the energies are.

The continuity conditions (4.17) are also important when solving boundary value problems, since it will dictate our choice of problem unknowns. For instance, when considering the diffusion of chemical species, the easiest choice will be to work with the chemical potentials as unknowns (Loix et al., 2008; Sun et al., 1999), instead of the chemical species concentrations, especially when it comes to applying Dirichlet-like boundary conditions in an FEM code.

5. Constitutive choices

The set of governing equations and interface conditions derived in Section 3 and the constitutive restrictions derived in Section 4 are given in their most general form. In order to guide the modeling of subcutaneous injections, we proceed to the following manipulations on the previously derived relations.

5.1. Lagrangian free energy

The application of the proposed general theory is aimed at the solution of boundary value problems. Given the importance of finite strains, the predominantly numerical solution methods are more easily applied when a Lagrangian formulation of the problem is used, thus motivating the following version, based on the introduction of the reference – i.e. per unit undeformed volume – mass densities M_s, M_f, M_f^a, M_i, M_i^a and energy density Ψ

$$\begin{aligned} &M_s := \mathrm{J}m_s,\ M_f := \mathrm{J}m_f,\ M_f^a := \mathrm{J}m_f^a, \quad M_i := \mathrm{J}m_i,\ M_i^a := \mathrm{J}m_i^a,\ 1 \le i \le n, \\ &\Psi\left(M_s, M_f, M_f^a, \{M_i\}_1^n, \{M_i^a\}_1^n, \theta, \mathcal{I}(\mathbf{B})\right) := \mathrm{J}\psi, \end{aligned} \tag{5.1}$$

where $\mathrm{J} := \det \mathbf{F}$ is the determinant of the deformation gradient of the skeleton (Coussy, 2004). A direct consequence of the above definitions and (4.6) and (4.8) are the following expressions for the relative chemical potentials, entropy and for the elastic stress tensor[25]

$$\begin{aligned} &\mu_s = \frac{\partial \Psi}{\partial M_s},\ \mu_f = \frac{\partial \Psi}{\partial M_f},\ \mu_f^a = \frac{\partial \Psi}{\partial M_f^a}, \quad \mu_i = \frac{\partial \Psi}{\partial M_i},\ \mu_i^a = \frac{\partial \Psi}{\partial M_i^a},\ 1 \le i \le n, \\ &\eta = -\frac{1}{\mathrm{J}}\frac{\partial \Psi}{\partial \theta}, \quad \boldsymbol{\sigma}^e = \frac{2}{\mathrm{J}}\mathbf{B}\cdot\frac{\partial \Psi}{\partial \mathbf{B}}. \end{aligned} \tag{5.2}$$

5.2. Porosity and saturation

We define the *Lagrangian porosity* Φ as the current volume of fluid per unit reference volume of tissue. By analogy, we introduce Φ^a as the current volume of blood per unit reference volume of tissue. Furthermore, we assume that the connected pore networks are always completely filled with fluid and blood. Introducing the *true density of the fluid*[26] ρ_f and $\{\rho_i\}_1^n$ the *true density of species* i[27] and the corresponding quantities for the blood ρ_f^a and $\{\rho_i^a\}_1^n$ yields the following *saturation conditions* (Coussy, 2004)

$$M_f = \Phi\rho_f, \quad M_f^a = \Phi^a\rho_f^a, \quad M_i = \Phi\rho_i, \quad M_i^a = \Phi^a\rho_i^a,\ 1 \le i \le n. \tag{5.3}$$

The Lagrangian free energy Ψ can be alternatively written as $\Psi(M_s, \Phi, \rho_f, \{\rho_i\}_1^n, \Phi^a, \{\rho_i^a\}_1^n, \theta, \mathcal{I}(\mathbf{C}))$.[28] Taking the partial derivative of Ψ with respect to ρ_f and ρ_i gives for the chemical potentials

$$\mu_f = \frac{1}{\Phi}\frac{\partial \Psi}{\partial \rho_f}, \quad \mu_i = \frac{1}{\Phi}\frac{\partial \Psi}{\partial \rho_i},\ 1 \le i \le n. \tag{5.4}$$

By introducing the porosity Φ, we added an extra variable to the problem, thus needing a supplementary equation to solve the boundary value problem. This additional equation naturally comes by taking the partial derivative of the reference free energy Ψ with respect to Φ[29]

$$\rho_f\mu_f + \sum_{i=1}^{n}\rho_i\mu_i = \frac{\partial \Psi}{\partial \Phi}. \tag{5.5}$$

[25] Since the invariants of the left and right Cauchy–Green tensors coincide, $\mathcal{I}(\mathbf{C}) = \mathcal{I}(\mathbf{B})$, for the more general case of an anisotropic skeleton $\boldsymbol{\sigma}^e = (2/J)\mathbf{F}\cdot(\partial\Psi/\partial\mathbf{C})\cdot\mathbf{F}^\intercal$.

[26] Mass of fluid per unit current volume of fluid.

[27] Mass of species i per unit current volume of fluid.

[28] For simplicity, we keep the same symbol Ψ for the free energy expressed in terms of the true densities.

[29] The Eq. (5.5) is nothing else but a general form of the well known thermodynamic identity for a mixture of $n+1$ chemical species that usually takes the form $\psi_f + p_f = \sum_{i=0}^{n}\rho_i\mu_i$ where $\rho_0 := \rho_f - \sum_{i=1}^{n}\rho_i$.

In the poro-mechanics theory, the relation (5.5) is usually postulated for the fluid (Coussy, 2004; Chapelle and Moireau, 2014), and directly used to simplify the algebra. In this work, the thermodynamic assumption arises naturally in a way that is similar to the results of Gurtin and Vargas (1971) in their remark (4.3).

By analogy to (5.4) the blood chemical potentials are

$$\mu_f^a = \frac{1}{\Phi^a}\frac{\partial \Psi}{\partial \rho_f^a}, \quad \mu_i^a = \frac{1}{\Phi^a}\frac{\partial \Psi}{\partial \rho_i^a}, \ 1 \le i \le n. \tag{5.6}$$

and the blood equation corresponding to (5.5)

$$\rho_f^a \mu_f^a + \sum_{i=1}^{n} \rho_i^a \mu_i^a = \frac{\partial \Psi}{\partial \Phi^a}. \tag{5.7}$$

5.3. Heat equation

Following the same procedure as in Chester and Anand (2011) for deriving the heat equation, one can substitute the definition of Ψ of (5.1) and (3.23) into the energy balance (3.19) and, applying the chain rule of time derivation, one can write the heat equation

$$\begin{aligned} &\frac{c}{\mathrm{J}}\dot{\theta} + \theta \boldsymbol{\nabla}\cdot\left(\frac{\mathbf{q}}{\theta}\right) - D - q - \frac{\theta}{\mathrm{J}}\left[\frac{\partial^2 \Psi}{\partial\theta\partial\mathbf{C}} : \dot{\mathbf{C}} + \frac{\partial^2 \Psi}{\partial\theta\partial M_f}\dot{M}_f\right. \\ &\left. + \frac{\partial^2 \Psi}{\partial\theta\partial M_f^a}\dot{M}_f^a + \sum_{i=1}^{n}\left\{\frac{\partial^2 \Psi}{\partial\theta\partial M_i}\dot{M}_i + \frac{\partial^2 \Psi}{\partial\theta\partial M_i^a}\dot{M}_i^a\right\}\right] = 0, \end{aligned} \tag{5.8}$$

where we defined the specific heat

$$c := -\theta\frac{\partial^2 \Psi}{\partial\theta^2}. \tag{5.9}$$

5.4. Free energy decomposition

We adopt an additive decomposition of the free energy according to the different physical phenomena involved

$$\Psi = \Psi_{mech} + \Psi_{int} + \Psi_{fluid} + \Psi_{elec} + \Psi_{int}^a + \Psi_{fluid}^a + \Psi_{elec}^a. \tag{5.10}$$

The component Ψ_{mech} is defined as the purely mechanical strain energy of the *dry* adipose tissue. This represents the strain energy of tissue that would be considered ex-vivo, with no interstitial fluid and no blood. The component Ψ_{fluid} is defined as the free energy carried by the fluid itself when the tissue is hydrated. The energy Ψ_{fluid}^a is the equivalent term for the fluid in the absorption system (blood). Moreover, the interstitial fluid and the blood are required to stay electrically neutral at all time. For application in numerical codes, it is convenient to treat the electroneutrality constraints by adding two energies Ψ_{elec} and Ψ_{elec}^a reflecting the energy penalty of the system due to its deviation from the neutral state. An alternative formulation with Lagrange multipliers could also be used (Huyghe and Janssen, 1997, 1999) and an example with Lagrange multiplier is treated in Section 7.

Since the energy Ψ_{mech}corresponds to the macroscopic mechanical deformation of the dry adipose tissue, one must still account for the energetic cost of the addition of a given mass of fluid, due to the fluid-induced mechanical dilation of pores. Hence one must add an interaction energy Ψ_{int} that represents the energy cost that the solid tissue must undertake so that the fluid volume fits within the pores. By analogy, the corresponding term for the absorption system is also defined as Ψ_{int}^a.

The physical mechanisms associated with the different energy components in (5.10), allow us to assume the functional dependence of each component of the free energy as follows

$$\begin{aligned} \Psi = \ & \Psi_{mech}(\theta, \mathcal{I}(\mathbf{C})) + \Psi_{int}(\Phi, \Phi^a, \mathrm{J}, \theta) + \Phi\psi_f(\rho_f, \{\rho_i\}_1^n, \theta) + \Psi_{elec}(\Phi, \rho_f, \{\rho_i\}_1^n) + \\ & \Psi_{int}^a(\Phi, \Phi^a, \mathrm{J}, \theta) + \Phi^a\psi_f^a(\rho_f^a, \{\rho_i^a\}_1^n, \theta) + \Psi_{elec}^a(\Phi^a, \rho_f^a, \{\rho_i^a\}_1^n), \end{aligned} \tag{5.11}$$

where ψ_f is defined as the free energy of the fluid per unit volume of interstitial fluid.[30] Similarly, the term ψ_f^a is the free energy of the blood per unit volume of blood.

[30] This allows us to define ψ_f from physical considerations of the fluid in its pure state (outside of the porous material).

Given the assumption about the different components of the free energy in (5.11), on can rewrite (5.2), (5.4), (5.5), (5.6) and (5.7)

$$
\begin{aligned}
&\mathrm{J}\eta = -\frac{\partial(\Psi_{mech}+\Psi_{int}+\Psi^a_{int})}{\partial\theta} - \Phi\frac{\partial\psi_f}{\partial\theta} - \Phi^a\frac{\partial\psi^a_f}{\partial\theta}, \quad \boldsymbol{\sigma} = \frac{2}{\mathrm{J}}\mathbf{B}\cdot\frac{\partial\Psi_{mech}}{\partial\mathbf{B}} + \frac{\partial(\Psi_{int}+\Psi^a_{int})}{\partial\mathrm{J}}\mathbf{I} - \left(m_f\mathbf{v}_r + m^a_f\mathbf{v}^a_r\right)\mathbf{v},\\
&\mu_f = \frac{\partial\psi_f}{\partial\rho_f} + \frac{1}{\Phi}\frac{\partial\Psi_{elec}}{\partial\rho_f}, \qquad \mu_i = \frac{\partial\psi_f}{\partial\rho_i} + \frac{1}{\Phi}\frac{\partial\Psi_{elec}}{\partial\rho_i},\ 1\le i\le n,\\
&\mu^a_f = \frac{\partial\psi^a_f}{\partial\rho^a_f} + \frac{1}{\Phi^a}\frac{\partial\Psi^a_{elec}}{\partial\rho^a_f}, \qquad \mu^a_i = \frac{\partial\psi^a_f}{\partial\rho^a_i} + \frac{1}{\Phi^a}\frac{\partial\Psi^a_{elec}}{\partial\rho^a_i},\ 1\le i\le n,\\
&\rho_f\mu_f + \sum_{i=1}^n \rho_i\mu_i = \psi_f + \frac{\partial(\Psi_{int}+\Psi^a_{int}+\Psi_{elec})}{\partial\Phi}, \qquad \rho^a_f\mu^a_f + \sum_{i=1}^n \rho^a_i\mu^a_i = \psi^a_f + \frac{\partial(\Psi_{int}+\Psi^a_{int}+\Psi^a_{elec})}{\partial\Phi^a}.
\end{aligned}
\tag{5.12}
$$

It is interesting to note that we retrieve in (5.12) the usual definitions of the chemical potentials, without introducing them as primitive fields. Also note that the supplementary equations $(5.12)_{7,8}$ are a mathematical consequence of the split (5.3) and do not need to be postulated as thermodynamic identities of the fluids (Gibbs relation).

5.5. Electroneutrality constraint

The interstitial fluid stays electrically neutral at all time, accounting for the presence of fixed charges attached to the collagen mesh. The electroneutrality constraint in the interstitial space takes the macroscopic form

$$
\frac{Q_F}{F_{\mathcal{A}}} + \Phi\sum_{i=1}^n \frac{z_i}{M^{\mathrm{mol}}_i}\rho_i = 0,
\tag{5.13}
$$

where Q_F is the density of charges attached to the skeleton (it is a charge per unit reference volume; we neglect here its dependence on the temperature), $F_{\mathcal{A}}$ is the Faraday constant, z_i is an integer representing the number of charges carried by one molecule of species i, M^{mol}_i is the molar mass of species i. In (5.13) we have also assumed that the solvent 0 is neutral ($z_0 = 0$) and used the saturation condition (5.3). The associated penalty energy is then defined as

$$
\Psi_{elec}(\Phi,\rho_f,\{\rho_i\}^n_1) = \frac{1}{2\zeta}\left(\frac{Q_F}{F_{\mathcal{A}}} + \Phi\sum_{i=1}^n \frac{z_i}{M^{\mathrm{mol}}_i}\rho_i\right)^2,
\tag{5.14}
$$

where $0 < \zeta \ll 1$ is the penalty parameter.

In a similar fashion, the electroneutrality constraint in blood vessels, accounting for the absence of fixed charges in the absorption system ($Q^a_F = 0$), takes the form

$$
\Phi^a\sum_{i=1}^n \frac{z_i}{M^{\mathrm{mol}}_i}\rho^a_i = 0,
\tag{5.15}
$$

and the corresponding penalty energy is

$$
\Psi^a_{elec}(\Phi^a,\rho^a_f,\{\rho^a_i\}^n_1) = \frac{1}{2\zeta^a}\left(\Phi^a\sum_{i=1}^n \frac{z_i}{M^{\mathrm{mol}}_i}\rho^a_i\right)^2,
\tag{5.16}
$$

where $0 < \zeta^a \ll 1$ is the associated penalty parameter. Also note that we did not drop the dependence on Φ^a in the constraint (5.15) in order to stay consistent with the dimensions of the energies.

Substituting (5.14) and (5.16) into $(5.12)_{3,4,5,6,7,8}$ yields

$$
\begin{aligned}
&\mu_f = \frac{\partial\psi_f}{\partial\rho_f}, \qquad \mu_i = \frac{\partial\psi_f}{\partial\rho_i} + \frac{z_i}{M^{\mathrm{mol}}_i\zeta}\left(\frac{Q_F}{F_{\mathcal{A}}} + \Phi\sum_{i=1}^n \frac{z_i}{M^{\mathrm{mol}}_i}\rho_i\right),\ 1\le i\le n,\\
&\mu^a_f = \frac{\partial\psi^a_f}{\partial\rho^a_f}, \qquad \mu^a_i = \frac{\partial\psi^a_f}{\partial\rho^a_i} + \frac{z_i\Phi^a}{M^{\mathrm{mol}}_i\zeta^a}\sum_{i=1}^n \frac{z_i}{M^{\mathrm{mol}}_i}\rho^a_i,\ 1\le i\le n,\\
&\rho_f\frac{\partial\psi_f}{\partial\rho_f} + \sum_{i=1}^n \rho_i\frac{\partial\psi_f}{\partial\rho_i} = \psi_f + \frac{\partial(\Psi_{int}+\Psi^a_{int})}{\partial\Phi}, \quad \rho^a_f\frac{\partial\psi^a_f}{\partial\rho^a_f} + \sum_{i=1}^n \rho^a_i\frac{\partial\psi^a_f}{\partial\rho^a_i} = \psi^a_f + \frac{\partial(\Psi_{int}+\Psi^a_{int})}{\partial\Phi^a}.
\end{aligned}
\tag{5.17}
$$

Note that the approach with penalty energies (5.14) and (5.16) is particularly suited to numerical solving involving a framework of energy minimization (e.g. variational principles and finite elements). In the case of an analytical solving in simplified frameworks (see e.g. Section 7), an alternative formulation involving Lagrange multipliers can be more tractable. Following the same approach as in Huyghe and Janssen (1997, 1999), the equations of (5.17) remain unchanged expect for the following

$$
\mu_i = \frac{\partial\psi_f}{\partial\rho_i} + \frac{z_iF_{\mathcal{A}}}{M^{\mathrm{mol}}_i}\lambda, \quad \mu^a_i = \frac{\partial\psi^a_f}{\partial\rho^a_i} + \frac{z_iF_{\mathcal{A}}}{M^{\mathrm{mol}}_i}\lambda^a, 1\le i\le n,
\tag{5.18}
$$

where the Lagrange multipliers λ and λ^a are two unknown fields to solve for, together with the algebraic equations (5.13) and (5.15).

6. Summary of governing equations and interface conditions

It is helpful at this point to recapitulate all governing equations, i.e. linear momentum, all mass balances and the heat equation, plus their associated interface conditions, below in (6.1)

$\mathbf{x} \in \upsilon$	$\mathbf{x} \in \hat{\mathrm{s}}$		
$m_t \dot{\mathbf{v}} - \boldsymbol{\nabla} \cdot \left(m_f \mathbf{v}_r + m_f^a \mathbf{v}_r^a \right) \mathbf{v} - \boldsymbol{\nabla} \cdot \boldsymbol{\sigma} - m_t \mathbf{b} = \mathbf{0},$	$\mathbf{n} \cdot [\![\boldsymbol{\sigma}]\!] + \boldsymbol{\nabla}_{\hat{\mathrm{s}}} \cdot \boldsymbol{\sigma}_{\hat{\mathrm{s}}} = \mathbf{0}$	and	$[\![\mathbf{u}]\!] = \mathbf{0},$
$\dot{m}_s + m_s \boldsymbol{\nabla} \cdot \mathbf{v}_s = 0,$		N/A,	
$\dot{m}_f + m_f \boldsymbol{\nabla} \cdot \mathbf{v}_s + \boldsymbol{\nabla} \cdot \left(m_f \mathbf{v}_r \right) = \sum_{i=0}^{n} r_i,$	$\mathbf{n} \cdot [\![m_f \mathbf{v}_r]\!] = 0$	and	$\left[\!\left[\mu_f + \frac{(c_f \mathbf{v}_r)^2}{2} \right]\!\right] = 0,$
$\dot{m}_f^a + m_f^a \boldsymbol{\nabla} \cdot \mathbf{v}_s + \boldsymbol{\nabla} \cdot \left(m_f^a \mathbf{v}_r^a \right) = - \sum_{i=0}^{n} r_i,$	$\mathbf{n} \cdot \left[\!\left[m_f^a \mathbf{v}_r^a \right]\!\right] = 0$	and	$\left[\!\left[\mu_f^a + \frac{\left(c_f^a \mathbf{v}_r^a \right)^2}{2} \right]\!\right] = 0,$
$\dot{m}_i + m_i \boldsymbol{\nabla} \cdot \mathbf{v}_s + \boldsymbol{\nabla} \cdot \left(\mathbf{j}_i + m_i \mathbf{v}_r \right) = r_i,$	$\mathbf{n} \cdot [\![\mathbf{j}_i + m_i \mathbf{v}_r]\!] = 0$	and	$[\![\mu_i]\!] = 0,$
$\dot{m}_i^a + m_i^a \boldsymbol{\nabla} \cdot \mathbf{v}_s + \boldsymbol{\nabla} \cdot \left(\mathbf{j}_i^a + m_i^a \mathbf{v}_r^a \right) = -r_i,$	$\mathbf{n} \cdot [\![\mathbf{j}_i^a + m_i^a \mathbf{v}_r^a]\!] = 0$	and	$[\![\mu_i^a]\!] = 0,$
$\frac{c}{\mathrm{J}} \dot{\theta} + \theta \boldsymbol{\nabla} \cdot \left(\frac{\mathbf{q}}{\theta} \right) - D - q$			
$- \frac{\theta}{\mathrm{J}} \left(\frac{\partial^2 \Psi}{\partial \theta \partial \mathbf{B}} : \dot{\mathbf{B}} + \frac{\partial^2 \Psi}{\partial \theta \partial M_f} \dot{M}_f + \frac{\partial^2 \Psi}{\partial \theta \partial M_f^a} \dot{M}_f^a \right.$	$\mathbf{n} \cdot [\![\mathbf{q}]\!] = 0$	and	$[\![\theta]\!] = 0.$
$\left. + \sum_{i=1}^{n} \left\{ \frac{\partial^2 \Psi}{\partial \theta \partial M_i} \dot{M}_i + \frac{\partial^2 \Psi}{\partial \theta \partial M_i^a} \dot{M}_i^a \right\} \right) = 0,$			

(6.1)

where the relationships between the current and reference mass densities – respectively m_s, m_f, m_f^a, m_i, m_i^a and M_s, M_f, M_f^a, M_i, M_i^a – and the arguments of the reference energy density Ψ are given in (5.1). We also recall from (4.10) the sufficient restrictions for $\mathbf{q}$, $\mathbf{v}_r$, $\mathbf{v}_r^a$, $\mathbf{j}_i$, $\mathbf{j}_i^a$ and r_i, and the definition of the dissipation D from (4.9). Moreover, accounting for the saturation conditions (5.3) and the energy decomposition hypothesis (5.11), the constitutive relations for the entropy, stress tensor and various chemical potentials are given by (5.12) for $\mathbf{x} \in \upsilon$ and (4.16) for $\mathbf{x} \in \hat{\mathrm{s}}$.

7. Illustrating the interplay between mechanics, chemistry and electroneutrality

Although necessary for the study of subcutaneous injections, the non-linear finite-strain effects require numerical solution of the relevant boundary value problems and will thus be the object of a subsequent study using the proposed theory. To illustrate the contribution of the different physical mechanisms introduced in the multiphysics finite strain model derived above we hereby propose an analytically tractable study of the injection process for the small strain, time independent case.

7.1. Modeling assumptions

(L-1) We restrict the study to an isothermal and stationary boundary value problem, an assumption justified when the injected fluid is close to the body temperature.

(L-2) We do not consider any surface tension.

(L-3) We only consider two chemical species in a solvent. The subscript c is used for the chemical species carrying a positive charge (cation), the subscript n is used for the chemical species carrying a negative charge (anion).

(L-4) All material constants involved are time and space independent.

(L-5) The absorption system is considered as a reservoir whose composition is not changed by the contribution of the interstitial fluid. Consequently, the equations pertaining to the absorption system are omitted in the boundary value problem definition. We consider the blood vessels to be part of the skeleton so that their mechanical contribution is included in the mechanical response of the skeleton. We also assume that the volume of blood in the tissue is constant and unaffected by the deformation of the tissue. This assumption yields that we consider Ψ_{int}^a contribution to be included in Ψ_{mech} in the energy decomposition (5.11).

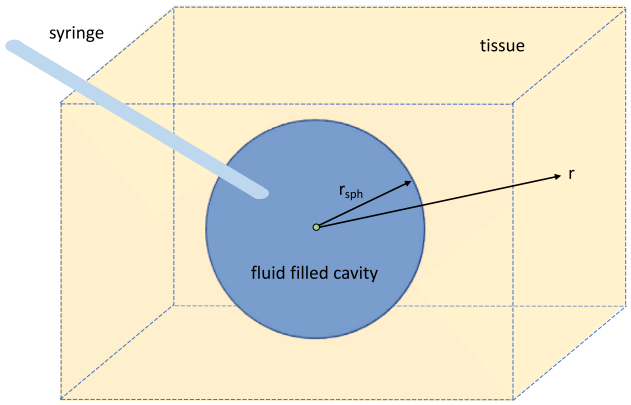

Fig. 3. Spherical cavity in an infinite medium injection boundary value problem.

(L-6) There are no external body forces.
(L-7) The linear regime of governing equations is considered with small strain kinematics and small perturbations from an equilibrium state (denoted with the superscript ^{e}) to be specified later. As a consequence, the quadratic terms in $\mathbf{v}_r$, $\mathbf{v}_r^a$, $\mathbf{v}$ are neglected in the considered regime.
(L-8) The equilibrium state is assumed to be stress-free and the skeleton is assumed to be at its reference configuration.
(L-9) For this closed-form analytical solving, the Lagrange multiplier formulation is used in place of the penalty energy approach, as discussed around Eqs. (5.17) and (5.18).

7.2. Dimensionless, perturbed variables

Consider a spherical cavity of initial radius r_{sph} within an infinite medium, as depicted in Fig. 3. The cavity is filled with a fluid whose pressure and chemical potentials are known injection parameters and denoted with a superscript ^{inj}. A spherically symmetric solution of the problem is considered and consequently all field variables are functions of the radial coordinate r.

Denote by $\boldsymbol{\varepsilon}$ the linearized strain tensor and by $\boldsymbol{\varepsilon}' = \boldsymbol{\varepsilon} - (\mathrm{tr}\boldsymbol{\varepsilon}/3)\mathbf{I}$ its deviatoric part. In the regime of small deformation, the initial equilibrium is represented by the superscript ^{e}. Following the assumption (L-8), the equilibrium state is such that the skeleton is in its reference unstressed configuration, represented by the superscript ^{0}:

$$\boldsymbol{\Phi}^e = \boldsymbol{\Phi}^0, \quad \mathbf{u}^e = \mathbf{0}, \quad \boldsymbol{\varepsilon}^e = \mathbf{0}, \quad \boldsymbol{\sigma}^e = \mathbf{0}, \quad p_f^e = 0, \tag{7.1}$$

where the hydrostatic pressure of the fluid p_f has been introduced in (B.10) and ρ_f^0 stands for the density of the fluid at the atmospheric reference pressure.

Only two chemical species are assumed to be present, with densities ρ_c (positively charged) and ρ_n (negatively charged). Taking into account (7.1), we define the following dimensionless perturbation quantities away from equilibrium

$$\delta\mathbf{u} := \frac{\mathbf{u}}{r_{sph}}, \quad \delta\boldsymbol{\varepsilon} := \boldsymbol{\varepsilon}, \quad \delta\boldsymbol{\Phi} := \frac{\boldsymbol{\Phi} - \boldsymbol{\Phi}^0}{\boldsymbol{\Phi}^0}, \quad \delta\rho_c := \frac{\rho_c - \rho_c^e}{\rho_c^e}, \quad \delta\rho_n := \frac{\rho_n - \rho_n^e}{\rho_n^e}, \quad \delta\rho_f := \frac{\rho_f - \rho_f^e}{\rho_f^e},$$

$$\delta\mu_f := \frac{\mu_f - \mu_f^e}{R\theta/\rho_0^e\left(\dfrac{\rho_c^e}{M_c^{\mathrm{mol}}} + \dfrac{\rho_n^e}{M_n^{\mathrm{mol}}}\right)}, \quad \delta\mu_c := \frac{\mu_c - \mu_c^e}{R\theta/M_c^{\mathrm{mol}}}, \quad \delta\mu_n := \frac{\mu_n - \mu_n^e}{R\theta/M_n^{\mathrm{mol}}}, \tag{7.2}$$

$$\delta\boldsymbol{\sigma} := \frac{\boldsymbol{\sigma}}{G}, \quad \delta p_f := \frac{p_f}{G}, \quad \delta\lambda := \frac{\lambda - \lambda^e}{R\theta/F_{\mathcal{A}}},$$

where R is the universal gas constant, $\rho_0^e = \rho_f^e - \rho_c^e - \rho_n^e$ is the equilibrium density of the solvent and the fluid pressure p_f is defined in (B.10).

7.3. Linearized boundary value problem

We introduce the dimensionless radius variable $\bar{\mathrm{r}}$ and the corresponding dimensionless nabla operator $\overline{\boldsymbol{\nabla}}$

$$\bar{\mathrm{r}} := \frac{\mathrm{r}}{r_{sph}}, \quad \overline{\boldsymbol{\nabla}} := r_{sph}\boldsymbol{\nabla}, \tag{7.3}$$

where r_{sph} is the inner radius of the spherical cavity (see Fig. 3). Due to its length, the linearization procedure of (6.1) is presented in detail in Appendix B and results in a system of four linear O.D.E.s.

The corresponding linear momentum equation $(6.1)_1$ yields

$$\frac{\partial}{\partial \bar{\mathrm{r}}}\left[\left(\frac{4}{3}+\frac{K}{G}-b_{Biot}\mathrm{G}_{p\epsilon}^{-1}\right)\mathrm{tr}\delta\boldsymbol{\epsilon}-b_{Biot}\left(\mathrm{G}_{pf}^{-1}\delta\mu_f+\mathrm{G}_{pc}^{-1}\delta\mu_c+\mathrm{G}_{pn}^{-1}\delta\mu_n\right)\right]=0, \tag{7.4}$$

where K and G are the bulk and shear modulus of the skeleton continuum, b_{Biot} is the Biot coefficient of the skeleton porous material as defined in (B.6) and (B.11). The scalars $\mathrm{G}_{p\epsilon}^{-1}$, G_{pf}^{-1}, G_{pc}^{-1} and G_{pn}^{-1} are coefficients of the inverse of the matrix $\mathbf{G}$ defined in (B.16).

The linearized equations for mass balances of the fluid $(6.1)_2$, the species c $(6.1)_3$ and n $(6.1)_4$ are in matrix notation

$$\overline{\boldsymbol{\nabla}}\cdot\left(\overline{\boldsymbol{\nabla}}\mathbf{A}\delta\boldsymbol{\mu}\right)-\mathbf{B}\delta\boldsymbol{\mu}=\mathbf{0},\quad \delta\boldsymbol{\mu}=\begin{bmatrix}\delta\mu_f\\ \delta\mu_c\\ \delta\mu_n\end{bmatrix}, \tag{7.5}$$

where the effective mobility matrix $\mathbf{A}$ and the effective absorption matrix $\mathbf{B}$ are defined in (B.21) and (B.23).

The four differential equations (7.4) and (7.5) are solved for the four unknown fields $\delta\mathrm{u}_\mathrm{r}(\bar{\mathrm{r}})$, $\delta\mu_f(\bar{\mathrm{r}})$, $\delta\mu_c(\bar{\mathrm{r}})$ and $\delta\mu_n(\bar{\mathrm{r}})$ using the following boundary conditions at $\bar{\mathrm{r}}=1$ and $\bar{\mathrm{r}}\to\infty$

$$\begin{aligned}&\delta\sigma_{\mathrm{rr}}\big|_{\bar{\mathrm{r}}=1}=-\delta p_f^{\mathrm{inj}},\quad \delta\mu_f\big|_{\bar{\mathrm{r}}=1}=\delta\mu_f^{\mathrm{inj}},\quad \delta\mu_c\big|_{\bar{\mathrm{r}}=1}=\delta\mu_c^{\mathrm{inj}},\quad \delta\mu_n\big|_{\bar{\mathrm{r}}=1}=\delta\mu_n^{\mathrm{inj}},\\ &\delta\sigma_{\mathrm{rr}}\big|_{\bar{\mathrm{r}}\to\infty}=0,\qquad \delta\mu_f\big|_{\bar{\mathrm{r}}\to\infty}=0,\qquad \delta\mu_c\big|_{\bar{\mathrm{r}}\to\infty}=0,\qquad \delta\mu_n\big|_{\bar{\mathrm{r}}\to\infty}=0.\end{aligned} \tag{7.6}$$

The values of the chemical potential perturbations at the surface of the spherical cavity $\bar{\mathrm{r}}=1$ are obtained from the hydrostatic pressure $\delta p_f^{\mathrm{inj}}$ and the chemical species densities $\delta\rho_c^{\mathrm{inj}}$ and $\delta\rho_n^{\mathrm{inj}}$ as described in (B.24).

The system of mass balances (7.5) only involves the perturbation chemical potentials $\delta\boldsymbol{\mu}$. To solve this system, we bring it to a diagonal form by introducing an auxiliary variable $\delta\boldsymbol{\xi}$ using the matrix $\mathbf{Q}$ that diagonalizes $\mathbf{A}^{-1}\mathbf{B}$

$$\delta\boldsymbol{\xi}=\mathbf{Q}^{-1}\delta\boldsymbol{\mu},\ \mathbf{Q}^{-1}\left(\mathbf{A}^{-1}\mathbf{B}\right)\mathbf{Q}=\mathbf{D}=\mathrm{diag}[D_i],\implies \overline{\boldsymbol{\nabla}}\cdot\left(\overline{\boldsymbol{\nabla}}\mathbf{A}\delta\boldsymbol{\mu}\right)-\mathbf{B}\delta\boldsymbol{\mu}=\mathbf{A}\mathbf{Q}[\overline{\boldsymbol{\nabla}}\cdot\left(\overline{\boldsymbol{\nabla}}\delta\boldsymbol{\xi}\right)-\mathbf{D}\delta\boldsymbol{\xi}]=\mathbf{0}. \tag{7.7}$$

The above system (7.7) can be written in the uncoupled form with respect to the auxiliary variable $\delta\boldsymbol{\xi}$ and accounting for the boundary conditions of (7.6) has the following solution in $\delta\boldsymbol{\xi}(\bar{\mathrm{r}})$ and hence for the perturbation chemical potentials $\delta\boldsymbol{\mu}(\bar{\mathrm{r}})$

$$\overline{\boldsymbol{\nabla}}\cdot\left(\overline{\boldsymbol{\nabla}}\delta\xi_i(\bar{\mathrm{r}})\right)-\mathrm{D}_i\delta\xi_i(\bar{\mathrm{r}})=0,\implies \delta\xi_i(\bar{\mathrm{r}})=\delta\xi_i^{\mathrm{inj}}[\exp(-\sqrt{\mathrm{D}_i}(\bar{\mathrm{r}}-1))]/\bar{\mathrm{r}};\ i=1,\dots,3,\implies \delta\boldsymbol{\mu}(\bar{\mathrm{r}})=\mathbf{Q}\delta\boldsymbol{\xi}(\bar{\mathrm{r}}). \tag{7.8}$$

These results are obtained considering that the coefficients $\mathrm{D}_i>0$ are positive real numbers, an assumption that holds true in all subsequent numerical calculations.

The linear momentum balance differential equation (7.4) has the following solution

$$\delta\mathrm{u}_\mathrm{r}(\bar{\mathrm{r}})=\frac{U_2}{\bar{\mathrm{r}}^2}+U_1\bar{\mathrm{r}}-\frac{1+\bar{\mathrm{r}}}{\bar{\mathrm{r}}}\mathbf{V}^\intercal\mathbf{Q}\begin{bmatrix}\frac{1}{\sqrt{\mathrm{D}_1}}\delta\xi_1(\bar{\mathrm{r}})\\ \frac{1}{\sqrt{\mathrm{D}_2}}\delta\xi_2(\bar{\mathrm{r}})\\ \frac{1}{\sqrt{\mathrm{D}_3}}\delta\xi_3(\bar{\mathrm{r}})\end{bmatrix},\quad \mathbf{V}=\frac{b_{Biot}}{\frac{4}{3}+\frac{K}{G}-b_{Biot}\mathrm{G}_{p\epsilon}^{-1}}\begin{bmatrix}\mathrm{G}_{pf}^{-1}\\ \mathrm{G}_{pc}^{-1}\\ \mathrm{G}_{pn}^{-1}\end{bmatrix}, \tag{7.9}$$

where U_1 and U_2 are integration constants to be determined by the stress boundary conditions. Using the normal component of the Cauchy stress tensor perturbation $\delta\sigma_{\mathrm{rr}}$

$$\delta\sigma_{\mathrm{rr}}(\bar{\mathrm{r}})=2\delta\epsilon_{\mathrm{rr}}(\bar{\mathrm{r}})+\left(\frac{K}{G}-\frac{2}{3}\right)\mathrm{tr}\delta\boldsymbol{\epsilon}(\bar{\mathrm{r}})-b_{Biot}\delta p_f(\bar{\mathrm{r}})=-\frac{4}{\bar{\mathrm{r}}}\delta\mathrm{u}_\mathrm{r}(\bar{\mathrm{r}})+U_1, \tag{7.10}$$

and applying the boundary conditions in (7.6) at $\bar{\mathrm{r}}=1$ and $\bar{\mathrm{r}}\to\infty$ we obtain the following result for $\delta\mathrm{u}_\mathrm{r}(\bar{\mathrm{r}})$

$$\delta\mathrm{u}_\mathrm{r}(\bar{\mathrm{r}})=\frac{\delta p_f^{\mathrm{inj}}}{4\bar{\mathrm{r}}^2}-\frac{1}{\bar{\mathrm{r}}^2}\mathbf{V}^\intercal\mathbf{Q}\begin{bmatrix}\frac{1}{\sqrt{\mathrm{D}_1}}\left((\bar{\mathrm{r}}+\bar{\mathrm{r}}^2)\delta\xi_1(\bar{\mathrm{r}})-2\delta\xi_1^{\mathrm{inj}}\right)\\ \frac{1}{\sqrt{\mathrm{D}_2}}\left((\bar{\mathrm{r}}+\bar{\mathrm{r}}^2)\delta\xi_2(\bar{\mathrm{r}})-2\delta\xi_2^{\mathrm{inj}}\right)\\ \frac{1}{\sqrt{\mathrm{D}_3}}\left((\bar{\mathrm{r}}+\bar{\mathrm{r}}^2)\delta\xi_3(\bar{\mathrm{r}})-2\delta\xi_3^{\mathrm{inj}}\right)\end{bmatrix}, \tag{7.11}$$

where $\delta\boldsymbol{\xi}^{\mathrm{inj}}=\mathbf{Q}^{-1}\delta\boldsymbol{\mu}^{\mathrm{inj}}$. In (7.11) and (7.8) we have thus obtained the four perturbation fields $\delta\mathrm{u}_\mathrm{r}(\bar{\mathrm{r}})$, $\delta\mu_f(\bar{\mathrm{r}})$, $\delta\mu_c(\bar{\mathrm{r}})$ and $\delta\mu_n(\bar{\mathrm{r}})$ which constitute the solution to the system of the four differential equation (7.4) and (7.5) with boundary conditions (7.6). Other quantities of interest, such as the perturbations of porosity $\delta\Phi$, pressure δp_f, fluid density $\delta\rho_f$ and chemical species densities $\delta\rho_c$, $\delta\rho_n$ are given in Appendix B.

Important information to estimate the efficiency of an injection is given by the integral over the whole volume of the absorption terms $(B.5)_2$

$$4\pi\mathrm{r}_{\mathrm{sph}}^2\int_1^\infty\bar{\mathrm{r}}'^2\begin{bmatrix}r_f/a_f\\ r_c/a_c\\ r_n/a_n\end{bmatrix}\mathrm{d}\bar{\mathrm{r}}'=-2\mathbf{B}\mathbf{Q}\begin{bmatrix}\frac{1}{\sqrt{\mathrm{D}_1}}\delta\xi_1^{\mathrm{inj}}\\ \frac{1}{\sqrt{\mathrm{D}_2}}\delta\xi_2^{\mathrm{inj}}\\ \frac{1}{\sqrt{\mathrm{D}_3}}\delta\xi_3^{\mathrm{inj}}\end{bmatrix}. \tag{7.12}$$

If the components of $(7.12)_2$ are negative, the corresponding species are absorbed by the poroelastic continuum, which is the desired behavior when injecting a fluid. In the opposite case the absorption system releases these species into the interstitial space.

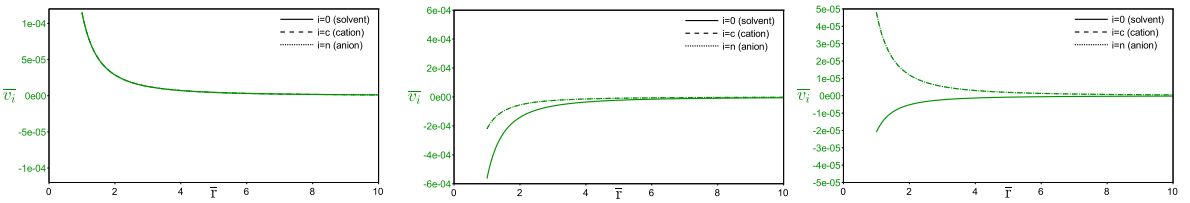

(a) $\delta\rho_c^{\text{inj}} = 0.01,\ \omega = 0.$ (b) $\delta\rho_c^{\text{inj}} = 0.01,\ \omega = \omega_{\max}.$ (c) $\delta\rho_c^{\text{inj}} = 0.01,\ \omega = 0.2\omega_{\max}.$

Fig. 4. Importance of accounting for the cross-coupling in the dissipation constitutive laws of the fluxes by just adding salt (NaCl) in the cavity ($\delta\rho_c^{\text{inj}} = 0.01$). Three different cases of the osmotic coefficient are considered: $\omega = 0$ in (a), $\omega = \omega_{\max}$ in (b) and $\omega = 0.2\omega_{\max}$ in (c). The vertical axis of each graph records the different dimensionless fluid velocities ($\overline{\mathrm{v}}_0$, $\overline{\mathrm{v}}_c$, $\overline{\mathrm{v}}_n$); solid green line corresponds to the solvent fluid ($\overline{\mathrm{v}}_0$), dashed green line to the cation velocity ($\overline{\mathrm{v}}_c$) and dotted green line to the anion velocity ($\overline{\mathrm{v}}_n$). The horizontal axis gives the dimensionless distance $\bar{\mathrm{r}}$ away from the cavity-tissue boundary ($\bar{\mathrm{r}} = 1$).

A final note is in order at this point. The solution in (7.8) and (7.11) is valid when $D_i \neq 0$, i.e. when the absorption terms $r_f, r_c, r_n \neq 0$. In the no-absorption case $r_f = r_c = r_n = 0$, the solution simplifies to

$$\delta \mathrm{u}_{\mathrm{r}}^{\mathrm{na}}(\bar{\mathrm{r}}) = \frac{\delta p_f^{\text{inj}}}{4\bar{\mathrm{r}}^2} + \frac{\bar{\mathrm{r}}^2 - 1}{2\bar{\mathrm{r}}^2}\mathbf{V}^{\intercal}\delta\boldsymbol{\mu}^{\text{inj}}, \quad \delta\mu_f^{\mathrm{na}}(\bar{\mathrm{r}}) = \frac{\delta\mu_f^{\text{inj}}}{\bar{\mathrm{r}}}, \quad \delta\mu_c^{\mathrm{na}}(\bar{\mathrm{r}}) = \frac{\delta\mu_c^{\text{inj}}}{\bar{\mathrm{r}}}, \quad \delta\mu_n^{\mathrm{na}}(\bar{\mathrm{r}}) = \frac{\delta\mu_n^{\text{inj}}}{\bar{\mathrm{r}}}, \tag{7.13}$$

7.4. Results from the simplified injection model

The results presented below in Figs. 4, 5 and 6 show the importance of chemical species absorption and diffusion as well as bound tissue charges on pressure, volume change and solvent, species flows using the context of the simple, linearized injection model described in Section 7.3. Depending on the case considered, the loading consists of changing the concentration of cations (e.g. Na^+) in the cavity ($\delta\rho_c^{inj}$), the bound charges in the tissue (Q_F) and the pressure (δp_f^{inj}). The corresponding changes of anions (e.g. Cl^-) in the cavity ($\delta\rho_n^{inj}$) are found from electroneutrality in (B.15) and the boundary conditions for each problem are calculated with the help of (B.24).

Dimensionless expressions are used for the solvent $\overline{\mathrm{v}}_0$, cation $\overline{\mathrm{v}}_c$ and anion $\overline{\mathrm{v}}_n$ velocities, which are normalized by a reference porous velocity $\mathrm{v}^{\text{porous}}$ defined using a characteristic time of permeation T_{pe} (Auton and MacMinn, 2017, 2018)

$$\overline{\mathrm{v}}_{0,c,n} = \frac{\mathrm{v}_{0,c,n}}{\mathrm{v}^{\text{porous}}}, \quad \mathrm{v}^{\text{porous}} := \frac{\mathrm{r}_{sph}}{T_{pe}}, \quad T_{pe} = \frac{\mu_v \mathrm{r}_{sph}^2}{k_h\,(K + 4G/3)}, \tag{7.14}$$

where G and K are the shear and bulk moduli of the skeleton, introduced in (B.6) and μ_v and k_h are the viscosity of the fluid and the hydraulic permeability of the porous medium, introduced in (B.17).

Similarly, we define the dimensionless absorption rates

$$\bar{r}_{0,c,n} = \frac{r_{0,c,n}\tau_0}{\boldsymbol{\Phi}^0\rho_f^e}, \tag{7.15}$$

where τ_0 is the absorption time of the solvent, introduced in (B.19).

(i) *The Importance of the osmotic efficiency coefficient ω*

The first objective is to show the importance of accounting for the cross-coupling in the dissipation constitutive laws in the velocities of the solvent (v_0) and the two chemical species ($\mathrm{v}_c, \mathrm{v}_n$). This coupling is modeled through the *osmotic efficiency coefficient* ω defined in (B.17) (see details in Loret et al. (2004)). Positive definiteness of the diffusion coefficients matrix in $(\mathrm{B.5})_1$ dictates a positive value of this coefficient with an upper bound $\omega_{\max}$ defined in (B.18).

We show in Fig. 4 the role of this coefficient by treating the simple problem of just adding salt (NaCl) in the cavity[31] ($\delta\rho_c^{\text{inj}} = 0.01$), without applying fluid pressure ($\delta p_f^{\text{inj}} = 0$), ignoring bound charges in the tissue ($Q_F = 0$) and absorption ($\mathrm{R}_{00} = \mathrm{R}_{cc} = \mathrm{R}_{nn} = 0 \implies \bar{r}_0 = \bar{r}_c = \bar{r}_n = 0$). We investigate three different cases: $\omega = 0$ in Fig. 4(a), $\omega = \omega_{\max}$ in Fig. 4(b) and $\omega = 0.2\omega_{\max}$ in Fig. 4(c). In each graph we plot the dimensionless different velocities ($\overline{\mathrm{v}}_0$, $\overline{\mathrm{v}}_c$, $\overline{\mathrm{v}}_n$); solid line corresponds to the solvent fluid ($\overline{\mathrm{v}}_0$), dashed line to the cation velocity ($\overline{\mathrm{v}}_c$) and dotted line to the anion velocity ($\overline{\mathrm{v}}_n$) as function of the dimensionless distance $\bar{\mathrm{r}}$ away from the cavity-tissue boundary ($\bar{\mathrm{r}} = 1$).

Note from Fig. 4(a) that in the absence of the osmotic efficiency coefficient ($\omega = 0$) the solvent and the salt move from the cavity into the tissue and the corresponding positive velocities decay to practically zero at a distance at about $\bar{\mathrm{r}} = 10$. The exact opposite happens in Fig. 4(b) when we consider the maximum value for the osmotic coefficient ($\omega = \omega_{\max}$) as the solvent and the salt move from the tissue into the cavity and the corresponding negative velocities decay to practically zero at the same distance as before. Both results seem rather unphysical, as one expects the solvent to move into the cavity and the salt into the tissue in an attempt to

[31] We only need to prescribe the Na^+ concentration ($\delta\rho_c^{\text{inj}}$). The corresponding Cl^- concentration ($\delta\rho_n^{\text{inj}}$) is determined from the electroneutrality constraint in (B.15).

balance chemical potentials in both regions. This is exactly what happens in Fig. 4(c) where an intermediate value of the osmotic efficiency coefficient is chosen ($\omega = 0.2\omega_{\max}$): the salt velocities are positive – from the cavity into the tissue – while the solvent velocity is negative from the tissue into the cavity, the expected behavior of the system. Henceforth, all numerical calculations are based on this osmotic efficiency coefficient ($\omega = 0.2\omega_{\max}$). Note that in all results of Fig. 4 the cation ($\bar{v}_c$) and anion ($\bar{v}_n$) velocities are the same to ensure electroneutrality.

(ii) *The importance of fixed charges and absorption under a diffusive regime (no injection pressure)*

For subcutaneous injection modeling the importance of accounting for the fixed charges in the tissue and the resulting impact of the electroneutrality balance must be established, as well as the influence of absorption of the chemical species into the blood. To highlight the role of these two mechanisms, the next simulations do not have an hydrostatic pressure applied in the cavity — we just introduce salt NaCl there. Since $Q_F \neq 0$ electroneutrality dictates a change in the cation and anion concentrations in the tissue (depending on the sign of Q_F) and hence a change in the corresponding concentrations in the cavity. We assume $\delta\rho_c^{\text{inj}} = 0$ for Na^+ – $\delta\rho_n^{\text{inj}} \neq 0$ for Cl^- is calculated by electroneutrality and is a function of Q_F – and follow the salt diffusion within the tissue and absorption by the blood. The response of the system due to the addition of salt in the cavity fixed charges in the tissue ($Q_F \neq 0$) but in the absence of injection pressure ($\delta p_f^{\text{inj}} = 0$) is presented in Fig. 5.

The response of a system with positive tissue charges ($Q_F > 0$) following the introduction of salt in the cavity but in the absence of absorption is presented in Figs. 5(a) and 5(b). Although there is no applied pressure at the cavity, the introduction of salt induces a pressure and porosity jump at the boundary according to Fig. 5(a). The solvent enters the tissue (positive velocity $\bar{v}_0 > 0$) while the excess Cl^- exists the tissue negative velocity $\bar{v}_n < 0$, as seen in Fig. 5(b). Notice also the very rapid decay of the pressure, volume change and fluxes away from the cavity boundary in the absence of absorption ($\bar{r}_0 \cdot \bar{r}_c \cdot \bar{r}_n = 0$ in Fig. 5(b)).

For the same loading and positive tissue charges ($Q_F > 0$) as before, but allowing for absorption, the results are presented in Figs. 5(c) and 5(d). Observe in Fig. 5(c) that now the pressure at the cavity boundary is zero and increases steeply to a maximum – corresponding to the location where the fluxes change in sign – at about $\bar{r} = 5$ before slowly decreasing. The porosity change $\delta\Phi$ and the skeleton volume change ($\text{tr}\delta\boldsymbol{\varepsilon}$) follow the evolution of the pressure and after reaching a maximum also decay slowly. Notice from Fig. 5(d) the reversal of the solvent velocity ($\bar{v}_0 < 0$) compared to Fig. 5(b), as the interstitial fluid exits the tissue along with the Cl^-. Moreover the solvent exits the tissue for the blood ($\bar{r}_0 < 0$) while the absorption rate for Cl^- is positive ($\bar{r}_n > 0$) as the negatively charged chemical species is absorbed in the tissue and the absorption rate of Na^+ is zero ($\bar{r}_c = 0$). Moreover, these chemical rates decay much faster than the pressure and porosity, recorded in Fig. 5(c).

The results of reversing the permanent tissue charges ($Q_F < 0$), while keeping the rest of the parameters as before (Figs. 5(c) and 5(d)) are presented in Figs. 5(e) and 5(f). Similarly to Fig. 5(c) but with its sign reversed, the pressure at the cavity boundary, starting from zero, drops rapidly to a minimum before increasing again at a much slower rate. Note in the same graph that the porosity and the skeleton volume also decrease. The same sign reversal in pressure and porosity and volume change observed between Figs. 5(c) and 5(e) also occurs for the fluxes and absorption rates as expected from electroneutrality, as evidenced by comparing Figs. 5(d) and 5(f). Notice that in view of our assumption that $\delta\rho_c^{inj} = 0$, the velocities and absorption rates for Na^+ are again zero.

The results presented in Fig. 5 illustrate the importance of accounting for the chemical mechanisms of fixed charges and absorption when calculating the mechanics quantities of pressure, porosity and volume changes, as it can change the qualitative and quantitative response of the tissue to the modeled injection.

(iii) *The importance of full chemo-mechanical coupling in the presence of injection pressure*

Finally the importance of the full chemo-mechanical coupling is established in Fig. 6 that compares the response of the system subjected only to an injection pressure in the cavity ($\delta p_f^{inj} = 0.01$), i.e. in the absence of chemical effects ($Q_F = \delta\rho_c^{inj} = \delta\rho_n^{inj} = 0$), presented in Figs. 6(a) and 6(b), and under full chemo-mechanical coupling ($Q_F > 0, \delta p_f^{inj} = 0.01, \delta\rho_c^{inj} = 0.01$), presented in Fig. 6(c) and in Fig. 6(d).

For the purely mechanical response of the system under an applied pressure at the cavity ($\delta p_f^{inj} = 0.01$) but in the absence of permanent tissue charges and chemical species ($Q_F = 0$, $\delta\rho_c^{inj} = \delta\rho_n^{inj} = 0$), the only fluid that plays a role is the solvent; diffusion as well absorption are both accounted for. The results in this case are the classical poroelasticity results for the solvent with a rapidly decaying positive pressure ($\delta p_f > 0$), porosity ($\delta\Phi > 0$) and skeleton volume change ($\text{tr}\delta\boldsymbol{\varepsilon} > 0$) observed in Fig. 6(a). As also expected from classical poroelasticity, we have a positive but rapidly decaying solvent velocity ($\bar{v}_0 > 0$) as the fluid enters the tissue by diffusion while it is also absorbed by the blood ($\bar{r}_0 < 0$). Since chemical effects are not accounted for, the velocities of the chemical species are zero ($\bar{v}_c = \bar{v}_n = 0$) as are the corresponding absorption rates ($\bar{r}_c = \bar{r}_n = 0$), as seen in Fig. 6(b).

A radically different picture emerges when a full chemo-mechanical coupling is considered ($Q_F > 0, \delta p_f^{inj} = 0.01, \delta\rho_c^{inj} = 0.01$). Even though a positive hydrostatic pressure is applied, a contraction in the tissue is observed since the hydrostatic pressure applied is low. Notice in Fig. 6(c) the sign reversal of the pressure ($\delta p_f < 0$), porosity ($\delta\Phi < 0$) and skeleton volume change ($\text{tr}\delta\boldsymbol{\varepsilon} < 0$) compared to the purely mechanical response in Fig. 6(a). These quantities all start from zero at the boundary, decrease rapidly to reach a minimum at about $\bar{r} = 5$ and subsequently increase slowly but at a much slower rate than in the purely mechanical case. A different from the purely mechanical case picture in Fig. 6(b) also emerges for the velocities and absorption rates when chemical effects are accounted for in Fig. 6(d). Although the solvent velocity is initially positive as the fluid enters the tissue, it changes sign at about $\bar{r} = 5$. Moreover solvent is absorbed by the tissue ($\bar{r}_0 > 0$) while Cl^- exits and is absorbed by the blood $\bar{r}_n < 0$.

From the above results in Fig. 6 we establish the importance of the full chemo-mechanical coupling for correctly modeling the fluxes in the tissue as well as the swelling behavior. Omitting the chemical and electroneutrality contribution in the modeling could lead to predicting the wrong swelling/shrinking behavior of the tissue, the wrong injection behavior – since the value one could predict a fluid injection whereas the injection pressure is not enough to counterbalance the osmotic contribution – and the wrong absorption equilibrium, since it is directly impacted by these conditions and the tissue does not necessarily absorb the injected fluid, as expected in an injection.

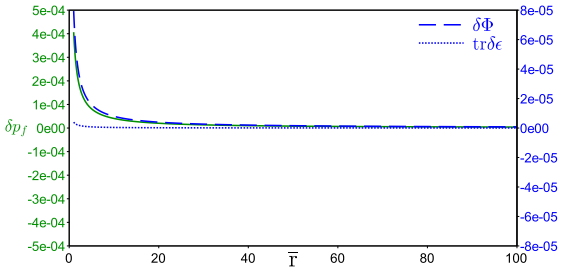

(a) $Q_F > 0$, $\delta p_f^{\text{inj}} = 0$, $\delta \rho_c^{\text{inj}} = 0$, $\bar{r}_0 = \bar{r}_c = \bar{r}_n = 0$.

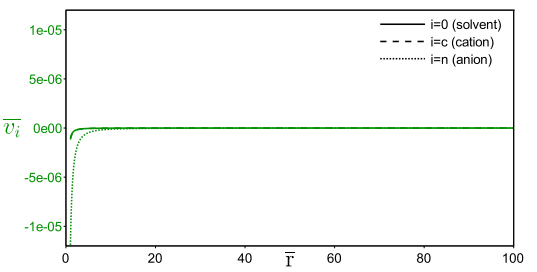

(b) $Q_F > 0$, $\delta p_f^{\text{inj}} = 0$, $\delta \rho_c^{\text{inj}} = 0$, $\bar{r}_0 = \bar{r}_c = \bar{r}_n = 0$.

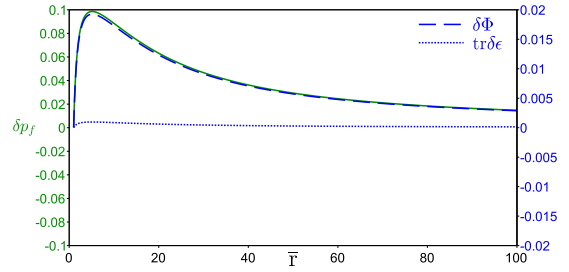

(c) $Q_F > 0$, $\delta p_f^{\text{inj}} = 0$, $\delta \rho_c^{\text{inj}} = 0$, $\bar{r}_0 \cdot \bar{r}_c \cdot \bar{r}_n \neq 0$.

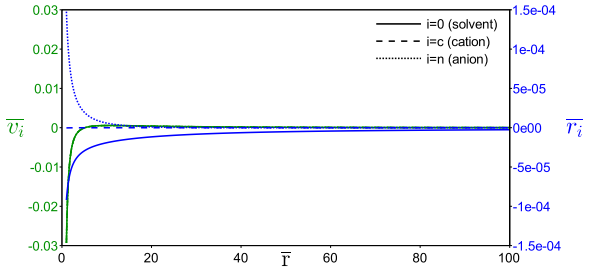

(d) $Q_F > 0$, $\delta p_f^{\text{inj}} = 0$, $\delta \rho_c^{\text{inj}} = 0$, $\bar{r}_0 \cdot \bar{r}_c \cdot \bar{r}_n \neq 0$.

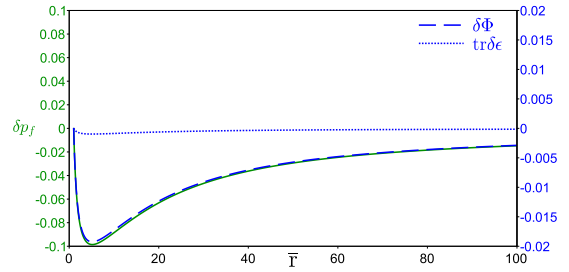

(e) $Q_F < 0$, $\delta p_f^{\text{inj}} = 0$, $\delta \rho_c^{\text{inj}} = 0$, $\bar{r}_0 \cdot \bar{r}_c \cdot \bar{r}_n \neq 0$.

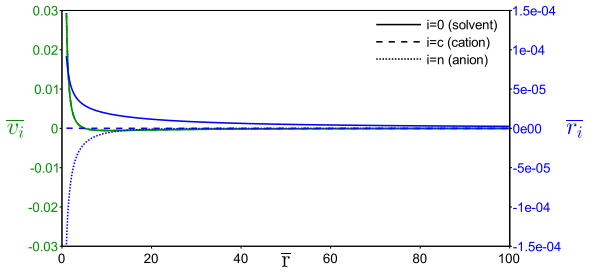

(f) $Q_F < 0$, $\delta p_f^{\text{inj}} = 0$, $\delta \rho_c^{\text{inj}} = 0$, $\bar{r}_0 \cdot \bar{r}_c \cdot \bar{r}_n \neq 0$.

Fig. 5. Importance of accounting for electroneutrality and absorption by adding salt in the cavity ($\delta \rho_c^{inj} = 0, \delta \rho_n^{inj} \neq 0$) but not imposing an injection pressure ($\delta p_f^{inj} = 0$). Three different cases are considered: $Q_F > 0$ without absorption ($\bar{r}_0 = \bar{r}_c = \bar{r}_n = 0$) in (a) and (b), $Q_F > 0$ with absorption ($\bar{r}_0 \cdot \bar{r}_c \cdot \bar{r}_n \neq 0$) in (c) and (d) and $Q_F < 0$ with absorption ($\bar{r}_0 \cdot \bar{r}_c \cdot \bar{r}_n \neq 0$) in (e) and (f). The left vertical axes of graphs (a), (c) and (e) record in solid green line the dimensionless pressure (δp_f) and their right vertical axes record in dashed blue line the porosity change ($\delta \Phi$) and in dotted blue line the skeleton's volume change ($\text{tr}\delta\epsilon$). The left vertical axes of graphs (b), (d) and (f) record the different dimensionless fluid velocities ($\bar{v}_0$, $\bar{v}_n$, $\bar{v}_c$); solid green line corresponds to the solvent fluid ($\bar{v}_0$), dashed green line to the cation velocity ($\bar{v}_c$) and dotted green line to the anion velocity ($\bar{v}_n$) and their right vertical axes record in blue lines the different absorption rates ($\bar{r}_0$ in solid lines, $\bar{r}_c$ in dashed lines and $\bar{r}_n$ in dotted lines). The horizontal axis gives the dimensionless distance $\bar{r}$ away from the cavity-tissue boundary ($\bar{r} = 1$).

8. Conclusion

The goal, as well as the novelty of this work, is the introduction of a thermodynamically consistent, objective and fully coupled continuum chemo-mechanical general theory for subcutaneous injections that considers the interaction of all the important physical mechanisms involved in this procedure. The proposed model, derived via the direct approach of continuum mechanics, using the Coleman–Noll procedure and employing the minimum set of hypotheses, accounts for finite strain poro-mechanics, where an interstitial fluid, carrying different charged species, is diffusing in a flexible porous matrix and absorbed by blood and/or lymph vessels. Electrochemistry is an integral part of the theory, as it generates an osmotic pressure, due to electrical charges attached to the tissue.

Inevitably, such a general nonlinear theory is rather difficult to use and meant for numerical calculations, due to the multitude of physical phenomena at work and the plethora of material parameters involved. It is impossible to obtain analytical results, an essential tool in understanding the influence of the different parameters in such a complex problem. To establish the importance of the full coupling (i.e. electro-chemical and poro-mechanical) in the modeling of a subcutaneous injection, we solve a simplified,

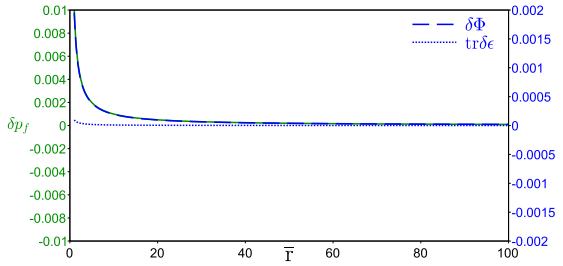

(a) $Q_F = 0$, $\delta p_f^{inj} = 0.01$, $\delta \rho_c^{inj} = 0$, $\bar{r}_0 \cdot \bar{r}_c \cdot \bar{r}_n \neq 0$.

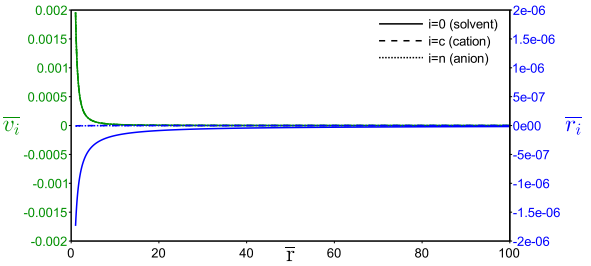

(b) $Q_F = 0$, $\delta p_f^{inj} = 0.01$, $\delta \rho_c^{inj} = 0$, $\bar{r}_0 \cdot \bar{r}_c \cdot \bar{r}_n \neq 0$.

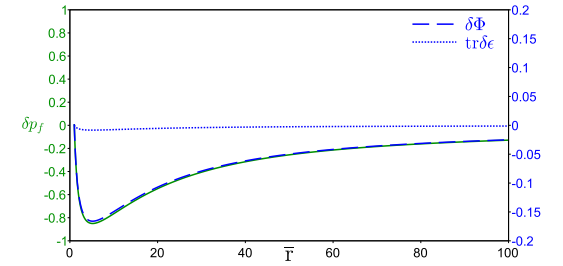

(c) $Q_F > 0$, $\delta p_f^{inj} = 0.01$, $\delta \rho_c^{inj} = 0.01$, $\bar{r}_0 \cdot \bar{r}_c \cdot \bar{r}_n \neq 0$.

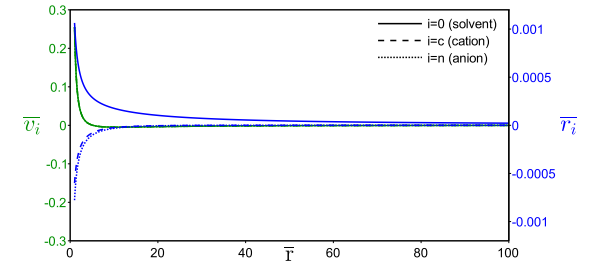

(d) $Q_F > 0$, $\delta p_f^{inj} = 0.01$, $\delta \rho_c^{inj} = 0.01$, $\bar{r}_0 \cdot \bar{r}_c \cdot \bar{r}_n \neq 0$.

Fig. 6. The importance of chemo-mechanical coupling in the presence of injection pressure ($\delta p_f^{inj} = 0.01$). Results for the purely mechanical response ($Q_F = 0$, $\delta \rho_c^{inj} = 0$) in the presence of absorption ($\bar{r}_0 \cdot \bar{r}_c \cdot \bar{r}_n \neq 0$) are presented in (a) and (b). Results for the fully coupled chemo-mechanical response with a positively charged tissue and added Na^+ in the cavity ($Q_F > 0$, $\delta \rho_c^{inj} = 0.01$) in (c) and (d). The left vertical axes of graphs (a) and (c) record in solid green line the dimensionless pressure (δp_f) and their right vertical axes record in dashed blue line the porosity change ($\delta \Phi$) and in dotted blue line the skeleton's volume change (tr$\delta\epsilon$). The left vertical axes of graphs (b) and (d) record the different dimensionless fluid velocities ($\bar{v}_0$, $\bar{v}_n$, $\bar{v}_c$); solid green line corresponds to the solvent fluid ($\bar{v}_0$), dashed green line to the cation velocity ($\bar{v}_c$) and dotted green line to the anion velocity ($\bar{v}_n$) and their right vertical axes record in blue lines the different absorption rates ($\bar{r}_0$ in solid lines, $\bar{r}_c$ in dashed lines and $\bar{r}_n$ in dotted lines). The horizontal axis gives the dimensionless distance $\bar{r}$ away from the cavity-tissue boundary ($\bar{r} = 1$).

linearized model problem that shows the importance of the osmotic efficiency coefficient, the fixed tissue-bound charges in finding the pressure, volume changes, interstitial fluid and chemical species velocities and absorption rates.

The power of the proposed fully coupled, nonlinear theory lies in the thermodynamically consistent inclusion of all the physical mechanisms of subcutaneous injections. Accounting for these couplings is shown to be of high importance for the prediction of subcutaneous injections key performance indicators, as illustrated by the linearized use-case as a proof of principle. By its nature, the model is intended for numerical analysis and the required calculations impose important challenges that constitute the next frontier for future work in this area (e.g. see Barré et al. (2023) for issues related to time-dependent problems in the linear regime.)

CRediT authorship contribution statement

Ludovic Gil: Writing – review & editing, Writing – original draft, Methodology, Investigation, Formal analysis, Conceptualization. **Michel Jabbour:** Writing – review & editing, Writing – original draft, Validation, Methodology, Investigation, Formal analysis, Conceptualization. **Nicolas Triantafyllidis:** Writing – review & editing, Writing – original draft, Validation, Supervision, Methodology, Investigation, Formal analysis, Conceptualization.

Declaration of competing interest

This work was funded by BD (Becton Dickinson and Company) through a CIFRE agreement between BD Medical - Pharmaceutical Systems and the Laboratoire de Mecanique des Solides at the Ecole Polytechnique.

Data availability

No data was used for the research described in the article.

Acknowledgments

This work has been conducted as part of the PhD thesis of the lead author (Gil, 2020) – under a CIFRE agreement between BD Medical - Pharmaceutical Systems and the Laboratoire de Mécanique des Solides at the Ecole Polytechnique – who gratefully acknowledges the help of his colleagues at both institutions.

Appendix A. Derivation details for constitutive restrictions

In this section, we apply the methodology introduced in Gil et al. (2022) to the current framework with the multiple-porosity networks and chemical species. The derivation of reversible restrictions in volume and on the surface are given respectively in Appendices A.1 and A.3, while the non-reversible restrictions are presented in Appendix A.2.

A.1. Constitutive restrictions in volume

The pointwise free-energy imbalance (3.24) for $\mathbf{x} \in \upsilon$ can then be written as

$$
\begin{aligned}
&-\left(\frac{\partial \psi}{\partial \theta}+\eta\right)\dot{\theta}-\frac{\partial \psi}{\partial \boldsymbol{\nabla} m_s}\cdot\dot{\widehat{\boldsymbol{\nabla} m_s}}-\frac{\partial \psi}{\partial \boldsymbol{\nabla} m_f}\cdot\dot{\widehat{\boldsymbol{\nabla} m_f}}-\frac{\partial \psi}{\partial \boldsymbol{\nabla} m_f^a}\cdot\dot{\widehat{\boldsymbol{\nabla} m_f^a}}\\
&-\left[\left(\frac{\partial \psi}{\partial \mathbf{F}}\cdot\mathbf{F}^{\mathsf{T}}\right)^{\mathsf{T}}+\left(\psi-m_s\frac{\partial \psi}{\partial m_s}-m_f\frac{\partial \psi}{\partial m_f}-m_f^a\frac{\partial \psi}{\partial m_f^a}-\sum_{i=1}^{n}\left\{m_i\frac{\partial \psi}{\partial m_i}+m_i^a\frac{\partial \psi}{\partial m_i^a}\right\}\right)\mathbf{I}\right]:\boldsymbol{\nabla}\mathbf{v}_s\\
&-\frac{\partial \psi}{\partial \boldsymbol{\nabla}\theta}\cdot\dot{\widehat{\boldsymbol{\nabla}\theta}}-\frac{\partial \psi}{\partial \mathbf{F}}\vdots\dot{\widehat{\mathbf{F}}}-\frac{\partial \psi}{\partial \mathbf{v}_s}\cdot\dot{\mathbf{v}}_s+\frac{\partial \psi}{\partial m_f}\boldsymbol{\nabla}\cdot\left(m_f\mathbf{v}_r\right)+\frac{\partial \psi}{\partial m_f^a}\boldsymbol{\nabla}\cdot\left(m_f^a\mathbf{v}_r^a\right)\\
&-\sum_{i=1}^{n}\left[\frac{\partial \psi}{\partial \boldsymbol{\nabla} m_i}\cdot\dot{\widehat{\boldsymbol{\nabla} m_i}}+\frac{\partial \psi}{\partial \boldsymbol{\nabla} m_i^a}\cdot\dot{\widehat{\boldsymbol{\nabla} m_i^a}}-\frac{\partial \psi}{\partial m_i}\boldsymbol{\nabla}\cdot\left(\mathbf{j}_i+m_i\mathbf{v}_r\right)-\frac{\partial \psi}{\partial m_i^a}\boldsymbol{\nabla}\cdot\left(\mathbf{j}_i^a+m_i^a\mathbf{v}_r^a\right)\right]\\
&-\boldsymbol{\nabla}\cdot\left(m_f\mathbf{v}_r+m_f^a\mathbf{v}_r^a\right)\frac{\mathbf{v}^2}{2}-(\boldsymbol{\nabla}\cdot\boldsymbol{\sigma})\cdot\mathbf{v}-\boldsymbol{\nabla}\cdot(\mathbf{h}-\mathbf{q})-\frac{\mathbf{q}}{\theta}\cdot\boldsymbol{\nabla}\theta\\
&-r_f\left(\frac{\partial \psi}{\partial m_f}-\frac{\partial \psi}{\partial m_f^a}\right)-\sum_{i=1}^{n}r_i\left(\frac{\partial \psi}{\partial m_i}-\frac{\partial \psi}{\partial m_i^a}\right)\geq 0.
\end{aligned}
\tag{A.1}
$$

For the sake of simplicity in the subsequent derivations, we define the *relative chemical potentials* as

$$
\mu_s(\mathcal{L}):=\frac{\partial \psi}{\partial m_s},\ \mu_f(\mathcal{L}):=\frac{\partial \psi}{\partial m_f},\ \mu_f^a(\mathcal{L}):=\frac{\partial \psi}{\partial m_f^a},\quad \mu_i(\mathcal{L}):=\frac{\partial \psi}{\partial m_i},\ \mu_i^a(\mathcal{L}):=\frac{\partial \psi}{\partial m_i^a},\ 1\leq i\leq n,
\tag{A.2}
$$

and also the *absolute chemical potentials* as[32]

$$
\tilde{\mu}_0(\mathcal{L}):=\mu_f,\ \tilde{\mu}_0^a(\mathcal{L}):=\mu_f^a,\quad \tilde{\mu}_i(\mathcal{L}):=\mu_i+\mu_f,\ \tilde{\mu}_i^a(\mathcal{L}):=\mu_i^a+\mu_f^a,\ 1\leq i\leq n.
\tag{A.3}
$$

Note that in this work, the *chemical potentials are introduced as a renaming of variables* as also proposed by Gurtin (1971) and Gurtin and Vargas (1971).

Results using arbitrary time rates

In order to extract all the reversible constitutive restrictions from (A.1), we will first consider the arbitrary variations of the time-rates in the set $\mathcal{L}^\star$ defined in (4.3). Given any admissible set $\mathcal{L}$, the quantities $\dot{\theta}$, $\dot{\widehat{\boldsymbol{\nabla} m_s}}$, $\dot{\widehat{\boldsymbol{\nabla} m_f}}$, $\dot{\widehat{\boldsymbol{\nabla} m_f}}$, $\dot{\widehat{\boldsymbol{\nabla} m_i}}$, $\dot{\widehat{\boldsymbol{\nabla} m_i^a}}$, $\dot{\widehat{\boldsymbol{\nabla}\theta}}$, $\dot{\widehat{\mathbf{F}}}$ and $\dot{\mathbf{v}}_s$ can be assigned arbitrarily and only appear linearly in (A.1), obtaining the following necessary (equality) restrictions

$$
\begin{aligned}
&\frac{\partial \psi}{\partial \boldsymbol{\nabla} m_s}=\frac{\partial \psi}{\partial \boldsymbol{\nabla} m_f}=\frac{\partial \psi}{\partial \boldsymbol{\nabla} m_f^a}=\mathbf{0},\quad \frac{\partial \psi}{\partial \boldsymbol{\nabla} m_i}=\frac{\partial \psi}{\partial \boldsymbol{\nabla} m_i^a}=\mathbf{0},\ 1\leq i\leq n,\\
&\eta=-\frac{\partial \psi}{\partial \theta},\quad \frac{\partial \psi}{\partial \boldsymbol{\nabla}\theta}=\mathbf{0},\quad \frac{\partial \psi}{\partial \mathbf{F}}=\mathbf{0},\quad \frac{\partial \psi}{\partial \mathbf{v}_s}=\mathbf{0},
\end{aligned}
\tag{A.4}
$$

implying that the free energy ψ is independent of $\boldsymbol{\nabla} m_s$, $\boldsymbol{\nabla} m_f$, $\boldsymbol{\nabla} m_f^a$, $\boldsymbol{\nabla} m_i$, $\boldsymbol{\nabla} m_i^a$, $\boldsymbol{\nabla}\theta$, $\mathbf{F}$ and $\mathbf{v}_s$. We further assume here that the material is isotropic and hence ψ and all the other fields are a function of $\mathbf{B}:=\mathbf{F}\cdot\mathbf{F}^{\mathsf{T}}$, the left Cauchy–Green tensor, instead of $\mathbf{F}$. Moreover, requiring the *Helmholtz*[33] *free energy* ψ to be objective, it must depend on the invariants $\mathcal{I}(\mathbf{B})$

$$
\psi=\psi(S,\mathbf{B})=\psi\left(m_s,m_f,m_f^a,\{m_i\}_1^n,\{m_i^a\}_1^n,\theta,\mathcal{I}(\mathbf{B})\right).
\tag{A.5}
$$

[32] Here, we follow the terminology used by Gurtin and Vargas (1971) and Fried and Gurtin (1999). Indeed, our expression of μ_i corresponds to the definition of the *relative chemical potential* in their work.

[33] We can now use this terminology since ψ is independent of velocities.

Note that (A.5) implies from (A.2) the same dependence for the chemical potentials

$$\mu_s = \mu_s(\mathcal{S}, \mathcal{I}(\mathbf{B})), \quad \mu_f = \mu_f(\mathcal{S}, \mathcal{I}(\mathbf{B})), \quad \mu_f^a = \mu_f^a(\mathcal{S}, \mathcal{I}(\mathbf{B})),$$
$$\mu_i = \mu_i(\mathcal{S}, \mathcal{I}(\mathbf{B})), \quad \mu_i^a = \mu_i^a(\mathcal{S}, \mathcal{I}(\mathbf{B})), \quad 1 \le i \le n, \tag{A.6}$$

and (A.1) can now be simplified to

$$\left(\boldsymbol{\sigma}^\star - \boldsymbol{\sigma}^e\right) : \boldsymbol{\nabla}\mathbf{v}_s + \boldsymbol{\sigma}^\star : \boldsymbol{\nabla}\left(c_f \mathbf{v}_r + c_f^a \mathbf{v}_r^a\right) - \boldsymbol{\nabla}\cdot\tilde{\mathbf{k}} - \sum_{i=1}^n \left(\mathbf{j}_i \cdot \boldsymbol{\nabla}\mu_i + \mathbf{j}_i^a \cdot \boldsymbol{\nabla}\mu_i^a\right)$$
$$-m_f \mathbf{v}_r \cdot \boldsymbol{\nabla}\mu_f - m_f^a \mathbf{v}_r^a \cdot \boldsymbol{\nabla}\mu_f^a - \frac{\mathbf{q}}{\theta}\cdot\boldsymbol{\nabla}\theta - \sum_{i=0}^n r_i\left(\tilde{\mu}_i - \tilde{\mu}_i{}^a\right) \ge 0, \tag{A.7}$$

where, the following grouping of terms have been identified: an *elastic stress tensor* $\boldsymbol{\sigma}^e$ and a *symmetrized stress tensor* $\boldsymbol{\sigma}^\star$[34]

$$\boldsymbol{\sigma}^e := 2\mathbf{B}\cdot\frac{\partial\psi}{\partial\mathbf{B}} + \left(\psi - m_s\mu_s - m_f\mu_f - m_f^a\mu_f^a - \sum_{i=1}^n \left\{m_i\mu_i + m_i^a\mu_i^a\right\}\right)\mathbf{I} = (\boldsymbol{\sigma}^e)^{\intercal},$$
$$\boldsymbol{\sigma}^\star := \boldsymbol{\sigma} + \left(m_f\mathbf{v}_r + m_f^a\mathbf{v}_r^a\right)\mathbf{v} = (\boldsymbol{\sigma}^\star)^{\intercal}, \tag{A.8}$$

and we have also introduced an *inertially modified* energy flux vector $\tilde{\mathbf{k}}$, related to the energy flux vector $\mathbf{h}$

$$\tilde{\mathbf{k}} := \mathbf{h} - \mathbf{q} - \left(m_f\mu_f + \sum_{i=1}^n m_i\mu_i\right)\mathbf{v}_r - \left(m_f^a\mu_f^a + \sum_{i=1}^n m_i\mu_i\right)\mathbf{v}_r^a$$
$$-\sum_{i=1}^n \left(\mu_i\mathbf{j}_i + \mu_i^a\mathbf{j}_i^a\right) + \boldsymbol{\sigma}^\star\cdot\mathbf{v} - \frac{\mathbf{v}^2}{2}\left(m_f\mathbf{v}_r + m_f^a\mathbf{v}_r^a\right). \tag{A.9}$$

At this point we require that $\boldsymbol{\sigma}^\star$ and $\tilde{\mathbf{k}}$ to be objective fields and hence to not depend on $\mathbf{v}_s$. It is shown in Gil et al. (2022) that there is no loss of generality in making such a hypothesis at this point of the derivation. Consequently, the term $\boldsymbol{\nabla}\mathbf{v}_s$ appears now linearly in (A.7) and, making it vary arbitrarily,[35] we obtain

$$\boldsymbol{\sigma}^\star = \boldsymbol{\sigma}^e. \tag{A.10}$$

Moreover, all the remaining terms of (A.7) are now constitutive and hence required to be objective, giving

$$-\boldsymbol{\nabla}\cdot\mathbf{k} - \frac{\mathbf{q}}{\theta}\cdot\boldsymbol{\nabla}\theta - \sum_{i=1}^n \mathbf{j}_i\cdot\boldsymbol{\nabla}\mu_i - \mathbf{v}_r\cdot\left[c_f\boldsymbol{\nabla}\cdot\boldsymbol{\sigma}^e + m_f\boldsymbol{\nabla}\mu_f + \sum_{i=1}^n m_i\boldsymbol{\nabla}\mu_i\right]$$
$$-\sum_{i=1}^n \mathbf{j}_i^a\cdot\boldsymbol{\nabla}\mu_i^a - \mathbf{v}_r^a\cdot\left[c_f^a\boldsymbol{\nabla}\cdot\boldsymbol{\sigma}^e + m_f^a\boldsymbol{\nabla}\mu_f^a + \sum_{i=1}^n m_i^a\boldsymbol{\nabla}\mu_i^a\right] - \sum_{i=0}^n r_i\left(\tilde{\mu}_i - \tilde{\mu}_i{}^a\right) \ge 0, \tag{A.11}$$

where we have defined

$$\mathbf{k} := \tilde{\mathbf{k}} - \boldsymbol{\sigma}^e\cdot\left(c_f\mathbf{v}_r + c_f^a\mathbf{v}_r^a\right). \tag{A.12}$$

The first step of the procedure is not complete yet since we have not exploited all the arbitrary quantities.

Results using arbitrary second order gradients

In order to advance further in the exploitation of (A.11), we recall the material frame indifference principle and the hypothesis of isotropy[36] made in (A.5). Following a rather lengthy manipulation, with details provided in the Appendix of Gil et al. (2022), we show that the constitutive vector $\mathbf{k}(\mathcal{L}_O)$ defined in (A.12) vanishes identically

$$\mathbf{k}(\mathcal{L}_O) = \mathbf{0}, \tag{A.13}$$

thus providing the expression for the sought objective energy flux vector $\mathbf{h}(\mathcal{L}_O)$ introduced in (3.18)

$$\mathbf{h} = \mathbf{q} + \frac{\mathbf{v}^2}{2}\left(m_f\mathbf{v}_r + m_f^a\mathbf{v}_r^a\right) - \boldsymbol{\sigma}^e\cdot\mathbf{v}_s$$
$$+\sum_{i=1}^n \mu_i\mathbf{j}_i + \left(m_f\mu_f + \sum_{i=1}^n m_i\mu_i\right)\mathbf{v}_r + \sum_{i=1}^n \mu_i^a\mathbf{j}_i^a + \left(m_f^a\mu_f^a + \sum_{i=1}^n m_i^a\mu_i^a\right)\mathbf{v}_r^a. \tag{A.14}$$

[34] The symmetry of $\boldsymbol{\sigma}^e$ follows by the isotropy of ψ and the symmetry of $\boldsymbol{\sigma}^\star$ follows from angular momentum in (3.17) and the definition of $\mathbf{v}$ in (2.6).

[35] See footnote 21 on the equivalence between the independently assigned time rate quantities $\boldsymbol{\nabla}\mathbf{v}_s$ and $\dot{\mathbf{F}}$ of $\mathcal{L}^\star$.

[36] Although a restrictive hypothesis, it allows us to find a unique energy flux $\mathbf{h}$ using the principle of material frame indifference.

This completes the first step of the procedure providing the necessary conditions, constitutive equalities for the entropy η, free energy ψ, stress $\boldsymbol{\sigma}$ and flux vectors $\mathbf{h}$ and $\mathbf{q}$ in $\mathbf{x} \in \upsilon$. The remaining terms in the entropy imbalance (A.11) represent the *dissipation* D of the system

$$\begin{aligned} D(\mathcal{L}_O) := \; & -\frac{\mathbf{q}}{\theta}\cdot\boldsymbol{\nabla}\theta - \mathbf{v}_r\cdot\left[c_f\boldsymbol{\nabla}\cdot\boldsymbol{\sigma}^e + m_f\boldsymbol{\nabla}\mu_f + \sum_{i=1}^{n} m_i\boldsymbol{\nabla}\mu_i\right] - \sum_{i=1}^{n}\mathbf{j}_i\cdot\boldsymbol{\nabla}\mu_i \\ & -\mathbf{v}_r^a\cdot\left[c_f^a\boldsymbol{\nabla}\cdot\boldsymbol{\sigma}^e + m_f^a\boldsymbol{\nabla}\mu_f^a + \sum_{i=1}^{n} m_i^a\boldsymbol{\nabla}\mu_i^a\right] - \sum_{i=1}^{n}\mathbf{j}_i^a\cdot\boldsymbol{\nabla}\mu_i^a - \sum_{i=0}^{n} r_i\left(\tilde{\mu}_i - \tilde{\mu}_i{}^a\right) \geq 0. \end{aligned} \tag{A.15}$$

The second step of the procedure extracts additional information from (A.15) and is presented in Appendix A.2.

A.2. Sufficient restrictions

We proceed with the second step of the procedure, described in Gil et al. (2022), starting from the positive dissipation inequality (A.15) and seeking restrictions on the admissible expressions for the constitutive vector fields $\mathbf{q}$, $\mathbf{v}_r$, $\mathbf{v}_r^a$, $\{\mathbf{j}_i\}_1^n$ and $\{\mathbf{j}_i^a\}_1^n$, designated henceforth by a generic symbol $\mathbf{v}(\mathcal{L}_O)$ and the scalar absorption/release mass rates of the chemicals r_i. We require these fields to be objective for any orthogonal tensor $\mathbf{Q} \in O(3)$,[37] which implies

$$\mathbf{Q}\cdot\mathbf{v}(\mathcal{S},\mathcal{G},\mathbf{B},\boldsymbol{\nabla}\mathbf{B}) = \mathbf{v}(\mathcal{S},\mathbf{Q}\cdot\mathcal{G},\mathbf{Q}\cdot\mathbf{B}\cdot\mathbf{Q}^{\intercal},\mathbf{Q}\cdot(\mathbf{Q}\cdot\boldsymbol{\nabla}\mathbf{B}\cdot\mathbf{Q}^{\intercal})). \tag{A.16}$$

Taking the particular case of $\mathbf{Q} = -\mathbf{I}$ (see discussion around equation (3.16) of Coleman and Noll (1963))

$$-\mathbf{v}(\mathcal{S},\mathcal{G},\mathbf{B},\boldsymbol{\nabla}\mathbf{B}) = \mathbf{v}(\mathcal{S},-\mathcal{G},\mathbf{B},-\boldsymbol{\nabla}\mathbf{B}). \tag{A.17}$$

Defining as homogeneous the state where the gradients of state variables vanish, i.e. $\mathcal{L}_O^h \subset \mathcal{L}_O$ (see definition in (4.1)), where $\mathcal{L}_O^h := \{\mathcal{S},\mathbf{0},\mathbf{B},\mathbf{0}\}$, (A.17) leads to the following conditions for $\mathbf{v}$ and its derivatives $\partial\mathbf{v}/\partial s$ evaluated at $\mathcal{L}_O^h$

$$\mathbf{v}|_{\mathcal{L}_O^h} = \mathbf{0}, \quad \left.\frac{\partial\mathbf{v}}{\partial s}\right|_{\mathcal{L}_O^h} = \mathbf{0}, \;\; \forall s \in \mathcal{S}. \tag{A.18}$$

Accounting for $(A.18)_1$, the remaining dissipation inequality (A.15) yields

$$-\sum_{i=0}^{n} r_i|_{\mathcal{L}_O^h}\left(\tilde{\mu}_i|_{\mathcal{L}_O^h} - \tilde{\mu}_i^a|_{\mathcal{L}_O^h}\right) \geq 0. \tag{A.19}$$

Moreover, since $r_i(\mathcal{L}_O)$ are required to be objective, the following conditions also hold:

$$\left.\frac{\partial r_i}{\partial\mathbf{g}}\right|_{\mathcal{L}_O^h} = \mathbf{0}, \;\; \forall\mathbf{g}\in\mathcal{G}, \quad \left.\frac{\partial r_i}{\partial\boldsymbol{\nabla}\mathbf{B}}\right|_{\mathcal{L}_O^h} = \mathbf{0}, \;\; 1 \leq i \leq n. \tag{A.20}$$

Due to objectivity and isotropy, the scalars r_i depend on the invariants $\mathcal{I}_1(\mathbf{B})$, $\mathcal{I}_2(\mathbf{B})$, $\mathcal{I}_3(\mathbf{B})$. Following Gurtin and Vargas (1971), we define an *equilibrium state* $\mathcal{L}_O^{h,e} := \{\mathcal{S}^e,\mathbf{0},\mathbf{B}^e,\mathbf{0}\}$ as the homogeneous state for which the absorption/release mass rates of the chemicals vanish

$$r_i|_{\mathcal{L}_O^{h,e}} = 0, \;\; 0 \leq i \leq n. \tag{A.21}$$

Accounting for the consequences of objectivity enumerated in (A.18) and (A.20), one can write the following Taylor expansion about the equilibrium state $\mathcal{L}_O^{h,e}$

$$\begin{aligned} \mathbf{v}(\mathcal{L}_O) &= \sum_{\mathbf{g}\in\mathcal{G}} \left.\frac{\partial\mathbf{v}}{\partial\mathbf{g}}\right|_{\mathcal{L}_O^{h,e}}\cdot\mathbf{g} + \left.\frac{\partial\mathbf{v}}{\partial\boldsymbol{\nabla}\mathbf{B}}\right|_{\mathcal{L}_O^{h,e}} \vdots\, \boldsymbol{\nabla}\mathbf{B} + O\left((\delta^e)^2\right), \\ r_i(\mathcal{L}_O) &= \sum_{s\in\mathcal{S}} \left.\frac{\partial r_i}{\partial s}\right|_{\mathcal{L}_O^{h,e}}(s-s^e) + \sum_{k=1}^{3} \left.\frac{\partial r_i}{\partial\mathcal{I}_k}\right|_{\mathcal{L}_O^{h,e}}\left(\mathcal{I}_k(\mathbf{B}) - \mathcal{I}_k(\mathbf{B}^e)\right) + O\left((\delta^e)^2\right), \;\; 0 \leq i \leq n, \end{aligned} \tag{A.22}$$

where $\delta^e := \left|\mathcal{L}_O - \mathcal{L}_O^{h,e}\right|$.

One can write the Taylor expansions close to an equilibrium state for the chemical potentials

$$\mu - \mu^e = \sum_{s\in\mathcal{S}} \left.\frac{\partial\mu}{\partial s}\right|_{\mathcal{L}_O^{h,e}}(s-s^e) + \sum_{k=1}^{3} \left.\frac{\partial\mu}{\partial\mathcal{I}_k}\right|_{\mathcal{L}_O^{h,e}}\left(\mathcal{I}_k - \mathcal{I}_k^e\right) + O\left(\left|\mathcal{L}_O - \mathcal{L}_O^{h,e}\right|^2\right), \tag{A.23}$$

where μ stands for either one of the chemical potentials μ_s, μ_f, μ_f^a, μ_i, μ_i^a and μ^e for their corresponding equilibrium counterparts, i.e. μ_s^e, μ_f^e, $\mu_f^{a,e}$, μ_i^e, $\mu_i^{a,e}$. Similarly for the gradients of the chemical potentials and the divergence of the elastic stress $\boldsymbol{\nabla}\cdot\boldsymbol{\sigma}^e$ one has

[37] Where $O(3)$ is the set of all orthogonal rank two tensors $\mathbf{Q}$, i.e. $\mathbf{Q}\cdot\mathbf{Q}^{\intercal} = 1$, where $\det\mathbf{Q} = \pm 1$.

the expansions

$$\begin{aligned}
\nabla\mu &= \sum_{s\in\mathcal{S}} \left.\frac{\partial\mu}{\partial s}\right|_{\mathcal{L}_O^{h,e}} \nabla s + \sum_{k=1}^{3} \left.\frac{\partial\mu}{\partial \mathcal{I}_k}\right|_{\mathcal{L}_O^{h,e}} \nabla \mathcal{I}_k + O\left(\left|\mathcal{L}_O - \mathcal{L}_O^{h,e}\right|^2\right),\\
\nabla\cdot\boldsymbol{\sigma}^e &= \sum_{s\in\mathcal{S}} \left.\frac{\partial(\nabla\cdot\boldsymbol{\sigma}^e)}{\partial s}\right|_{\mathcal{L}_O^{h,e}} \nabla s + \sum_{k=1}^{3} \left.\frac{\partial(\nabla\cdot\boldsymbol{\sigma}^e)}{\partial \mathcal{I}_k}\right|_{\mathcal{L}_O^{h,e}} \nabla \mathcal{I}_k + O\left(\left|\mathcal{L}_O - \mathcal{L}_O^{h,e}\right|^2\right).
\end{aligned} \tag{A.24}$$

As in Gurtin and Vargas (1971) and Gil et al. (2022), we assume that the systems (A.23) and (A.24) are invertible such that we can write the following Taylor expansions up to order $O\left(\left|\mathcal{L}_O - \mathcal{L}_O^{h,e}\right|^2\right)$ close to the equilibrium state

$$\begin{aligned}
&\mathbf{q} = -\mathbf{K}_{\theta,\theta}\cdot\nabla\theta - \mathbf{K}_{\theta,s}\cdot\nabla\mu_s - \mathbf{K}_{\theta,f}\cdot\nabla\mu_f - \mathbf{K}_{\theta,p}\cdot\nabla p - \mathbf{K}_{\theta,p^a}\cdot\nabla p^a - \sum_{j=1}^{n}\left\{\mathbf{K}_{\theta,j}\cdot\nabla\mu_j + \mathbf{K}_{\theta,j^a}\cdot\nabla\mu_j^a\right\},\\
&\mathbf{v}_r = -\mathbf{K}_{f,\theta}\cdot\nabla\theta - \mathbf{K}_{f,s}\cdot\nabla\mu_s - \mathbf{K}_{f,f}\cdot\nabla\mu_f - \mathbf{K}_{f,p}\cdot\nabla p - \mathbf{K}_{f,p^a}\cdot\nabla p^a - \sum_{j=1}^{n}\left\{\mathbf{K}_{f,j}\cdot\nabla\mu_j + \mathbf{K}_{f,j^a}\cdot\nabla\mu_j^a\right\},\\
&\mathbf{v}_r^a = -\mathbf{K}_{f^a,\theta}\cdot\nabla\theta - \mathbf{K}_{f^a,s}\cdot\nabla\mu_s - \mathbf{K}_{f^a,f}\cdot\nabla\mu_f - \mathbf{K}_{f^a,p}\cdot\nabla p - \mathbf{K}_{f^a,p^a}\cdot\nabla p^a - \sum_{j=1}^{n}\left\{\mathbf{K}_{f^a,j}\cdot\nabla\mu_j + \mathbf{K}_{f^a,j^a}\cdot\nabla\mu_j^a\right\},\\
&1\le i\le n,\\
&\mathbf{j}_i = -\mathbf{K}_{i,\theta}\cdot\nabla\theta - \mathbf{K}_{i,s}\cdot\nabla\mu_s - \mathbf{K}_{i,f}\cdot\nabla\mu_f - \mathbf{K}_{i,p}\cdot\nabla p - \mathbf{K}_{i,p^a}\cdot\nabla p^a - \sum_{j=1}^{n}\left\{\mathbf{K}_{i,j}\cdot\nabla\mu_j + \mathbf{K}_{i,j^a}\cdot\nabla\mu_j^a\right\},\\
&\mathbf{j}_i^a = -\mathbf{K}_{i^a,\theta}\cdot\nabla\theta - \mathbf{K}_{i^a,s}\cdot\nabla\mu_s - \mathbf{K}_{i^a,f}\cdot\nabla\mu_f - \mathbf{K}_{i^a,p}\cdot\nabla p - \mathbf{K}_{i^a,p^a}\cdot\nabla p^a - \sum_{j=1}^{n}\left\{\mathbf{K}_{i^a,j}\cdot\nabla\mu_j + \mathbf{K}_{i^a,j^a}\cdot\nabla\mu_j^a\right\},\\
&0\le i\le n,\\
&r_i = -\mathsf{R}_{i,\theta}(\theta-\theta^e) - \sum_{j=0}^{n}\left\{\mathsf{R}_{i,j}\left[\tilde{\mu}_j - \tilde{\mu}_j{}^a - \left(\tilde{\mu}_j{}^e - \tilde{\mu}_j{}^{a,e}\right)\right] + \mathsf{R}_{i,j^a}\left(\tilde{\mu}_j{}^a - \tilde{\mu}_j{}^{a^e}\right)\right\} - \mathsf{R}_{i,s}\left(\mu_s-\mu_s^e\right) - \sum_{k=1}^{3}\mathsf{R}_{i,\mathcal{I}_k}\left(\mathcal{I}_k - \mathcal{I}_k^e\right),
\end{aligned} \tag{A.25}$$

where the following auxiliary notations have been introduced

$$\nabla p := c_f\nabla\cdot\boldsymbol{\sigma}^e + m_f\nabla\mu_f + \sum_{i=1}^{n} m_i\nabla\mu_i, \quad \nabla p^a := c_f^a\nabla\cdot\boldsymbol{\sigma}^e + m_f^a\nabla\mu_f^a + \sum_{i=1}^{n} m_i^a\nabla\mu_i^a. \tag{A.26}$$

Note that when writing the Taylor expansions (A.25), we have already grouped some terms in order to simplify the subsequent algebra. There is no loss of generality in using these expressions modulo a redefinition of the expansion coefficients. In particular, the reader can notice that there is no explicit term in $\nabla\mu_f^a$ in (A.25) since it is embedded in the definition of ∇p^a while there is an explicit dependence of $\nabla\mu_f$ as it is necessary to be able to account for the variations of $\nabla\cdot\boldsymbol{\sigma}$ in ∇p. Substituting (A.25) into the dissipation (A.15) gives

$$\begin{aligned}
&\theta^{-1}\left[\mathbf{K}_{\theta,\theta}\cdot\nabla\theta + \mathbf{K}_{\theta,s}\cdot\nabla\mu_s + \mathbf{K}_{\theta,f}\cdot\nabla\mu_f + \mathbf{K}_{\theta,p}\cdot\nabla p + \mathbf{K}_{\theta,p^a}\cdot\nabla p^a + \sum_{j=1}^{n}\left\{\mathbf{K}_{\theta,j}\cdot\nabla\mu_j + \mathbf{K}_{\theta,j^a}\cdot\nabla\mu_j^a\right\}\right]\cdot\nabla\theta\\
&+\left[\mathbf{K}_{f,\theta}\cdot\nabla\theta + \mathbf{K}_{f,s}\cdot\nabla\mu_s + \mathbf{K}_{f,f}\cdot\nabla\mu_f + \mathbf{K}_{f,p}\cdot\nabla p + \mathbf{K}_{f,p^a}\cdot\nabla p^a + \sum_{j=1}^{n}\left\{\mathbf{K}_{f,j}\cdot\nabla\mu_j + \mathbf{K}_{f,j^a}\cdot\nabla\mu_j^a\right\}\right]\cdot\nabla p\\
&+\sum_{i=1}^{n}\left[\mathbf{K}_{i,\theta}\cdot\nabla\theta + \mathbf{K}_{i,s}\cdot\nabla\mu_s + \mathbf{K}_{i,f}\cdot\nabla\mu_f + \mathbf{K}_{i,p}\cdot\nabla p + \mathbf{K}_{i,p^a}\cdot\nabla p^a + \sum_{j=1}^{n}\left\{\mathbf{K}_{i,j}\cdot\nabla\mu_j + \mathbf{K}_{i,j^a}\cdot\nabla\mu_j^a\right\}\right]\cdot\nabla\mu_i\\
&+\left[\mathbf{K}_{f^a,\theta}\cdot\nabla\theta + \mathbf{K}_{f^a,s}\cdot\nabla\mu_s + \mathbf{K}_{f^a,f}\cdot\nabla\mu_f + \mathbf{K}_{f^a,p}\cdot\nabla p + \mathbf{K}_{f^a,p^a}\cdot\nabla p^a + \sum_{j=1}^{n}\left\{\mathbf{K}_{f^a,j}\cdot\nabla\mu_j + \mathbf{K}_{f^a,j^a}\cdot\nabla\mu_j^a\right\}\right]\cdot\nabla p^a\\
&+\sum_{i=1}^{n}\left[\mathbf{K}_{i^a,\theta}\cdot\nabla\theta + \mathbf{K}_{i^a,s}\cdot\nabla\mu_s + \mathbf{K}_{i^a,f}\cdot\nabla\mu_f + \mathbf{K}_{i^a,p}\cdot\nabla p + \mathbf{K}_{i^a,p^a}\cdot\nabla p^a + \sum_{j=1}^{n}\left\{\mathbf{K}_{i^a,j}\cdot\nabla\mu_j + \mathbf{K}_{i^a,j^a}\cdot\nabla\mu_j^a\right\}\right]\cdot\nabla\mu_i^a\\
&+\sum_{i=0}^{n}\left[\mathsf{R}_{i,\theta}(\theta-\theta^e) + \sum_{j=0}^{n}\left\{\mathsf{R}_{i,j}\left[\tilde{\mu}_j - \tilde{\mu}_j{}^a - \left(\tilde{\mu}_j{}^e - \tilde{\mu}_j{}^{a,e}\right)\right] + \mathsf{R}_{i,j^a}\left(\tilde{\mu}_j{}^a - \tilde{\mu}_j{}^{a^e}\right)\right\}\right.\\
&\qquad\left.+\mathsf{R}_{i,s}\left(\mu_s-\mu_s^e\right) + \sum_{k=1}^{3}\mathsf{R}_{i,\mathcal{I}_k}\left(\mathcal{I}_k - \mathcal{I}_k^e\right)\right]\left(\tilde{\mu}_i - \tilde{\mu}_i{}^a\right) \ge 0.
\end{aligned} \tag{A.27}$$

Requiring the inequality (A.27) to hold for any arbitrarily small values of $\nabla\theta$, $\nabla\mu_s$, $\nabla\mu_f$, ∇p, $\nabla\mu_i$, ∇p^a, $\nabla\mu_i^a$, $\theta-\theta^e$, $\left[\tilde{\mu}_j - \tilde{\mu}_j{}^a - \left(\tilde{\mu}_j{}^e - \tilde{\mu}_j{}^{a,e}\right)\right]$, $\tilde{\mu}_j{}^a - \tilde{\mu}_j{}^{a^e}$, $\mu_s-\mu_s^e$ and $\mathcal{I}_k - \mathcal{I}_k^e$, we obtain the conditions

$$\begin{aligned}
&\mathbf{K}_{\theta,s} = \mathbf{K}_{\theta,f} = \mathbf{0}, \quad \mathbf{K}_{f,s} = \mathbf{K}_{f^a,s} = \mathbf{K}_{f,f} = \mathbf{K}_{f^a,f} = \mathbf{0}, \quad \mathbf{K}_{i,s} = \mathbf{K}_{i^a,s} = \mathbf{K}_{i,f} = \mathbf{K}_{i^a,f} = \mathbf{0}, \qquad 1\le i\le n,\\
&\mathsf{R}_{i,\theta} = 0, \quad \mathsf{R}_{i,ja} = \mathsf{R}_{i,s} = 0, \quad \mathsf{R}_{i,\mathcal{I}_k} = 0, \qquad 0\le i\le n, \quad 0\le j\le n, \quad 1\le k\le 3,
\end{aligned} \tag{A.28}$$

which yields the expression (4.10). Moreover, by (A.23), we have

$$\tilde{\mu}_i - \tilde{\mu}_i{}^a = \tilde{\mu}_i{}^e - \tilde{\mu}_i{}^{a,e} + O\left(\left|\mathcal{L}_O - \mathcal{L}_O^{h,e}\right|\right), \quad 0 \le i \le n. \tag{A.29}$$

Substituting $(A.25)_6$ and (A.29) into (A.19) in an homogeneous state and accounting for $(A.28)_4$, $(A.28)_5$, $(A.28)_6$ give

$$\sum_{i,j=0}^{n} \mathsf{R}_{i,j}\left[\tilde{\mu}_j - \tilde{\mu}_j{}^a - \left(\tilde{\mu}_j{}^e - \tilde{\mu}_j{}^{a,e}\right)\right]\left(\tilde{\mu}_i{}^e - \tilde{\mu}_i{}^{a,e}\right) + O\left(\left|\mathcal{L}_O^h - \mathcal{L}_O^{h,e}\right|^2\right) \ge 0. \tag{A.30}$$

Since (A.30) must hold for any $\left[\tilde{\mu}_j - \tilde{\mu}_j{}^a - \left(\tilde{\mu}_j{}^e - \tilde{\mu}_j{}^{a,e}\right)\right]$, the following restriction holds

$$\sum_{i=0}^{n} \mathsf{R}_{i,j}\left(\tilde{\mu}_i{}^e - \tilde{\mu}_i{}^{a,e}\right) = 0, \quad 0 \le j \le n, \tag{A.31}$$

thus proving the restriction (4.14).

A.3. Constitutive restrictions on surface

As seen in Section 3, there are interface conditions associated respectively with the mass balances, linear momentum balance, energy balance and entropy imbalance. Substituting the expression (A.14) in (3.24), and making use of (2.4), (A.10), $(3.4)_2$, $(3.10)_2$, $(3.6)_2$, $(3.12)_2$ and $(3.15)_2$, the pointwise free-energy imbalance (3.24) for $\mathbf{x} \in \hat{\mathsf{s}}$ yields

$$\begin{aligned} &\dot{\psi}_{\hat{\mathsf{s}}} + \eta_{\hat{\mathsf{s}}}\dot{\theta} - \boldsymbol{\sigma}_{\hat{\mathsf{s}}} : \left(\boldsymbol{\nabla}_{\hat{\mathsf{s}}}\mathbf{v}_s\right) + \sum_{i=1}^{n}\left\{\mathbf{n}\cdot\left(\mathbf{j}_i + m_i\mathbf{v}_r\right)[\![\mu_i]\!] + \mathbf{n}\cdot\left(\mathbf{j}_i^a + m_i^a\mathbf{v}_r^a\right)[\![\mu_i^a]\!]\right\} \\ &+\mathbf{n}\cdot\left(m_f\mathbf{v}_r\right)\left[\!\left[\mu_f + \left(c_f\mathbf{v}_r\right)^2/2\right]\!\right] + \mathbf{n}\cdot\left(m_f^a\mathbf{v}_r^a\right)\left[\!\left[\mu_f^a + \left(c_f^a\mathbf{v}_r^a\right)^2/2\right]\!\right] \le 0. \end{aligned} \tag{A.32}$$

The inequality (A.32) must hold for any admissible thermodynamic process. Following the framework of Gurtin and Jabbour (2002) for moving interface and assuming without loss of generality, an elastic membrane on the surface s with $\psi_{\hat{\mathsf{s}}}(\mathbf{F}_{\mathsf{s}}, \theta)$, one obtains the constitutive equalities for the surface entropy $\eta_{\hat{\mathsf{s}}}$ and stress tensor $\boldsymbol{\sigma}_{\hat{\mathsf{s}}}$

$$\eta_{\hat{\mathsf{s}}} = -\frac{\partial\psi_{\hat{\mathsf{s}}}}{\partial\theta}, \quad \boldsymbol{\sigma}_{\hat{\mathsf{s}}} = \left(\frac{\partial\psi_{\hat{\mathsf{s}}}}{\partial\mathbf{F}_{\hat{\mathsf{s}}}}\cdot\mathbf{F}_{\hat{\mathsf{s}}}^{\mathsf{T}}\right)^{\mathsf{T}}. \tag{A.33}$$

Assuming no dissipation at the discontinuity surface (called *ideal surface*), the inequality (A.32) yields an equality at the interface $\mathbf{x} \in \hat{\mathsf{s}}$ since $\mathbf{v}_r$, $\mathbf{v}_r^a$, μ_f, μ_f^a, μ_i and μ_i^a are thermodynamically independent (Hou et al., 1989; Lai et al., 1991; Sun et al., 1999; Liu, 2014). The resulting jump/continuity conditions for the chemical potentials are

$$\left[\!\left[\mu_f + \left(c_f\mathbf{v}_r\right)^2/2\right]\!\right] = 0, \quad \left[\!\left[\mu_f^a + \left(c_f^a\mathbf{v}_r^a\right)^2/2\right]\!\right] = 0, \quad [\![\mu_i]\!] = 0, \quad [\![\mu_i^a]\!] = 0, \ 1 \le i \le n. \tag{A.34}$$

Appendix B. Linearized boundary value problem

In Appendix B.1, the assumptions in Section 7.1 are used to simplify the system of field equations and interface conditions as well as the saturation condition, electroneutrality constraint and the constitutive relations. Explicit, general (nonlinear) expressions for the free-energy are given in Appendix B.2. In Appendix B.3 we present the linearization procedure of the various constitutive relations. Finally in Appendix B.4 we introduce auxiliary variables for the linearized mass balance equations and present the corresponding boundary value problem.

B.1. Simplified governing equations

Accounting for the assumptions (L-1) to (L-7) of Section 7.1, the system of field equations and interface conditions simplifies into

$$\begin{array}{l|lll} \boldsymbol{\nabla}\cdot\boldsymbol{\sigma} = \mathbf{0}, & \mathbf{n}\cdot[\![\boldsymbol{\sigma}]\!] = \mathbf{0} & \text{and} & [\![\mathbf{u}]\!] = \mathbf{0}, \\ \boldsymbol{\nabla}\cdot\left(m_f\mathbf{v}_r\right) = r_c + r_n + r_0, & \mathbf{n}\cdot[\![m_f\mathbf{v}_r]\!] = 0 & \text{and} & [\![\mu_f]\!] = 0, \\ \boldsymbol{\nabla}\cdot\left(\mathbf{j}_c + m_c\mathbf{v}_r\right) = r_c, & \mathbf{n}\cdot[\![\mathbf{j}_c + m_c\mathbf{v}_r]\!] = 0 & \text{and} & [\![\mu_c]\!] = 0, \\ \boldsymbol{\nabla}\cdot\left(\mathbf{j}_n + m_n\mathbf{v}_r\right) = r_n, & \mathbf{n}\cdot[\![\mathbf{j}_n + m_n\mathbf{v}_r]\!] = 0 & \text{and} & [\![\mu_n]\!] = 0. \end{array} \tag{B.1}$$

From the assumptions (L-1), (L-3), (L-4) and (L-5), the free-energy of the isotropic continuum (5.11) gives

$$\Psi = \Psi_{mech}(\mathcal{I}(\mathbf{B})) + \Psi_{int}(\Phi, \mathrm{J}) + \Phi\psi_f(\rho_f, \rho_c, \rho_n), \tag{B.2}$$

and the constitutive relations (5.12) become

$$\boldsymbol{\sigma} = \frac{2}{\mathrm{J}}\mathbf{B}\cdot\frac{\partial \Psi_{mech}}{\partial \mathbf{B}} + \frac{\partial \Psi_{int}}{\partial \mathrm{J}}\mathbf{I}, \qquad \mu_f = \frac{\partial \psi_f}{\partial \rho_f}, \qquad \mu_c = \frac{\partial \psi_f}{\partial \rho_c} + \frac{z_c F_{\mathcal{A}}}{M_c^{\mathrm{mol}}}\lambda, \qquad \mu_n = \frac{\partial \psi_f}{\partial \rho_n} + \frac{z_n F_{\mathcal{A}}}{M_n^{\mathrm{mol}}}\lambda, \tag{B.3}$$

where a Lagrange multiplier is used, following assumption (L-9). The electroneutrality constraint (5.13) and the consequence of the saturation condition (5.12) yield

$$\frac{Q_F}{F_{\mathcal{A}}} + \Phi\left(\frac{z_c}{M_c^{\mathrm{mol}}}\rho_c + \frac{z_n}{M_n^{\mathrm{mol}}}\rho_n\right) = 0, \quad \rho_f\frac{\partial \psi_f}{\partial \rho_f} + \rho_c\frac{\partial \psi_f}{\partial \rho_c} + \rho_n\frac{\partial \psi_f}{\partial \rho_n} = \psi_f + \lambda F_{\mathcal{A}}\left(\frac{z_c\rho_c}{M_c^{\mathrm{mol}}} + \frac{z_n\rho_n}{M_n^{\mathrm{mol}}}\right) + \frac{\partial \Psi_{int}}{\partial \Phi}. \tag{B.4}$$

The constitutive relations (4.10) become

$$\begin{bmatrix} m_f\mathbf{v}_r \\ \mathbf{j}_c \\ \mathbf{j}_n \end{bmatrix} = -\begin{bmatrix} \mathrm{K}_{ww} & \mathrm{K}_{wc} & \mathrm{K}_{wn} \\ \mathrm{K}_{cw} & \mathrm{K}_{cc} & \mathrm{K}_{cn} \\ \mathrm{K}_{nw} & \mathrm{K}_{nc} & \mathrm{K}_{nn} \end{bmatrix}\begin{bmatrix} \boldsymbol{\nabla}\mu_f + \frac{\rho_c}{\rho_f}\boldsymbol{\nabla}\mu_c + \frac{\rho_n}{\rho_f}\boldsymbol{\nabla}\mu_n \\ \boldsymbol{\nabla}\mu_c \\ \boldsymbol{\nabla}\mu_n \end{bmatrix},$$

$$\begin{bmatrix} r_0 \\ r_c \\ r_n \end{bmatrix} = -\begin{bmatrix} \mathrm{R}_{00} & \mathrm{R}_{0c} & \mathrm{R}_{0n} \\ \mathrm{R}_{c0} & \mathrm{R}_{cc} & \mathrm{R}_{cn} \\ \mathrm{R}_{n0} & \mathrm{R}_{nc} & \mathrm{R}_{nn} \end{bmatrix}\begin{bmatrix} \mu_f - \mu_f^a \\ \mu_c + \mu_f - \mu_c^a - \mu_f^a \\ \mu_n + \mu_f - \mu_n^a - \mu_f^a \end{bmatrix}, \tag{B.5}$$

where μ_f^a, μ_c^a and μ_n^a are constant scalars, as implied by (L-5).

B.2. Free-energy choices

We start by stating explicit, nonlinear forms for the free energy terms in (B.2). The term Ψ_{mech} pertaining to the strain energy of the skeleton matrix is taken to follow a Neo-Hookean,[38] hyperelastic model

$$\Psi_{mech}(\mathbf{B}) = \frac{G}{2}\left[(I_1(\mathbf{B}) - 3 - \ln I_3(\mathbf{B})) + \left(\frac{K}{G} - \frac{2}{3}\right)(I_3(\mathbf{B})^{1/2} - 1)^2\right], \tag{B.6}$$

where G and K are respectively the shear and bulk moduli of the porous skeleton's initial (as $\mathbf{B} \to \mathbf{I}$), linearly elastic response and $I_i(\mathbf{B}), i = 1, \ldots, 3$ are the invariants of the right Green strain tensor $\mathbf{B}$. Substituting (B.6) into $(B.3)_1$, the Cauchy stress-tensor takes the form

$$\boldsymbol{\sigma} = \frac{G}{\mathrm{J}}\left[(\mathbf{B} - \mathbf{I}) + \left(\frac{K}{G} - \frac{2}{3}\right)(I_3 - I_3^{1/2})\mathbf{I}\right] + \frac{\partial \Psi_{int}}{\partial \mathrm{J}}\mathbf{I}. \tag{B.7}$$

Different expressions for the large strain definition of the interaction energy Ψ_{int} can be found in the literature (Gil, 2020; Chapelle and Moireau, 2014). For simplicity we do not give any of the explicit nonlinear forms for Ψ_{int} but will record in (B.11) its small strain limit properties required for the linearization process.

Following Gil (2020), we adopt the following free energy for the fluid

$$\begin{aligned} \psi_f = \; & \rho_0\mu_0^0 + \rho_c\mu_c^0 + \rho_n\mu_n^0 - \frac{1}{\chi_\theta}\left(1 - \frac{\rho_f}{\rho_f^0} + \ln\frac{\rho_f}{\rho_f^0}\right) \\ & - R\theta\left[\frac{\rho_c}{M_c^{\mathrm{mol}}}\left(1 - \ln\left(\frac{\rho_c/M_c^{\mathrm{mol}}}{\rho_0/M_0^{\mathrm{mol}}}\gamma_c\right)\right) + \frac{\rho_n}{M_n^{\mathrm{mol}}}\left(1 - \ln\left(\frac{\rho_n/M_n^{\mathrm{mol}}}{\rho_0/M_0^{\mathrm{mol}}}\gamma_n\right)\right)\right], \end{aligned} \tag{B.8}$$

where μ_0^0, μ_c^0 and μ_n^0 are the reference potentials of the solvent and species c and n in an ideal solution, χ_θ is the isothermal compressibility coefficient of the fluid mixture, ρ_f^0 is the reference fluid density at the reference hydrostatic pressure (e.g. atmospheric pressure assumed equal to zero as reference here), $\rho_0 = \rho_f - \rho_c - \rho_n$ is the density of the solvent, R is the universal gas constant, γ_c and γ_n are the activity coefficients of species c and n accounting for the non-ideal mixture of the fluid.

Note that χ_θ and ρ_f^0 should depend on the composition of the fluid mixture and therefore on the concentrations of the species c and n in the solvent. In the case of high dilution of the species in the solvent, based on the experimental data of Perman and Urry

[38] This is the simplest and most popular soft matter energy density model that satisfies polyconvexity (and is hence rank-one convex) and goes to infinity ($\Psi_{mech} \to \infty$) as its volume change tends to zero ($I_3 \to 0$).

(1929), one can assume that both χ_θ and ρ_f^0 only depend on the mass ratio of solvent $c_0 = 1-(\rho_c+\rho_n)/\rho_f$. Substituting (B.8) into $(B.3)_{2,3,4}$, the chemical potentials are

$$\begin{aligned}
\mu_f = \;& \mu_0^0 - \frac{R\theta}{\rho_0}\left(\frac{\rho_c}{M_c^{\rm mol}}+\frac{\rho_n}{M_n^{\rm mol}}\right)+\frac{\rho_f-\rho_f^0}{\chi_\theta\rho_f^0\rho_f}\left(1-\frac{\rho_c+\rho_n}{\rho_f^0\rho_f}\frac{\partial\rho_f^0}{\partial c_0}\right)+\frac{\rho_c+\rho_n}{(\chi_\theta\rho_f)^2}\left(1-\frac{\rho_f}{\rho_f^0}+\ln\frac{\rho_f}{\rho_f^0}\right)\frac{\partial\chi_\theta}{\partial c_0},\\
\mu_c = \;& \mu_c^0-\mu_0^0+\frac{R\theta}{M_c^{\rm mol}}\ln\left(\frac{\rho_c\gamma_c M_0^{\rm mol}}{\rho_0 M_c^{\rm mol}}\right)+\frac{R\theta}{\rho_0}\left(\frac{\rho_c}{M_c^{\rm mol}}+\frac{\rho_n}{M_n^{\rm mol}}\right)+\frac{z_c F_{\mathcal{A}}}{M_c^{\rm mol}}\lambda\\
& -\frac{1}{(\chi_\theta)^2\rho_f}\frac{\partial\chi_\theta}{\partial c_0}\left(1-\frac{\rho_f}{\rho_f^0}+\ln\frac{\rho_f}{\rho_f^0}\right)+\frac{\rho_f-\rho_f^0}{\chi_\theta(\rho_f^0)^2\rho_f}\frac{\partial\rho_f^0}{\partial c_0},\\
\mu_n = \;& \mu_n^0-\mu_0^0+\frac{R\theta}{M_n^{\rm mol}}\ln\left(\frac{\rho_n\gamma_n M_0^{\rm mol}}{\rho_0 M_n^{\rm mol}}\right)+\frac{R\theta}{\rho_0}\left(\frac{\rho_c}{M_c^{\rm mol}}+\frac{\rho_n}{M_n^{\rm mol}}\right)+\frac{z_n F_{\mathcal{A}}}{M_n^{\rm mol}}\lambda\\
& -\frac{1}{(\chi_\theta)^2\rho_f}\frac{\partial\chi_\theta}{\partial c_0}\left(1-\frac{\rho_f}{\rho_f^0}+\ln\frac{\rho_f}{\rho_f^0}\right)+\frac{\rho_f-\rho_f^0}{\chi_\theta(\rho_f^0)^2\rho_f}\frac{\partial\rho_f^0}{\partial c_0},
\end{aligned}\tag{B.9}$$

and the saturation condition $(B.4)_2$ yields with the help of (B.9)

$$p_f := \frac{1}{\chi_\theta}\ln\frac{\rho_f}{\rho_f^0}=\frac{\partial\Psi_{int}}{\partial\boldsymbol{\Phi}},\tag{B.10}$$

where for an easier interpretation of the results, we define the left-hand side of (B.10) as the hydrostatic pressure of the fluid p_f.

B.3. Linearization of the constitutive relations

We proceed with the linearization of the constitutive relations (B.3), (B.4), (B.5) given in Appendix B.1 using the energy densities in Appendix B.2 and recall the definitions of the non-dimensional perturbations introduced in (7.2).

The small strain limit of the derivatives of the interaction energy density Ψ_{int} (Gil, 2020; Chapelle and Moireau, 2014) are

$$\frac{\partial\Psi_{int}}{\partial \mathrm{J}}=-b_{Biot}\frac{\partial\Psi_{int}}{\partial\boldsymbol{\Phi}},\quad \frac{\partial\Psi_{int}}{\partial\boldsymbol{\Phi}}=\frac{K_m}{b_{Biot}-\boldsymbol{\Phi}^0}\left(\boldsymbol{\Phi}-\boldsymbol{\Phi}^0-b_{Biot}\mathrm{tr}\boldsymbol{\varepsilon}\right);\quad b_{Biot}=1-\frac{K}{K_m},\tag{B.11}$$

where b_{Biot} is Biot's coefficient and K_m is the bulk modulus of the solid material making the porous medium (Coussy, 2004). For the case of subcutaneous tissue, the bulk of the solid material K_m is close to the one of a lipid cell whereas the linearized skeleton bulk K is expected to be closer to the subcutaneous injection pressure (Thomsen et al., 2014).[39] Therefore, the Biot coefficient is expected to be close to 1 in the linearized case, as illustrated by the values considered in Appendix B.5. For large deformations, the tissue bulk compressibility is expected to be asymmetric with a compression bulk close to the one of the lipid cell (almost incompressible cells tessellation) and a swelling bulk of the order of the injection pressures of Thomsen et al. (2014), representing the swelling of the pores.[40] The non-dimensional perturbations of the Cauchy stress and of the chemical potentials can be written at order 1 in term of the perturbation variables in view of $(B.3)_1$, $(B.11)_1$ and (B.10)

$$\delta\boldsymbol{\sigma}=2\delta\boldsymbol{\varepsilon}'+\left(\frac{K}{G}\mathrm{tr}\delta\boldsymbol{\varepsilon}-b_{Biot}\delta p_f\right)\mathbf{I}.\tag{B.12}$$

[39] One could also estimate it with expressions similar to Hashin–Shtrikman's bounds (Gil, 2020).

[40] One can refer to the work of Gil (2020) for a proposal of an explicit expression of the asymmetric strain energy of tissue.

The linearization of the expressions for the chemical potential (B.9) and fluid pressure (B.10) yields the following relations between the chemical potential perturbations and δp_f, $\delta \rho_c$, $\delta \rho_n$, $\delta \lambda$ and $\delta \rho_f$

$$\begin{bmatrix} \delta\mu_f \\ \delta\mu_c \\ \delta\mu_n \end{bmatrix} = \begin{bmatrix} \mathrm{C}_{fp} & \mathrm{C}_{fc} & \mathrm{C}_{fn} & 0 & \mathrm{C}_{ff} \\ \mathrm{C}_{cp} & \mathrm{C}_{cc} & \mathrm{C}_{cn} & z_c & \mathrm{C}_{cf} \\ \mathrm{C}_{np} & \mathrm{C}_{nc} & \mathrm{C}_{nn} & z_n & \mathrm{C}_{nf} \end{bmatrix} \begin{bmatrix} \delta p_f \\ \delta \rho_c \\ \delta \rho_n \\ \delta \lambda \\ \delta \rho_f \end{bmatrix},$$

$$\mathrm{C}_{fp} = \frac{G M_c^{\mathrm{mol}} M_n^{\mathrm{mol}} \rho_0^e}{\rho_f^e R\theta \left(\rho_c^e M_n^{\mathrm{mol}} + \rho_n^e M_c^{\mathrm{mol}}\right)} \left(1 - \frac{\rho_c^e + \rho_n^e}{\rho_f^{e2}} \left.\frac{\partial \rho_f^0}{\partial c_0}\right|_e\right), \quad \mathrm{C}_{ff} = \frac{\rho_f^e}{\rho_0^e},$$

$$\mathrm{C}_{fc} = -\frac{\rho_c^e}{\rho_0^e} - \frac{\rho_c^e M_n^{\mathrm{mol}}}{\rho_c^e M_n^{\mathrm{mol}} + \rho_n^e M_c^{\mathrm{mol}}}, \quad \mathrm{C}_{fn} = -\frac{\rho_n^e}{\rho_0^e} - \frac{\rho_n^e M_c^{\mathrm{mol}}}{\rho_c^e M_n^{\mathrm{mol}} + \rho_n^e M_c^{\mathrm{mol}}},$$

$$\mathrm{C}_{cp} = \frac{M_c^{\mathrm{mol}} G}{R\theta \rho_f^{e2}} \left.\frac{\partial \rho_f^0}{\partial c_0}\right|_e, \quad \mathrm{C}_{cf} = -\frac{\rho_f^e}{\rho_0^e}\left(1 + \frac{\rho_c^e M_n^{\mathrm{mol}} + \rho_n^e M_c^{\mathrm{mol}}}{\rho_0^e M_n^{\mathrm{mol}}}\right), \tag{B.13}$$

$$\mathrm{C}_{np} = \frac{M_n^{\mathrm{mol}} G}{R\theta \rho_f^{e2}} \left.\frac{\partial \rho_f^0}{\partial c_0}\right|_e, \quad \mathrm{C}_{nf} = -\frac{\rho_f^e}{\rho_0^e}\left(1 + \frac{\rho_c^e M_n^{\mathrm{mol}} + \rho_n^e M_c^{\mathrm{mol}}}{\rho_0^e M_c^{\mathrm{mol}}}\right),$$

$$\mathrm{C}_{cc} = \frac{\left(\rho_f^e - \rho_n^e\right)^2 + \rho_c^e \rho_n^e M_c^{\mathrm{mol}}/M_n^{\mathrm{mol}}}{\left(\rho_0^e\right)^2}, \quad \mathrm{C}_{cn} = \frac{\rho_n^e}{\left(\rho_0^e\right)^2}\left[\rho_c^e + \rho_n^e\left(1 + 2\frac{M_c^{\mathrm{mol}}}{M_n^{\mathrm{mol}}}\right)\right],$$

$$\mathrm{C}_{nn} = \frac{\left(\rho_f^e - \rho_c^e\right)^2 + \rho_c^e \rho_n^e M_n^{\mathrm{mol}}/M_c^{\mathrm{mol}}}{\left(\rho_0^e\right)^2}, \quad \mathrm{C}_{nc} = \frac{\rho_c^e}{\left(\rho_0^e\right)^2}\left[\rho_n^e + \rho_c^e\left(1 + 2\frac{M_n^{\mathrm{mol}}}{M_c^{\mathrm{mol}}}\right)\right].$$

Taking into account that the fluid density at reference hydrostatic pressure ρ_f^0 is a function of the mass ratio of solvent c_0 (see comment before (B.9)) the linearization of the hydrostatic pressure (B.10) gives the following relation between the perturbation of fluid density in terms of the perturbations of the pressure and species concentrations

$$\begin{aligned} &\delta\rho_f = \mathrm{P}_p \delta p_f + \mathrm{P}_c \delta\rho_c + \mathrm{P}_n \delta\rho_n, \\ &\left[\mathrm{P}_p,\ \mathrm{P}_c,\ \mathrm{P}_n\right] := \left[\chi_\theta^e G (\rho_f^e)^2, -\rho_c^e (\partial\rho_f^0/\partial c_0)_e, -\rho_n^e (\partial\rho_f^0/\partial c_0)_e\right] / \left[(\rho_f^e)^2 - \left(\rho_c^e + \rho_n^e\right)(\partial\rho_f^0/\partial c_0)_e\right]. \end{aligned} \tag{B.14}$$

The linearization of the electroneutrality constraint $(\mathrm{B.4})_1$ and the saturation condition (B.10) gives

$$\begin{aligned} &\delta\rho_c = \mathrm{E}_n \delta\rho_n + \mathrm{E}_{\boldsymbol{\Phi}} \delta\boldsymbol{\Phi}, \qquad \mathrm{tr}\delta\boldsymbol{\varepsilon} = \mathrm{S}_{\boldsymbol{\Phi}} \delta\boldsymbol{\Phi} + \mathrm{S}_p \delta p_f, \\ &\mathrm{E}_n = -\frac{\rho_n^e z_n M_c^{\mathrm{mol}}}{\rho_c^e z_c M_n^{\mathrm{mol}}}, \qquad \mathrm{E}_{\boldsymbol{\Phi}} = \frac{Q_F M_c^{\mathrm{mol}}}{F_{\mathcal{A}} \boldsymbol{\Phi}^0 \rho_c^e z_c}, \qquad \mathrm{S}_{\boldsymbol{\Phi}} = \frac{\boldsymbol{\Phi}^0}{b_{Biot}}, \qquad \mathrm{S}_p = -\frac{G}{N b_{Biot}}. \end{aligned} \tag{B.15}$$

The system of four partial differential equations (B.1) shall be solved as a function of the continuous variables at the interface, namely $\delta\mathbf{u}$, $\delta\mu_f$, $\delta\mu_c$ and $\delta\mu_n$. Once these fields are found, we invert the linearized constitutive laws to access the values of pressures, densities, porosity and Lagrange multiplier. Combining (B.13) and $(\mathrm{B.15})_2$ and substituting $(\mathrm{B.15})_1$ and (B.14) yield the following (invertible) linear system

$$\begin{bmatrix} \delta\mu_f \\ \delta\mu_c \\ \delta\mu_n \\ \mathrm{tr}\delta\boldsymbol{\varepsilon} \end{bmatrix} = \underbrace{\begin{bmatrix} \mathrm{C}_{fp} + \mathrm{C}_{ff}\mathrm{P}_p & \mathrm{C}_{fn} + \mathrm{C}_{ff}\mathrm{P}_n + \left(\mathrm{C}_{fc} + \mathrm{C}_{ff}\mathrm{P}_c\right)\mathrm{E}_n & 0 & \left(\mathrm{C}_{fc} + \mathrm{C}_{ff}\mathrm{P}_c\right)\mathrm{E}_{\boldsymbol{\Phi}} \\ \mathrm{C}_{cp} + \mathrm{C}_{cf}\mathrm{P}_p & \mathrm{C}_{cn} + \mathrm{C}_{cf}\mathrm{P}_n + \left(\mathrm{C}_{cc} + \mathrm{C}_{cf}\mathrm{P}_c\right)\mathrm{E}_n & z_c & \left(\mathrm{C}_{cc} + \mathrm{C}_{cf}\mathrm{P}_c\right)\mathrm{E}_{\boldsymbol{\Phi}} \\ \mathrm{C}_{np} + \mathrm{C}_{nf}\mathrm{P}_p & \mathrm{C}_{nn} + \mathrm{C}_{nf}\mathrm{P}_n + \left(\mathrm{C}_{nc} + \mathrm{C}_{nf}\mathrm{P}_c\right)\mathrm{E}_n & z_n & \left(\mathrm{C}_{nc} + \mathrm{C}_{nf}\mathrm{P}_c\right)\mathrm{E}_{\boldsymbol{\Phi}} \\ \mathrm{S}_p & 0 & 0 & \mathrm{S}_{\boldsymbol{\Phi}} \end{bmatrix}}_{\mathbf{G}} \begin{bmatrix} \delta p_f \\ \delta\rho_n \\ \delta\lambda \\ \delta\boldsymbol{\Phi} \end{bmatrix}, \tag{B.16}$$

which is complemented by the electroneutrality constraint $(\mathrm{B.15})_1$ and pressure definition (B.14) to access the values of $\delta\rho_c$ and $\delta\rho_f$.

Following Loret et al. (2004), we write the following general form of the coefficients of $(B.5)_1$ relating the relative velocity and the chemical species fluxes to the corresponding chemical potential gradients

$$\begin{aligned} &\mathrm{K}_{ww} = (\rho_f^e)^2 \frac{k_h}{\mu_v}, \quad \mathrm{K}_{cc} = \boldsymbol{\Phi}^0 \rho_c^e \frac{M_c^{\mathrm{mol}} D_c^\star}{R\theta}, \quad \mathrm{K}_{nn} = \boldsymbol{\Phi}^0 \rho_n^e \frac{M_n^{\mathrm{mol}} D_n^\star}{R\theta}, \\ &\mathrm{K}_{wc} = \mathrm{K}_{cw} = -\omega \frac{\rho_c^e}{\rho_f^e} \mathrm{K}_{ww}, \quad \mathrm{K}_{wn} = \mathrm{K}_{nw} = -\omega \frac{\rho_n^e}{\rho_f^e} \mathrm{K}_{ww}, \quad \mathrm{K}_{cn} = \mathrm{K}_{nc} = 0, \end{aligned} \tag{B.17}$$

where k_h is the linear intrinsic permeability of the tissue, μ_v the dynamic viscosity of the fluid, ω is the *osmotic coefficient*, $D_c^\star$ and $D_n^\star$ are the effective diffusivity coefficients of species c and n in the tissue and the following inequalities must hold to ensure that the 3×3 matrix is positive semi-definite

$$k_h \geq 0, \quad \mu_v \geq 0, \quad 0 \leq \omega \leq \omega_{max} := \left[\frac{\boldsymbol{\Phi}^0 \mu_v}{R\theta k_h} \left(\frac{\rho_c^e}{M_c^{\mathrm{mol}} D_c^\star} + \frac{\rho_n^e}{M_n^{\mathrm{mol}} D_n^\star} \right)^{-1} \right]^{1/2}. \tag{B.18}$$

Similarly, following Gil (2020), we postulate the following form of the coefficients in the relation between absorption and chemical potentials of the different species $(B.5)_2$

$$\begin{aligned} &\mathrm{R}_{00} = \frac{\rho_0^e M_0^{\mathrm{mol}}}{R\theta\tau_0}, \quad \mathrm{R}_{cc} = \frac{\rho_c^e M_c^{\mathrm{mol}}}{R\theta\tau_c}, \quad \mathrm{R}_{nn} = \frac{\rho_n^e M_n^{\mathrm{mol}}}{R\theta\tau_n}, \\ &\mathrm{R}_{0c} = \mathrm{R}_{0n} = \mathrm{R}_{c0} = \mathrm{R}_{cn} = \mathrm{R}_{n0} = \mathrm{R}_{nc} = 0, \end{aligned} \tag{B.19}$$

where τ_0, τ_c and τ_n are respectively the characteristic times of absorption of the solvent and the species c and n.

B.4. Linearized mass balance equations

Having linearized the constitutive relations of the problem, we can now proceed with the mass balance equations. For the divergence terms of the $(B.1)_{2,3,4}$, we define the following auxiliary variables $\delta\boldsymbol{\alpha}$ in terms of $\delta\boldsymbol{\mu}$

$$\underbrace{\begin{bmatrix} \delta\alpha_f \\ \delta\alpha_c \\ \delta\alpha_n \end{bmatrix}}_{\delta\boldsymbol{\alpha}} := \underbrace{\begin{bmatrix} \mathrm{A}_{ff} & \mathrm{A}_{fc} & \mathrm{A}_{fn} \\ \mathrm{A}_{cf} & \mathrm{A}_{cc} & \mathrm{A}_{cn} \\ \mathrm{A}_{nf} & \mathrm{A}_{nc} & \mathrm{A}_{nn} \end{bmatrix}}_{\mathbf{A}} \underbrace{\begin{bmatrix} \delta\mu_f \\ \delta\mu_c \\ \delta\mu_n \end{bmatrix}}_{\delta\boldsymbol{\mu}},$$

$$\begin{aligned} &\mathrm{A}_{ff} = 1, \quad \mathrm{A}_{cf} = \mathrm{A}_{nf} = 1 - \omega, \quad \mathrm{A}_{fc} = \frac{(1-\omega)\,\rho_c^e M_n^{\mathrm{mol}}}{\rho_c^e M_n^{\mathrm{mol}} + \rho_n^e M_c^{\mathrm{mol}}}, \quad \mathrm{A}_{fn} = \frac{(1-\omega)\,\rho_n^e M_c^{\mathrm{mol}}}{\rho_c^e M_n^{\mathrm{mol}} + \rho_n^e M_c^{\mathrm{mol}}}, \\ &\mathrm{A}_{cc} = \left(1 - \omega + \frac{\boldsymbol{\Phi}^0 D_c^\star \mu_v M_c^{\mathrm{mol}} \rho_0^e}{R\theta k_h \rho_c^e \rho_f^e} \right) \frac{\mathrm{A}_{fc}}{\mathrm{A}_{cf}}, \quad \mathrm{A}_{cn} = \left(1 - \omega \frac{\rho_f^e + \rho_0^e}{\rho_f^e} \right) \frac{\mathrm{A}_{fn}}{\mathrm{A}_{nf}}, \\ &\mathrm{A}_{nc} = \left(1 - \omega \frac{\rho_f^e + \rho_0^e}{\rho_f^e} \right) \frac{\mathrm{A}_{fc}}{\mathrm{A}_{cf}}, \quad \mathrm{A}_{nn} = \left(1 - \omega + \frac{\boldsymbol{\Phi}^0 D_n^\star \mu_v M_n^{\mathrm{mol}} \rho_0^e}{R\theta k_h \rho_n^e \rho_f^e} \right) \frac{\mathrm{A}_{fn}}{\mathrm{A}_{nf}}. \end{aligned} \tag{B.20}$$

The fluxes in the divergence terms of $(B.1)_{2,3,4}$ can then be written as

$$\begin{aligned} &\begin{bmatrix} m_f^e \mathbf{v}_r \\ \mathbf{j}_c + m_c^e \mathbf{v}_r \\ \mathbf{j}_n + m_n^e \mathbf{v}_r \end{bmatrix} = -\frac{1}{\mathrm{r}_{\mathrm{sph}}} \begin{bmatrix} a_f \overline{\boldsymbol{\nabla}} \delta\alpha_f \\ a_c \overline{\boldsymbol{\nabla}} \delta\alpha_c \\ a_n \overline{\boldsymbol{\nabla}} \delta\alpha_n \end{bmatrix}, \\ &a_f = R\theta \frac{(\rho_f^e)^2}{\rho_0^e} \left(\frac{\rho_c^e M_n^{\mathrm{mol}} + \rho_n^e M_c^{\mathrm{mol}}}{M_c^{\mathrm{mol}} M_n^{\mathrm{mol}}} \right) \frac{k_h}{\mu_v}, \quad a_c = \frac{\rho_c^e}{\rho_f^e} a_f, \quad a_n = \frac{\rho_n^e}{\rho_f^e} a_f. \end{aligned} \tag{B.21}$$

Consequently, the mass balances $(B.1)_{2,3,4}$ can be written in the following dimensionless form

$$\underbrace{\frac{\mathrm{r}_{\mathrm{sph}}^2}{a_f} r_f}_{-\delta\beta_f} + \overline{\boldsymbol{\nabla}} \cdot \left(\overline{\boldsymbol{\nabla}} \delta\alpha_f \right) = 0, \quad \underbrace{\frac{\mathrm{r}_{\mathrm{sph}}^2}{a_c} r_c}_{-\delta\beta_c} + \overline{\boldsymbol{\nabla}} \cdot \left(\overline{\boldsymbol{\nabla}} \delta\alpha_c \right) = 0, \quad \underbrace{\frac{\mathrm{r}_{\mathrm{sph}}^2}{a_n} r_n}_{-\delta\beta_n} + \overline{\boldsymbol{\nabla}} \cdot \left(\overline{\boldsymbol{\nabla}} \delta\alpha_n \right) = 0, \tag{B.22}$$

where we have introduced the auxiliary variable $\delta\boldsymbol{\beta}$ in terms of $\delta\boldsymbol{\mu}$

$$\underbrace{\begin{bmatrix}\delta\beta_f\\ \delta\beta_c\\ \delta\beta_n\end{bmatrix}}_{\delta\boldsymbol{\beta}} = \underbrace{\begin{bmatrix} \left(\dfrac{\rho_0^e M_0^{\mathrm{mol}}}{\tau_0}+\dfrac{\rho_c^e M_c^{\mathrm{mol}}}{\tau_c}+\dfrac{\rho_n^e M_n^{\mathrm{mol}}}{\tau_n}\right)\dfrac{\mathrm{r}_{\mathrm{sph}}^2\left(\rho_c^e M_n^{\mathrm{mol}}+\rho_n^e M_c^{\mathrm{mol}}\right)}{a_f M_c^{\mathrm{mol}} M_n^{\mathrm{mol}}\rho_0^e} & \dfrac{\mathrm{r}_{\mathrm{sph}}^2\rho_c^e}{a_f\tau_c} & \dfrac{\mathrm{r}_{\mathrm{sph}}^2\rho_n^e}{a_f\tau_n} \\ \dfrac{\mathrm{r}_{\mathrm{sph}}^2\rho_c^e M_c^{\mathrm{mol}}}{a_c\tau_c\rho_0^e}\left(\dfrac{\rho_c^e}{M_c^{\mathrm{mol}}}+\dfrac{\rho_n^e}{M_n^{\mathrm{mol}}}\right) & \dfrac{\mathrm{r}_{\mathrm{sph}}^2\rho_c^e}{a_c\tau_c} & 0 \\ \dfrac{\mathrm{r}_{\mathrm{sph}}^2\rho_n^e M_n^{\mathrm{mol}}}{a_n\tau_n\rho_0^e}\left(\dfrac{\rho_c^e}{M_c^{\mathrm{mol}}}+\dfrac{\rho_n^e}{M_n^{\mathrm{mol}}}\right) & 0 & \dfrac{\mathrm{r}_{\mathrm{sph}}^2\rho_n^e}{a_n\tau_n} \end{bmatrix}}_{\mathbf{B}} \begin{bmatrix}\delta\mu_f\\ \delta\mu_c\\ \delta\mu_n\end{bmatrix}. \tag{B.23}$$

Combining the above relations (B.20) to (B.23), we arrive in the compact form of the linearized mass balance equations, namely: $\overline{\boldsymbol{\nabla}}\cdot\left(\overline{\boldsymbol{\nabla}}\mathbf{A}\delta\boldsymbol{\mu}\right)-\mathbf{B}\delta\boldsymbol{\mu}=\mathbf{0}$, which is reported in (7.5). The corresponding boundary conditions in terms of $\delta\boldsymbol{\mu}$ are recorded in (7.6).

Note that the chemical potentials are not the fields that one can naturally control and measure in an experiment. One must instead work with a hydrostatic pressure $\delta p_f^{\mathrm{inj}}$ and concentrations of chemical species $\delta\rho_c^{\mathrm{inj}}$ and $\delta\rho_n^{\mathrm{inj}}$ respecting the electroneutrality constraint in the injection fluid cavity (where $Q_F=0$). Using (B.13), the set of chemical potentials at $\bar{\mathrm{r}}=1$ are thus found to be

$$\begin{bmatrix}\delta\mu_f^{\mathrm{inj}}\\ \delta\mu_c^{\mathrm{inj}}\\ \delta\mu_n^{\mathrm{inj}}\end{bmatrix} = \begin{bmatrix}\mathrm{C}_{fp}+\mathrm{C}_{ff}\mathrm{P}_p & \mathrm{C}_{fc}+\mathrm{C}_{ff}\mathrm{P}_c & \mathrm{C}_{fn}+\mathrm{C}_{ff}\mathrm{P}_n\\ \mathrm{C}_{cp}+\mathrm{C}_{cf}\mathrm{P}_p & \mathrm{C}_{cc}+\mathrm{C}_{cf}\mathrm{P}_c & \mathrm{C}_{cn}+\mathrm{C}_{cf}\mathrm{P}_n\\ \mathrm{C}_{np}+\mathrm{C}_{nf}\mathrm{P}_p & \mathrm{C}_{nc}+\mathrm{C}_{nf}\mathrm{P}_c & \mathrm{C}_{nn}+\mathrm{C}_{nf}\mathrm{P}_n\end{bmatrix}\begin{bmatrix}\delta p_f^{\mathrm{inj}}\\ \delta\rho_c^{\mathrm{inj}}\\ \delta\rho_n^{\mathrm{inj}}\end{bmatrix}. \tag{B.24}$$

B.5. Parameters used in the linear model

The values of the parameters used in Section 7 are gathered in (B.25). Their orders of magnitude have been estimated based on existing work and estimations in the literature (e.g. Thomsen et al. (2014), Comley and Fleck (2011), Zheng et al. (2021), Leng et al. (2021a), de Lucio et al. (2023) and Swartz and Fleury (2007)) as well as some hypothesis for the simplicity of the analytical work.

Symbol	Value	Unit	Description
Q_F	$\pm 1e3$	C m^{-3}	Density of charges attached to tissue
$F_{\mathcal{A}}$	96485	C mol^{-1}	Faraday constant
θ	300	K	Temperature
R	8.314	J K^{-1} mol^{-1}	Universal gas constant
$\mathrm{r}_{\mathrm{sph}}$	$1e{-4}$	m	Spherical inclusion radius
K	$1e5$	Pa	Skeleton bulk modulus
G	$1e3$	Pa	Skeleton shear modulus
Φ^0	0.05	–	Porosity
K_m	$1e7$	Pa	Bulk modulus of material making the porous structure
k_h	$1e{-13}$	m^2	Linear intrinsic permeability of the tissue
μ_v	$3.5e{-3}$	Pa s	Dynamic viscosity of the fluid
χ_θ	$4.6e{-10}$	Pa^{-1}	Fluid compressibility coefficient
ρ_f^e	$1e3$	kg m^{-3}	Equilibrium fluid density
ρ_c^e	3	kg m^{-3}	Equilibrium cation density
$\left.\dfrac{\partial\rho_f^0}{\partial c_0}\right\vert_e$	1	kg m^{-3}	Mixture fluid density evolution
M_c^{mol}	$22.98e{-3}$	kg mol^{-1}	Molar mass of cation (Na^+)
M_n^{mol}	$35.45e{-3}$	kg mol^{-1}	Molar mass of anion (Cl^-)
M_0^{mol}	$22e{-3}$	kg mol^{-1}	Molar mass of solvent (water)
z_c	+1	–	Number of charge of cation (Na^+)
z_n	−1	–	Number of charge of anion (Cl^-)
$D_c^\star$; $D_n^\star$	$1e{-10}$	m^2 s^{-1}	Effective diffusivity coefficients of species in tissue
τ_0 ; τ_c ; τ_n	$1e3$	s	Absorption timescale of species and solvent

(B.25)

References

Alkhouli, N., Mansfield, J., Green, E., Bell, J., Knight, B., Liversedge, N., Tham, J.C., Welbourn, R., Shore, A.C., Kos, K., Winlove, C.P., 2013. The mechanical properties of human adipose tissues and their relationships to the structure and composition of the extracellular matrix. Am. J. Physiol.-Endocrinol. Metab. 305 (12), E1427–E1435. http://dx.doi.org/10.1152/ajpendo.00111.2013.

Anand, L., 2012. A Cahn–Hilliard-type theory for species diffusion coupled with large elastic–plastic deformations. J. Mech. Phys. Solids 60 (12), 1983–2002. http://dx.doi.org/10.1016/j.jmps.2012.08.001.

Aukland, K., Nicolaysen, G., 1981. Interstitial fluid volume: local regulatory mechanisms. Physiol. Rev. 61 (3), 556–643. http://dx.doi.org/10.1152/physrev.1981.61.3.556.

Auton, L.C., MacMinn, C.W., 2017. From arteries to boreholes: steady-state response of a poroelastic cylinder to fluid injection. Proc. R. Soc. A URL: https://doi.org/10.1098/rspa.2016.0753.

Auton, L.C., MacMinn, C.W., 2018. From arteries to boreholes: transient response of a poroelastic cylinder to fluid injection. Proc. R. Soc. A URL: https://doi.org/10.1098/rspa.2018.0284.

Barré, M., Grandmont, C., Moireau, P., 2023. Analysis of a linearized poromechanics model for incompressible and nearly incompressible materials. Evol. Equ. Control Theory 12, 846–906.

Biot, M.A., 1941. General theory of three-dimensional consolidation. J. Appl. Phys. 12 (2), 155–164. http://dx.doi.org/10.1063/1.1712886.

Biot, M.A., 1972. Theory of finite deformations of porous solids. Indiana Univ. Math. J. URL: https://www.jstor.org/stable/24890361.

Brassart, L., Suo, Z., 2013. Reactive flow in solids. J. Mech. Phys. Solids 61 (1), 61–77. http://dx.doi.org/10.1016/j.jmps.2012.09.007.

Chapelle, D., Moireau, P., 2014. General coupling of porous flows and hyperelastic formulations—from thermodynamics principles to energy balance and compatible time schemes. Eur. J. Mech. B Fluids 46, 82–96. http://dx.doi.org/10.1016/j.euromechflu.2014.02.009.

Chester, S.A., Anand, L., 2010. A coupled theory of fluid permeation and large deformations for elastomeric materials. J. Mech. Phys. Solids 58 (11), 1879–1906. http://dx.doi.org/10.1016/j.jmps.2010.07.020.

Chester, S.A., Anand, L., 2011. A thermo-mechanically coupled theory for fluid permeation in elastomeric materials: Application to thermally responsive gels. J. Mech. Phys. Solids 59 (10), 1978–2006. http://dx.doi.org/10.1016/j.jmps.2011.07.005.

Coleman, B.D., Noll, W., 1963. The thermodynamics of elastic materials with heat conduction and viscosity. Arch. Ration. Mech. Anal. 13 (1), 167–178. http://dx.doi.org/10.1007/bf01262690.

Comley, K., Fleck, N., 2010. A micromechanical model for the Young's modulus of adipose tissue. Int. J. Solids Struct. 47 (21), 2982–2990. http://dx.doi.org/10.1016/j.ijsolstr.2010.07.001.

Comley, K., Fleck, N., 2011. Deep penetration and liquid injection into adipose tissue. J. Mech. Mater. Struct. 6 (1–4), 127–140. http://dx.doi.org/10.2140/jomms.2011.6.127.

Comley, K., Fleck, N., 2012. The compressive response of porcine adipose tissue from low to high strain rate. Int. J. Impact Eng. 46, 1–10. http://dx.doi.org/10.1016/j.ijimpeng.2011.12.009.

Coussy, O., 2004. Poromechanics. John Wilez and Sons, Ltd.

Coussy, O., Dormieux, L., Detournay, E., 1998. From mixture theory to biot's approach for porous media. Int. J. Solids Struct. 35 (34–35), 4619–4635. http://dx.doi.org/10.1016/s0020-7683(98)00087-0.

de Lucio, M., Leng, Y., Hans, A., Bilionis, I., Brindise, M., Ardekani, A.M., Vlachos, P.P., Gomez, H., 2023. Modeling large-volume subcutaneous injection of monoclonal antibodies with anisotropic porohyperelastic models and data-driven tissue layer geometries. J. Mech. Behav. Biomed. Mater..

Dormieux, L., Coussy, O., de Buhan, P., 1991. Modélisation mécanique d'un milieu polyphasique par la méthode des puissances virtuelles. C. R. Acad. Sci. Paris t. 313, Serie II, 863–868.

Fried, E., Gurtin, M., 1999. Coherent solid-state phase transitions with atomic diffusion: A thermomechanical treatment. J. Stat. Phys. 95 (5), 1361–1427. http://dx.doi.org/10.1023/A:1004535408168.

Gajo, A., Loret, B., 2003. Finite element simulations of chemo-mechanical coupling in elastic–plastic homoionic expansive clays. Comput. Methods Appl. Mech. Engrg. 192 (31–32), 3489–3530. http://dx.doi.org/10.1016/s0045-7825(03)00355-4.

Gajo, A., Loret, B., 2007. The mechanics of active clays circulated by salts, acids and bases. J. Mech. Phys. Solids 55 (8), 1762–1801. http://dx.doi.org/10.1016/j.jmps.2007.01.005.

Gil, L., 2020. A General Continuum Theory of Finite Strain Chemoporomechanics with Application to Subcutaneous Injections (Ph.D. thesis). Ecole Polytechnique.

Gil, L., Jabbour, M., Triantafyllidis, N., 2022. The role of the relative fluid velocity in an objective continuum theory of finite strain poroelasticity. J. Elasticity URL: https://link.springer.com/article/10.1007/s10659-022-09903-6.

Guin, L., Jabbour, M., Triantafyllidis, N., 2018. The p-n junction under nonuniform strains: general theory and application to photovoltaics. J. Mech. Phys. Solids 110, 54–79. http://dx.doi.org/10.1016/j.jmps.2017.09.004.

Gurtin, M.E., 1971. On the thermodynamics of chemically reacting fluid mixtures. Arch. Ration. Mech. Anal. 43 (3), 198–212. http://dx.doi.org/10.1007/bf00251452.

Gurtin, M.E., Fried, E., Anand, L., 2010. The Mechanics and Thermodynamics of Continua. Cambridge University Press.

Gurtin, M.E., Jabbour, M.E., 2002. Interface evolution in three dimensions with curvature-dependent energy and surface diffusion: Interface-controlled evolution, phase transitions, epitaxial growth of elastic films. Arch. Ration. Mech. Anal. 163 (3), 171–208. http://dx.doi.org/10.1007/s002050200193.

Gurtin, M.E., Vargas, A.S., 1971. On the classical theory of reacting fluid mixtures. Arch. Ration. Mech. Anal. 43 (3), 179–197. http://dx.doi.org/10.1007/bf00251451.

Herlin, C., Chica-Rosa, A., Subsol, G., Gilles, B., Macri, F., Beregi, J.P., Captier, G., 2015. Three-dimensional study of the skin/subcutaneous complex using in vivo whole body 3T MRI: review of the literature and confirmation of a generic pattern of organization. Surg. Radiol. Anat. 37 (7), 731–741. http://dx.doi.org/10.1007/s00276-014-1409-0.

Herlin, C., Gilles, B., Subsol, G., Captier, G., 2014. Generic 3D geometrical and mechanical modeling of the skin/subcutaneous complex by a procedural hybrid method. In: Biomedical Simulation. Springer International Publishing, pp. 173–181. http://dx.doi.org/10.1007/978-3-319-12057-7_20.

Hong, W., Zhao, X., Zhou, J., Suo, Z., 2008. A theory of coupled diffusion and large deformation in polymeric gels. J. Mech. Phys. Solids 56 (5), 1779–1793. http://dx.doi.org/10.1016/j.jmps.2007.11.010.

Hou, J.S., Holmes, M.H., Lai, W.M., Mow, V.C., 1989. Boundary conditions at the cartilage-synovial fluid interface for joint lubrication and theoretical verifications. J. Biomech. Eng. 111 (1), 78. http://dx.doi.org/10.1115/1.3168343.

Huyghe, J., Janssen, J., 1997. Quadriphasic mechanics of swelling incompressible porous media. Internat. J. Engrg. Sci. 35 (8), 793–802. http://dx.doi.org/10.1016/s0020-7225(96)00119-x.

Huyghe, J., Janssen, J., 1999. Thermo-chemo-electro-mechanical formulation of saturated charged porous solids. Transp. Porous Media 34 (1/3), 129–141. http://dx.doi.org/10.1023/a:1006509424116.

Jabbour, M.E., Bhattacharya, K., 2003. A continuum theory of multispecies thin solid film growth by chemical vapor deposition. J. Elasticity 73 (1–3), 13–74. http://dx.doi.org/10.1023/b:elas.0000030018.40095.d5.

Lai, W.M., Hou, J.S., Mow, V.C., 1991. A triphasic theory for the swelling and deformation behaviors of articular cartilage. J. Biomech. Eng. 113 (3), 245. http://dx.doi.org/10.1115/1.2894880.

Lai, W.M., Mow, V.C., Roth, V., 1981. Effects of nonlinear strain-dependent permeability and rate of compression on the stress behavior of articular cartilage. J. Biomech. Eng. 103 (2), 61. http://dx.doi.org/10.1115/1.3138261.

Leng, Y., Ardekani, A.M., Gomez, H., 2021a. A poro-viscoelastic model for the subcutaneous injection of monoclonal antibodies. J. Mech. Phys. Solids 155, 104537.

Leng, Y., de Lucio, M., Gomez, H., 2021b. Using poro-elasticity to model the large deformation of tissue during subcutaneous injection. Comput. Methods Appl. Mech. Engrg. 384, 113919. http://dx.doi.org/10.1016/j.cma.2021.113919, URL: https://www.sciencedirect.com/science/article/pii/S0045782521002565.

Levitt, D.G., 2003. The pharmacokinetics of the interstitial space in humans. BMC Clin. Pharmacol. 3 (1), http://dx.doi.org/10.1186/1472-6904-3-3.
Liu, I.-S., 2014. A solid–fluid mixture theory of porous media. Internat. J. Engrg. Sci. 84, 133–146. http://dx.doi.org/10.1016/j.ijengsci.2014.07.002.
Loix, F., Simões, F.M., Loret, B., 2008. Articular cartilage with intra and extrafibrillar waters – simulations of mechanical and chemical loadings by the finite element method. Comput. Methods Appl. Mech. Engrg. 197 (51–52), 4840–4857. http://dx.doi.org/10.1016/j.cma.2008.07.004.
Loret, B., Gajo, A., Simões, F.M., 2004. A note on the dissipation due to generalized diffusion with electro-chemo-mechanical couplings in heteroionic clays. Eur. J. Mech. A Solids 23 (5), 763–782. http://dx.doi.org/10.1016/j.euromechsol.2004.04.004.
Loret, B., Simões, F.M., 2004. Articular cartilage with intra- and extrafibrillar waters: a chemo-mechanical model. Mech. Mater. 36 (5–6), 515–541. http://dx.doi.org/10.1016/s0167-6636(03)00074-7.
Loret, B., Simões, F.M., 2005. A framework for deformation, generalized diffusion, mass transfer and growth in multi-species multi-phase biological tissues. Eur. J. Mech. A Solids 24 (5), 757–781. http://dx.doi.org/10.1016/j.euromechsol.2005.05.005.
McGurk, S., 2010. Ganong's review of medical physiology – 23rd edition Kim E Barratt Ganong's review of medical physiology – 23rd editionet al |McGraw Hill medical|726pp|£41.99978 0 07160567 00071605673. Nurs. Stand. 24 (20), 30. http://dx.doi.org/10.7748/ns.24.20.30.s35.
McLennan, D.N., Porter, C.J., Charman, S.A., 2005. Subcutaneous drug delivery and the role of the lymphatics. Drug Discov. Today: Technol. 2 (1), 89–96. http://dx.doi.org/10.1016/j.ddtec.2005.05.006.
Müller, I., 1967. On the entropy inequality. Arch. Ration. Mech. Anal. 26 (2), 118–141. http://dx.doi.org/10.1007/bf00285677.
Müller, I., 1968. A thermodynamic theory of mixtures of fluids. Arch. Ration. Mech. Anal. 28 (1), 1–39. http://dx.doi.org/10.1007/bf00281561.
Noll, W., 1974. La mécanique classique, Basée sur un axiome d'objectivité. In: The Foundations of Mechanics and Thermodynamics. Springer Berlin Heidelberg, pp. 135–144. http://dx.doi.org/10.1007/978-3-642-65817-4_8.
Perman, E.P., Urry, W.D., 1929. The compressibility of aqueous solutions. Proc. R. Soc. Lond. Ser. A Math. Phys. Eng. Sci. 126 (800), 44–78. http://dx.doi.org/10.1098/rspa.1929.0204.
Richter, W.F., Bhansali, S.G., Morris, M.E., 2012. Mechanistic determinants of Biotherapeutics absorption following SC administration. AAPS J. 14 (3), 559–570. http://dx.doi.org/10.1208/s12248-012-9367-0.
Richter, W.F., Jacobsen, B., 2014. Subcutaneous absorption of Biotherapeutics: Knowns and unknowns. Drug Metab. Dispos. 42 (11), 1881–1889. http://dx.doi.org/10.1124/dmd.114.059238.
Rini, C.J., Roberts, B.C., Vaidyanathan, A., Li, A., Klug, R., Sherman, D.B., Pettis, R.J., 2022. Enabling faster subcutaneous delivery of larger volume, high viscosity fluids. Expert Opin. Drug Deliv..
Schwarzenbach, F., Berteau, C., Filipe-Santos, O., Wang, T., Rojas, H., Granger, C., 2015. Evaluation of the impact of viscosity, injection volume, and injection flow rate on subcutaneous injection tolerance. Med. Devices: Evid. Res. 473. http://dx.doi.org/10.2147/mder.s91019.
Sun, D.N., Gu, W.Y., Guo, X.E., Lai, W.M., Mow, V.C., 1999. A mixed finite element formulation of triphasic mechano-electrochemical theory for charged, hydrated biological soft tissues. Internat. J. Numer. Methods Engrg. 45 (10), 1375–1402. http://dx.doi.org/10.1002/(sici)1097-0207(19990810)45:10<1375::aid-nme635>3.0.co;2-7.
Swartz, M.A., Fleury, M.E., 2007. Interstitial flow and its effects in soft tissues. Annu. Rev. Biomed. Eng. 9 (1), 229–256. http://dx.doi.org/10.1146/annurev.bioeng.9.060906.151850.
Thomsen, M., Hernandez-Garcia, A., Mathiesen, J., Poulsen, M., Sørensen, D.N., Tarnow, L., Feidenhans, R., 2014. Model study of the pressure build-up during subcutaneous injection. PLoS ONE 9 (8), e104054. http://dx.doi.org/10.1371/journal.pone.0104054.
Thomsen, M., Poulsen, M., Bech, M., Velroyen, A., Herzen, J., Beckmann, F., Feidenhansl, R., Pfeiffer, F., 2012. Visualization of subcutaneous insulin injections by x-ray computed tomography. Phys. Med. Biol. 57 (21), 7191–7203. http://dx.doi.org/10.1088/0031-9155/57/21/7191.
Thomsen, M., Rasmussen, C.H., Refsgaard, H.H., Pedersen, K.-M., Kirk, R.K., Poulsen, M., Feidenhans, R., 2015. Spatial distribution of soluble insulin in pig subcutaneous tissue: Effect of needle length, injection speed and injected volume. Eur. J. Pharm. Sci. 79, 96–101. http://dx.doi.org/10.1016/j.ejps.2015.08.012.
Truesdell, C., Noll, W., 1992. The Non-Linear Field Theories of Mechanics. Springer Berlin Heidelberg, http://dx.doi.org/10.1007/978-3-662-13183-1.
Wiig, H., Swartz, M.A., 2012. Interstitial fluid and lymph formation and transport: Physiological regulation and roles in inflammation and cancer. Physiol. Rev. 92 (3), 1005–1060. http://dx.doi.org/10.1152/physrev.00037.2011.
Woodley, W.D., Morel, D.R., Sutter, D.E., Pettis, R.J., Bolick, N.G., 2022. Clinical evaluation of large volume subcutaneous injection tissue effects, pain, and acceptability in healthy adults. Clin. Transl. Sci..
Woodley, W.D., Yue, W., Morel, D.R., Lainesse, A., Pettis, R.J., Bolick, N.G., 2021. Clinical evaluation of an investigational 5 ml wearable injector in healthy human subjects. Clin. Transl. Sci..
Wu, J.Z., Cutlip, R.G., Andrew, M.E., Dong, R.G., 2007. Simultaneous determination of the nonlinear-elastic properties of skin and subcutaneous tissue in unconfined compression tests. Skin Res. Technol. 13 (1), 34–42. http://dx.doi.org/10.1111/j.1600-0846.2007.00182.x.
Xiao, Y., Bhattacharya, K., 2001. Modeling electromechanical properties of ionic polymers. In: Bar-Cohen, Y. (Ed.), Smart Structures and Materials 2001: Electroactive Polymer Actuators and Devices. SPIE, http://dx.doi.org/10.1117/12.432658.
Zheng, F., Hou, P., Corpstein, C.D., Xing, L., Li, T., 2021. Multiphysics modeling and simulation of subcutaneous injection and absorption of Biotherapeutics: Model development. Pharm. Res. 38, 607–624.